Titre: Title:	Compensation of Relevant and Compensable Volumetric Errors for Five-Axis Machine Tools Based on Differential Kinematics
Auteur: Author:	Mehrdad Givi
Date:	2015
Type:	Mémoire ou thèse / Dissertation or Thesis
Référence: Citation:	Givi, M. (2015). Compensation of Relevant and Compensable Volumetric Errors for Five-Axis Machine Tools Based on Differential Kinematics [Thèse de doctorat, École Polytechnique de Montréal]. PolyPublie. https://publications.polymtl.ca/1773/

URL de PolyPublie: PolyPublie URL:	https://publications.polymtl.ca/1773/
Directeurs de recherche: Advisors:	J. R. René Mayer
Programme: Program:	Génie mécanique

UNIVERSITÉ DE MONTRÉAL

COMPENSATION OF RELEVANT AND COMPENSABLE VOLUMETRIC ERRORS FOR FIVE-AXIS MACHINE TOOLS BASED ON DIFFERENTIAL KINEMATICS

MEHRDAD GIVI

DÉPARTEMENT DE GÉNIE MÉCANIQUE

ÉCOLE POLYTECHNIQUE DE MONTRÉAL

THÈSE PRÉSENTÉE EN VUE DE L'OBTENTION

DU DIPLÔME DE PHILOSOPHIAE DOCTOR

(GÉNIE MÉCANIQUE)

JUILLET 2015

UNIVERSITÉ DE MONTRÉAL

ÉCOLE POLYTECHNIQUE DE MONTRÉAL

Cette thèse intitulée :

COMPENSATION OF RELEVANT AND COMPENSABLE VOLUMETRIC ERRORS FOR FIVE-AXIS MACHINE TOOLS BASED ON DIFFERENTIAL KINEMATICS

présentée par : GIVI, Mehrdad

en vue de l'obtention du diplôme de : Philosophiae Doctor

a été dûment acceptée par le jury d'examen constitué de :

M. ACHICHE Sofiane, Ph. D., président

M. MAYER René, Ph. D., membre et directeur de recherche

M. BARON Luc, Ph. D., membre

M. DONMEZ Alkan, Ph. D., membre externe

DEDICATION

To my family

for their sincere love

ACKNOWLEDGEMENTS

This work could not have been succeeded to this extent without support of my research director, colleagues, friends and family.

In full gratitude, I would like to express my special appreciation to my tremendous supervisor and research director, Professor René Mayer, for his sincere and excellent guidance, caring, patience, availability and suggestions during my research.

I greatly acknowledge Professors Luc Baron, Sofiane Achiche and Alkan Donmez for the time devoted to evaluate my thesis and for their acceptance to participate in the jury.

I would like to thank Mr. Guy Gironne, CNC machine technician and also Mr. François Menard, CMM technician at École Polytechnique Montréal for their technical assistance during the experiments at Virtual Manufacturing Research Laboratory (LRFV).

The financial support of the NSERC Canadian Network for Research and Innovation in Machining Technology (CANRIMT) for this research is acknowledged.

I take this opportunity to extend my sincerest thanks to all of my colleagues and teammates at École Polytechnique especially Maryam Aramesh, Rahman Mizanur and Anna Los for their valuable emotional and technical supports during all these years.

A special thanks to my family. Words cannot express how grateful I am to my father, mother, sister and brother-in-law for all of their continuous supports and encouragements.

RÉSUMÉ

Les erreurs géométriques d'une machine-outil ont un impact direct sur la précision des pièces usinées. Cette thèse traite de la compensation d'erreur des machines-outils CNC à cinq-axe. Dans la première phase, une formulation générale de l'erreur volumétrique et un système de compensation hors ligne sont proposés pour améliorer la précision de la pièce. En utilisant la cinématique des corps rigides et les paramètres d'erreur estimés de la machine, les commandes de position de la machine contenues dans un code G standard sont utilisées pour calculer l'erreur de position de l'outil. Le Jacobien, exprimant le différentiel entre l'espace articulaire et l'espace cartésien, est également développé et utilisé pour calculer les modifications de commande articulaire de telle sorte que l'effet des erreurs de la machine peut être annulé par de petits changements directement sur le code G.

Lorsque la compensation est implémentée, sa validation est requise. Des machines à mesurer tridimensionnelles (MMT) ou d'autres dispositifs de mesure externes sont couramment utilisés pour mesurer la précision de la pièce usinée à des fins de validation. Dans ce travail, une série de tests de défauts surfaciques issus de l'usinage sont proposés pour comparer la précision d'usinage avant et après la compensation en utilisant des mesures sur machine seulement. Les écarts sur les surfaces produites découlent de l'erreur volumétrique et proviennent d'erreurs géométriques spécifiques de la machine qui sont mesurées en utilisant un palpeur placé sur la machine erronée elle-même. L'effet de la stratégie de compensation est ensuite validé en comparant l'écart entre les surfaces avec usinage compensé et non compensé. Les résultats des mesures sont compatibles avec les valeurs d'erreur volumétrique prévues et montrent une amélioration de la précision (réduction de décalage) d'environ 90% après compensation.

Finalement, deux nouvelles notions, la pertinence de l'erreur et l'aptitude à la compenser, sont introduites et quantifiées pour la machine-outil. La compensation des erreurs pertinentes et compensables seulement conduit à une compensation optimisée dans laquelle des modifications de commandes minimales mais efficaces sont faites. Une pièce est conçue spécialement pour le test, contenant des caractéristiques communes est usinée, en utilisant les cinq axes d'usinage simultanément, pour la validation expérimentale. Les résultats de simulation montrent jusqu'à 75% de réduction dans la 1-norme des compensations linéaires et angulaires alors que les erreurs pertinentes demeurent efficacement corrigées.

ABSTRACT

Machine tool geometric errors directly impact on the accuracy of machined parts. This thesis addresses the error compensation in five-axis CNC machine tools. In the first phase, a general volumetric error formulation and an off-line compensation scheme are proposed to improve part accuracy. Using rigid body kinematics and estimated machine error parameters, the machine position commands contained in a standard G-code are used to calculate the tool erroneous location. The Jacobian, expressing the differential joint space to Cartesian space relationship, is also developed and used to calculate minute joint command modifications so that the effect of machine errors can be canceled by making small changes directly to the G-code.

When compensation is implemented, its validation is sought. Coordinate measuring machines (CMM) or other external measurement devices are commonly used to measure the accuracy of the machined part for validation purpose. In this work, a series of surface mismatch producing machining tests are proposed to compare the machining accuracy before and after the compensation using only on-machine measurements. The produced surface mismatches that represent the volumetric error and come from specific machine geometric errors are measured using touch probing by the erroneous machine itself. The effect of the compensation strategy is then validated by comparing the surface mismatch value for compensated and uncompensated slots. The measurement results are compatible with the predicted volumetric error values and show an accuracy improvement (mismatch reduction) of about 90 % after compensation for the machine tested.

Finally, two new notions, error relevance and error compensability, are introduced and quantified. Compensation of only relevant and compensable errors leads to an optimized compensation in which minimal but effective command modifications are made. A specially designed test part containing common features is machined, using up to five-axis simultaneous machining, for the experimental validation. Simulation results show up to 75% reduction in the 1-norm of the linear and angular compensations while the relevant errors are still effectively corrected.

TABLE OF CONTENTS

LIST OF TABLES

LIST OF FIGURES

INTRODUCTION

With the burgeoning demand for machined parts with complicated shapes and high accuracy, as in the aerospace industry, the use of five-axis machine tools has been increasing. Applying five-axis machining, the cutting tool can be orientated relative to the part so that shorter machining time, fewer setups, jigs and fixture are required. However, the complex structure of these machines due to the presence of two rotary axes compared to three-axis ones, may cause further volumetric inaccuracy of the tool tip position.

In recent decades, computer numerically control (CNC) of machine tools provided more flexibility and productivity and reduced manual work and operator-related error sources. Machine tools manufacturers' goal is to minimize the possible error sources when designing, manufacturing and assembling machines to improve the quality of their production and stay competitive. However, reaching to higher levels of accuracy leads to exponentially rising costs. Thus, error prediction and compensation is a worthwhile approach for accuracy enhancement. Machined part dimensions and tolerances, particularly in the aerospace industry, are consistently controlled according to drawing tolerance. The dimensional imperfections of the machined part may come from machine errors like geometric errors of machine joints and components, thermal and cutting force induced errors and so on. The geometric error is a significant one that adversely influences the overall accuracy and cause unwanted deviations of tool location called "volumetric error". Prediction and compensation of the volumetric error in multi-axis machine tools have been the subjects of much research in recent decades.

Problem definition

To compensate the volumetric error in a machine tool, a precise model of geometric and kinematic parameters is required. A general and common understanding of the volumetric error which can be quantified using a mathematical formulation is a perquisite to reach an effective compensation. Once error compensation is implemented, its validation and optimization are also sought.

In addition, the machine structure (topology), the feature to be machined, the machining process and also tool geometry are effective factors in compensation strategy selection, validation and optimization. There is a lack of knowledge about the relationship between the compensation

scheme and the above-mentioned factors. In the present thesis, strategies and techniques are proposed to answer following the main research question:

- How to compensate the relevant and compensable volumetric error in five-axis machine tools?

This can be detailed in the form of below questions:

- How to calculate and predict the components of volumetric error in a five-axis machine?
- Is it possible to predict the volumetric error using the original G-code and then compensate errors through G-code modification?
- How to validate the compensation effectiveness using on-machine measurement (OMM) without an external measurement device?
- Do all volumetric error components require compensation?
- Is it possible to compensate all components of the volumetric error by changing original axes commands?

Objectives

To effectively compensate the volumetric error in a five-axis machine tool, these specific objectives are defined:

1. Develop an exact mathematical formulation to predict the volumetric error vector that relies solely on original axes positions and the machine error parameters.
2. Propose a fast and easy method for validation of error compensation effectiveness in machine tools without using CMM.
3. Reduce the demand on volumetric error compensation by considering the tool geometry and the feature to be machined.
4. Quantify the machine capability to compensate all volumetric error components by G-code adjustment.

Hypotheses

- Volumetric error twist in a five-axis machine tool can be predicted using a general modeling formulation, original G-code, machine tool error parameters and then compensated by minute adjustments in original commands of the machine axes.
- The effectiveness of a compensation strategy can be validated using OMM and without need for an external measurement device such as CMM.
- Minimal and effective modifications in axes positions can be calculated and implemented in an optimized compensation strategy in which only relevant and compensable error components are attempted to be compensated.

Assumptions

The assumptions considered in this research are as follow:

- Rigid body kinematics: the mathematical model of the machine tool is developed assuming that the machine joints and structure are rigid. Therefore, the error components of each joint are not influenced by the movement of other;
- estimated values for machine joints errors are known as input of the compensation function and also they remain constant after estimation and before machining tests are done;
- the machine tool is supposed to be able to accurately track the programmed commands and uploaded to the CNC controller;
- machine error values are sufficiently small to assume small, but not negligible, angular errors and approximation of the equations in the first article;
- nominal dimensions and location coordinate of the feature to be machined and tool geometry are known for the third paper when studying relevance of the error components.

CHAPTER 1 THEORY AND LITERATURE REVIEW

Basically, for the volumetric error compensation in machine tools, three steps should be taken into consideration; 1) Modeling of the machine tool and its errors, 2) Error measurement and identification, 3) Implementation of a compensation strategy. In this chapter, general definitions and concepts of error sources in multi-axis machine tools, as a perquisite for machine modeling and compensation, are presented. This is followed by an introduction about machine error measurement and identification techniques and then error elimination (reduction) strategies. Since error elimination or compensation is the main subject of the work, this will be explained in details in this chapter and the next chapters in the form of research articles.

1.1 Error sources and classifications

Error is “the difference between the actual response of a machine to a command issued according to the accepted protocol of that machine's operation and the response to that command anticipated by that protocol” [Hocken, 1980]. Various error sources may lead to overall machine inaccuracy and imperfections in machined part dimensions and geometry. Generally, machine errors are classified into two categories namely quasi-static errors and dynamic errors. Quasi-static errors are associated with the structure of the machine tool itself and do not depend on the particular operating conditions of the machine. The sources of these errors include geometric errors, errors due to the dead weight of the machine components and those due to thermally induced strains in the machine structure. Such errors slowly vary in time and accounted about seventy percent of the total error of machine tools. Thus quasi-static errors are a major error focus in error compensation research. On the other hand, dynamic errors are related to the dynamic behavior of the machine and usually depend on machining conditions during cutting operation such as spindle error motions, vibration of the machine structure, tool deflection and servo control and contouring errors [Hocken, 1980].

In this section, brief introductions to some of these errors are separately presented.

1.1.1 Thermal errors

Thermal errors or temperature induced errors are due to internal or external heat/cold sources. In addition to quasi-static errors due to thermally induced strains in the machine structure, dynamic behavior of the machine also produces thermal error. The movement of machine elements and

continuous running of motors and pumps during the machining process generate considerable heat. Significant expansion coefficients and expansion coefficient differences result in thermal distortion of machine elements [Schwenke et al., 2008]. Thermal factors contribute 40-70% of total dimensional and shape errors of the machined part. Six sources of thermal deformation are identified; 1) heat from the cutting process, 2) heat generated by the machine, 3) heating or cooling provided by cooling system, 4) environmental temperature, 5) effect of people, 6) thermal memory from previous environments [Bryan, 1990]. The heat transferring across the machine structure depends on the distribution of contact pressure along each joint and can be described based on the theory of thermo-elastic behavior [Attia et al., 1979]. A certain percentage of the total power of the machine is converted to thermal energy because of the frictional resistance exists in moving elements. Continuous movements of bearings, gears, hydraulic oil, drives, clutches, motors, pumps and guideways during machining operations cause temperatures to rise in the machine tool. Spindle growth, thermal expansion of the ball screws and thermal distortion of the column are some of its consequences that may influence the relative position and orientation of the tool. Additionally, heat generated by the shearing action during cutting (some of which is transferred to the deformed chip) should be considered as an important heat source [Ramesh et al., 2000].

The thermal errors can be categorized in two groups. The first group includes the position independents thermal errors (PITE) which vary with temperature but not the axis position. These errors don't depend on the joints positions and mostly affect the machine offsets. The second group is function of both axis position and temperature. These are called position dependent thermal errors (PDTE) and usually produce linear positioning errors [Allen et al., 1997].

The non-linear and time-varying nature of the thermally induced errors that come from non-uniform temperature distribution in machine structures and also the complexity of heat transfer mechanism makes it complicated to model and predict the thermal errors [Mou, 1997]. But, thermal errors cannot be neglected in machine tool accuracy improvement; particularly when a “real-time” compensation strategy is implemented. Thermal effect of heat produced during machining is possible to be detected using temperature sensors and considering the thermal errors in machine model for error compensation purpose. Reduction of external and internal heat sources, control of heat flow, usage of high volume of coolant, redesign the machine tool and

making machine components less sensitive to the heat flow are some proposed strategies to minimize thermal errors [Ramesh et al., 2000].

1.1.2 Load induced errors

The major sources of load induced errors can be divided into three categories, i.e. 1) strain resulting from the machine tool assembling, 2) strain resulting from the dead weight of the machine elements, 3) strain resulting from workpiece weight [Hocken, 1980].

1.1.2.1 Machine tool materials and assembling

The instability of the materials may result in geometric distortion in machine structure such as long-term dimensional length changes. Slow relaxation of metallurgical stress (e.g., iron casting or steel weldments) is the main reason of such instabilities. However, this error source can be minimized through stress-relieving methods such as vibration at liquid-metal solidification stage, vibration in solid state, commercial stress-relief annealing, weathering, etc. Great stress relief is achievable in good quality iron casting or steel weldments by means of long-cycle stress relieving process. Another error source is due to machine foundation and its mounting. Using a minimum but efficient number of physical constraints to constrain the machine body (e.g. kinematic mounting) provides the highest accuracy. This approach is mostly applicable for small and medium-size machine tools for which the foundation problems can be eliminated. For large machine tools, the properties of bedplate, foundation, and soil structure, static deformation and damping behavior of foundation and also, its long-term dimensional stability are of importance to reduce the error sources [Hocken, 1980].

1.1.2.2 Self-loading forces

Due to the finite stiffness of the load-bearing elements, static deformations may occur especially in large machine tools in which larger and heavier components are used and their displacement may cause deformations out of allowed limits. For instance, a vertical straightness and a pitch error motion may occur in straight guideways due to the weight of the moving slide. This is called " quasi-rigid behavior" [Schwenke et al., 2008]. Sometimes, the motion of one component affects the motion of another one (cross-coupling).For example, in the bridge-type machine tool shown in Figure 1-1a, a roll error (rotation around X-axis) may occur as a result of the Y

carriage movement across the table. Figure 1-1b clearly illustrates that the changes in Y position of the cross carriage mounted on the bridge is affecting the positioning error of the X table.

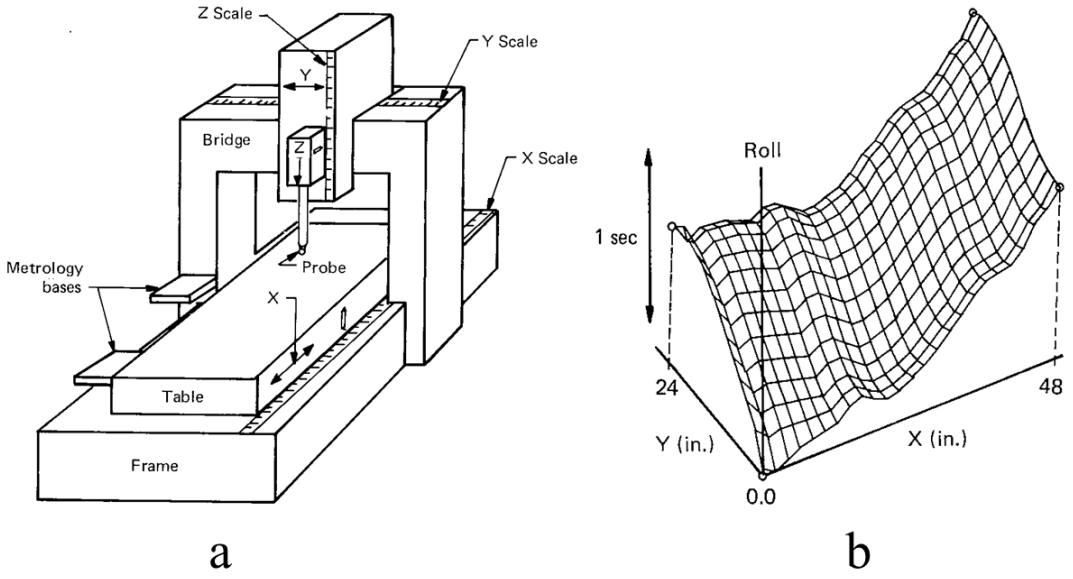

Figure 1-1 a) Schematic of a bridge-type machine b) roll error of the X-table [Hocken, 1980]

1.1.3 Dynamic force induced errors and vibrations

The presence of significant dynamic forces during cutting processes influences the overall accuracy by excessively deforming the tool and work piece or deformation of machine tool structure. Depending on the stiffness of the machine structure, its accuracy is affected by such forces.

Vibration of the machine tool during cutting operations is another source of volumetric error especially in milling processes in which the tool experiences periodic forced vibration. The magnitude and the phase of these vibrations depend on several factors such as the spindle speed and the number of teeth on the cutter, cutting coefficients of the tool/workpiece system, the radial and axial depths of cut, the feed per tooth and the cutter helix angle [Schmitz et al., 2008]. Vibration induced errors are not easily compensable due to very often unknown amplitude and the phase angle of the vibration frequencies. The resultant relative motions between tool and workpiece have detrimental effects on the surface roughness as well as tool wear. Sometimes vibrations come from external sources through foundation, bearing defects, interrupted cuts, etc. This type of vibration is named *forced vibrations*. On the other hand, *self-excited vibration* which

is associated with machine vibrations in one or several natural frequencies while there is no external noise or factor [Hocken, 1980]. Finally, in the case of high speed machining (high feed rate and velocity), forces caused by acceleration and decelerations of machine parts vary during machining process and may result in significant errors [Cano et al., 2008].

Tool deflection occurs due to machining forces and produces surface location errors. In the case of milling, the tooth either deflects towards the surface in up-milling thus causing an over cut form error, or deflects away from the surface in down milling causing an undercut form error. The periodic force at the contact point of tool and feature leads to vibration as Schmitz et.al [Schmitz et al., 1999] investigated the effect of spindle speed (tooth passing frequency) on tool deflection in high speed machining and found both system natural frequency and flexibility as the important factors to choose the depth of cut for a stable operation.

Some researchers have neglected the effect of cutting force induced errors considering that for the finishing process, the cutting forces are too small to influence the overall accuracy. However, in cases of machining some materials like hardened steel to final form (without finishing operation), large forces may be the source of considerable errors and this has to be considered in an overall compensation process [Ramesh et al., 2000]. Errors induced by cutting forces can be particularly dominant also in turning thin workpieces (where a significant elastic deflection occurs in workpiece) or in boring small diameter holes (where tool is subject to have a significant deflection) [Li, 2001].

1.1.4 Fixture dependent errors

A fixture is an element that holds the workpiece on the machine table during machining. Errors in fixture and setup are related to geometric inaccuracies or misalignments of the locating element. Furthermore, if the workpiece is not fixed well or if the fixture is too compliant, its deformation or displacement may become a significant source of error. Therefore, the appropriate fixture elements and locators, clamping sequence, clamping intensity and the contact area of workpiece are of importance to avoid the fixture dependent geometric errors [Hockenberger, 1994; De Meter et al., 1997; Ramesh et al., 2000].

1.1.5 Contouring and servo errors

After modeling the part to be machined in a manufacturing process, usually a computer-aided machining software is used to generate a desired tool path for machining. Due to interpolation and discretization methods applied for tool path generation of complex shape parts, there may be some differences between the generated tool path and the numerical model of the part. Approximations occur in the inverse kinematic transformation during the post-processing phase are also, should be considered as a source of error in machine tool. Reversal spike and servo mismatch are examples of control system and servo setting error sources. Accurate path tracking for contouring is not always possible due to the loss of joint coordination or CNC controllers' limitations especially during high speed motions. Each machine axis may have follow-up errors, influencing the overall accuracy [Lavernhe et al., 2008; Andolfatto et al., 2011]. In other words, unavoidable tracking imperfection between the commanded and actual positions may occur due to the servo controller dynamics that result in contouring errors. The *contour error* can be defined as the normal distance, of the actual tool tip, from the desired (reference) tool path while *tool orientation contour error* can be defined as the normal angular deviation of the tool axis from the desired orientation trajectory [Koren, 1983]. Modeling, evaluation and compensation of contouring errors are studied in some researches [Kwon, 1996; Sencer et al., 2009].

1.1.6 Geometric errors

Machine tool accuracy is directly affected by manufacturing defects, surface straightness and roughness of the machine components and bearing pre-loads. Geometric errors include firstly, the straightness error of the guideways upon which a machine axis carriage moves and secondly, the link geometric errors which may result from shape and assembly errors of the machine structural components.

1.2 Description of the machine errors

According to causality principle, Ekinci et al. [Ekinci et al., 2007] proposed a hierarchal classification of machine errors. As shown in Figure 1-2., geometric errors of the guideways directly lead to kinematic errors in moving joints which would be called "error motions". The second group of the errors considered in the kinematic chain model is called "link geometric errors".

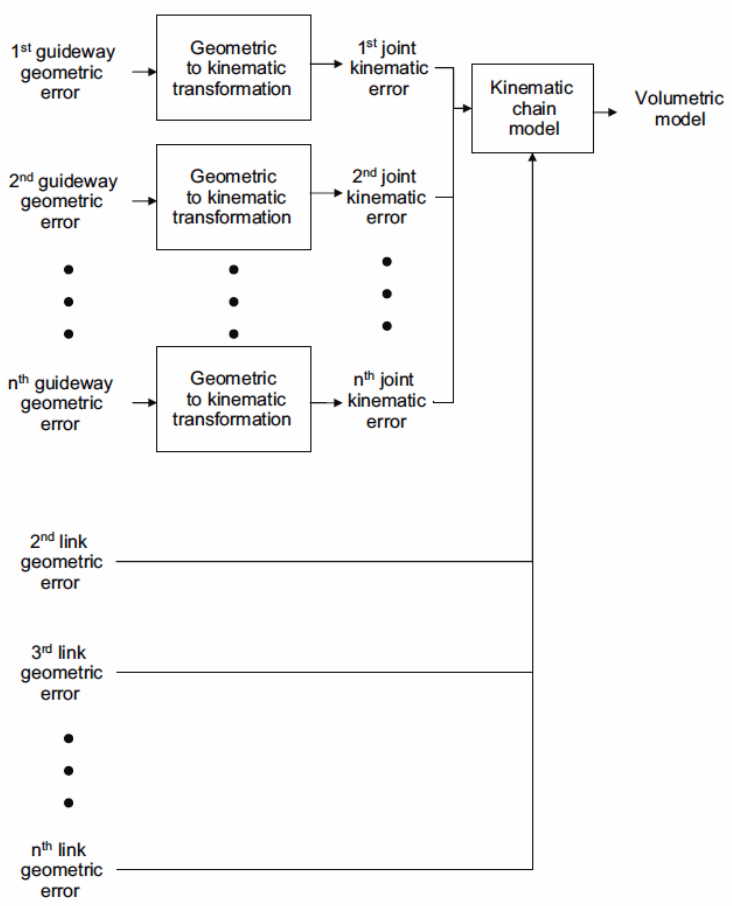

Figure 1-2 Machine error analysis according to causality principle [Ekinci et al., 2007]

The error motions are position dependent geometric parameters (PDGEPs) while the link errors are called position independent geometric parameters (PIGEPs). Link errors are basically associated with misalignment of a structural component and its deviation from the nominal position and orientation in the machine coordinate system such as out of squareness, angular offset and rotary axes separation errors [Abbaszadeh-Mir et al., 2002]:

In next section, all possible motion errors and link errors for multi-axis machine tools are described based on the standard ISO 230. Other common notations for such errors are compared in [Ibaraki et al., 2012].

1.2.1 Error motions

As shown in Figure 1-3, a linear axis (Z-axis for example) could have six motion errors when it moves. These errors are listed in Table 1-1 where the notation is based on ISO 230-1[ISO230-1, 2012]. If, the behavior of the machine is assumed as a rigid body, such errors depend only on the

nominal movement of the axis of concern and so, the location of the other axes does not affect them [Schwenke et al., 2008].

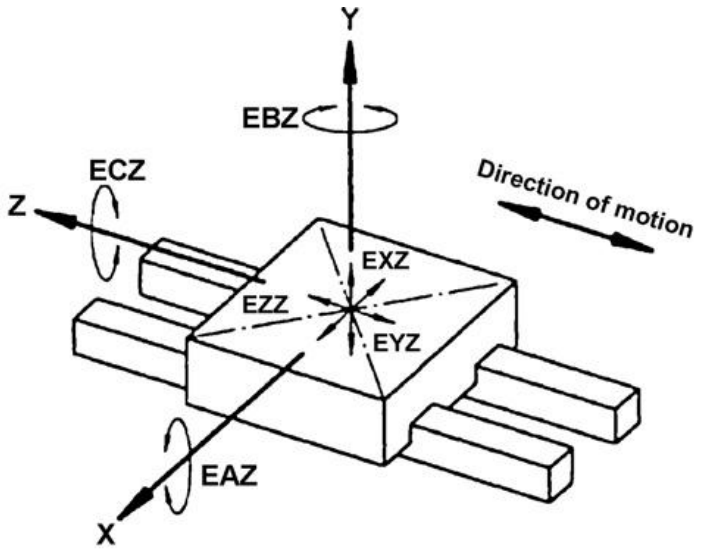

Figure 1-3 Error motions of a horizontal Z-axis [ISO230-1, 2012]

Table 1-1 Error motions of a horizontal Z-axis, notation is according to ISO 230-1

Error description	Error symbol
Straightness error motion of Z in X direction	EXZ
Straightness error motion of Z in Y direction	EYZ
Positioning error in Z direction	EZZ
Pitch error motion of Z (tilt error motion around X)	EAZ
Yaw error motion of Z (tilt error motion around Y)	EBZ
Roll error motion of Z	ECZ

The same possible errors may exist for a nominal rotational movement (for example C-axis) as shown in Figure 1-4 and listed in Table 1-2.

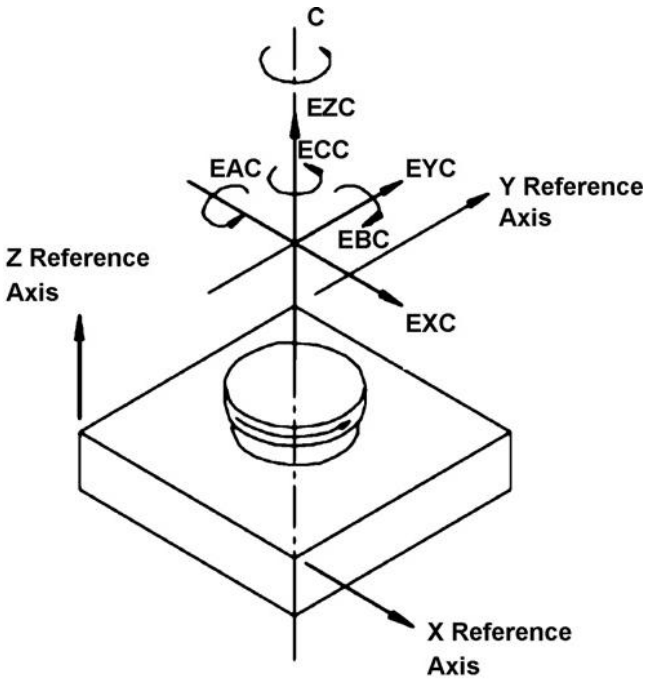

Figure 1-4 Error motions of a rotary C-axis [ISO230-7, 2006]

Table 1-2 Error motions of a rotary C-axis, notation is according to ISO 230-1

Error description	Error symbol
Radial error motion of C in X direction	EXC
Radial error motion of C in Y direction	EYC
Axial error motion of C	EZC
Tilt error motion of C around X	EAC
Tilt error motion of C around Y	EBC
Angular position error of C	ECC

1.2.2 Link errors

To define the link errors relative to the reference coordinate, generally a “reference straight line (average location and orientation) is assumed as the nominal axis (linear or rotational) according to ISO 230-1. A linear motion axis can be defined as a vector with a zero position on the vector. Thus, there are only two squareness errors and the zero position error for it as shown in Figure 1-5 and Table 1-3.

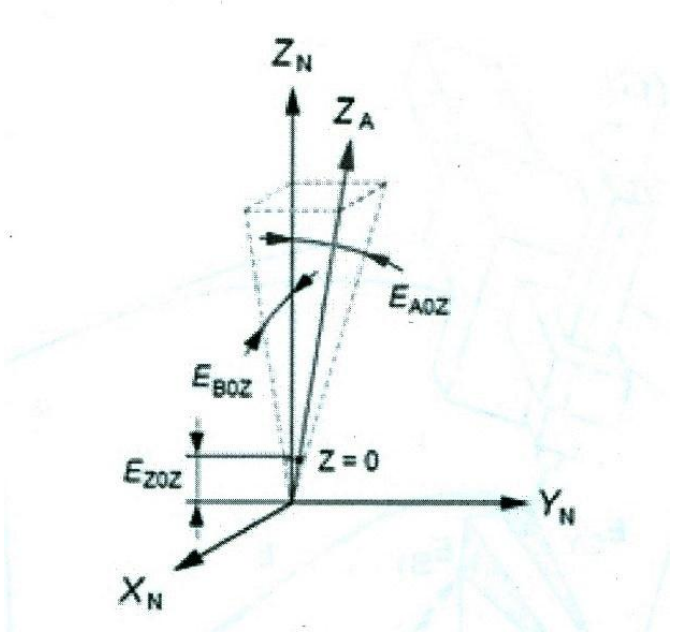

Figure 1-5 Link errors of a linear axis, Z [ISO230-1, 2012]

Table 1-3 Link errors of a linear Z-axis, notation is according to ISO 230-1

Error description	Error symbol
Zero position of Z	E_{ZOZ}
Squareness of Z related to Y	E_{AOZ}
Squareness of Z related to X	E_{BOZ}

A rotary axis has also two translational errors in addition to the ones of a linear axis as shown in Figure 1-6 and Table 1-4.

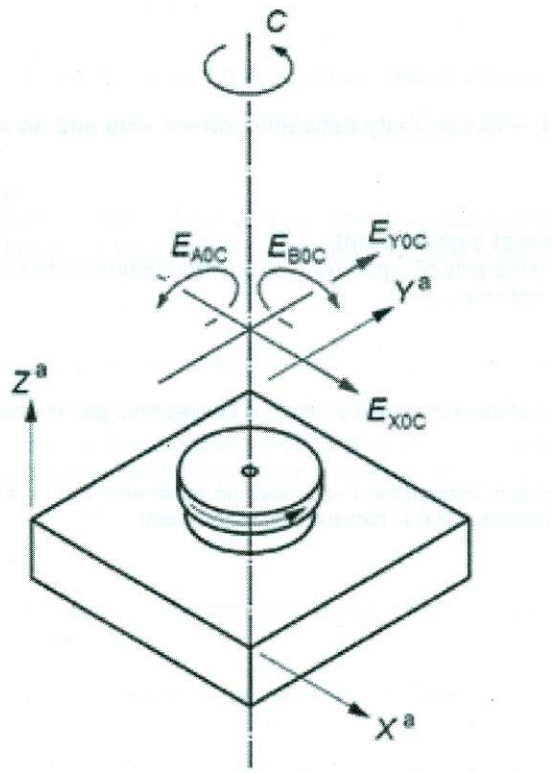

Figure 1-6 Link errors of a rotary axis, C [ISO230-1, 2012]

Table 1-4 Link errors of a rotary C-axis, notation is according to ISO 230-1

Error description	Error symbol
Position error of C in X direction	E_{XOC}
Position error of C in Y direction	E_{YOC}
Out-of-squareness of C relative to Y direction	E_{AOC}
Out-of-squareness of C relative to X direction	E_{BOC}
Angular position error of C	E_{COC}

The total number of errors of a particular machine tool depends on the number of axes. In three-axis machine tools, there are only three prismatic joints whereas, a five axis machine tool is a kinematic chain made of three prismatic and two rotary axes and can be in various arrangement of sequential manners. Everett et al. [Everett et al., 1988], proposed Eq. 1-1 to determine N, the minimum number of fixed value parameters required to define a serial kinematic chain, the robot base frame and end effector frame (regardless of the modeling scheme);

$$N = 4R + 2P + 6 \tag{1-1}$$

where R is the number of rotary axes and P is the number of prismatic axes. Thus, N=20 in five-axis machines. If six parameters among of these 20 parameters are assumed to define the tool frame location and another six to locate the work piece relative to the work piece axis branch, then, only eight link error parameters are remained for the machine internal structure. If the spindle axis and its five error parameters (the rotational error around spindle axis is not accounted as an error) are also considered, a total of 13 link errors are required for error modeling of the five axis machine tool [Zargarbashi et al., 2009].

Based on Abbaszadeh-Mir research [Abbaszadeh-Mir et al., 2002], potentially 42 PIGEPs or link errors are considered for prediction of tool location error respect to the feature in five-axis machine tools; six PIGEPs per axis, six parameters to describe the pose error (positioning and orienting error) of the work piece and an additional six error parameters for the pose of the tool frame in the spindle. Using mathematical analysis of the sensitivity Jacobian matrix, its rank and singular value decomposition (SVD), eight independent error parameters can be determined as the minimum but sufficient set of link error parameters required for estimation of the volumetric error. This is also mentioned in ISO 230-1 (Annex A). In this standard, first, position and orientation error parameters for each axis of a five-axis machine tool (Figure 1-7) are presented. If the coordinate system is defined using the linear axes of motion of the machine, a set of minimum number of error parameter to fully characterize the five-axis machine tool can be extracted as seen in Table 1-5. Note that the possible errors of the spindle axis are not shown in this table [ISO230-1, 2012].

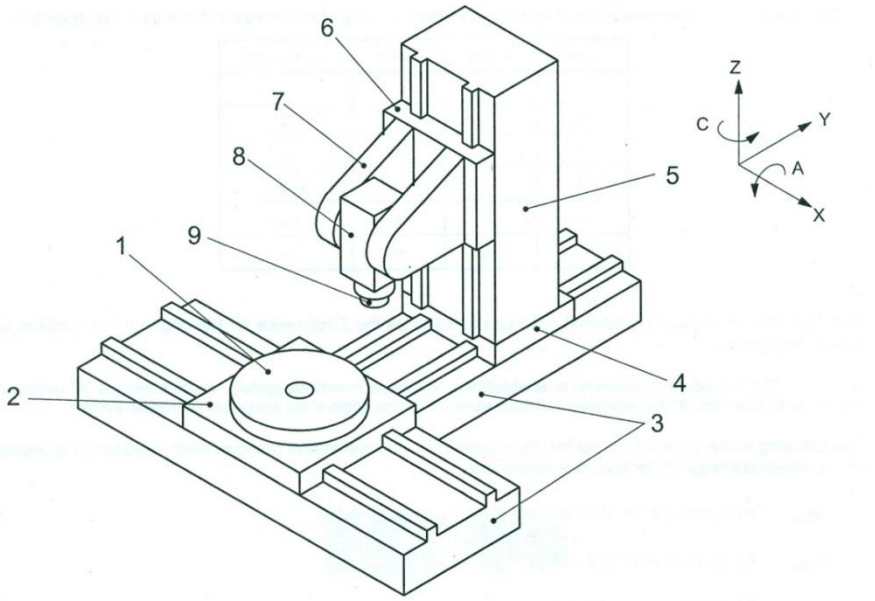

Figure 1-7 A five-axis machine tool configuration; 1) rotary C-axis 2) X-axis 3) bed 4) Y-axis 5) column 6) Z-axis 7) yoke 8) A-axis 9) Spindle [ISO230-1, 2012]

Table 1-5 Minimum number of error parameter to fully characterize a five-axis machine tool

C-axis	X-axis	Y-axis	Z-axis	A-axis
0	(0)	-	-	-
0	-	(0)	-	E_{YOA}
-	-	-	(0)	0
E_{AOC}	-	0	E_{AOZ}	(0)
E_{BOC}	0	-	E_{BOZ}	E_{BOA}
(0)	0	E_{COY}	-	E_{COA}

1.2.3 Volumetric error

The term “volumetric error” refers to the resulting error in position and orientation of the machine tool end effector (tool or stylus tip) related to the workpiece or feature to be machined or measured. The term “volumetric accuracy” for three-axis machine is defined as” the maximum range of relative deviations between actual and ideal position in X-, Y-, Z-axis directions and the maximum range of orientation deviations for A-, B- and C-axis directions for X-, Y- and Z-axis motions in the volume concerned [ISO230-1, 2012]. This definition is valid for the rotary axes accuracy in five-axis machine tools too. This error is defined in the working volume of the machine and can be measured using calibrated artifacts or telescoping ball-bar. In chapter three, a general mathematical formulation for volumetric error and also a graphical representations of that will be explained.

1.3 Machine tool modeling

Most machine tools are serial kinematic chain made of successive joints and moving components to provide a desired relative location between cutter tool and the feature to be machined. The common modeling approaches are as follows;

- **Rigid body kinematics** is one of the most widely used techniques for simulation and modeling of the machine tools. Based on rigid body kinematics, machine tool axes and links are connected to each other like a chain but error motions of each axis are not influenced by other axes position. The direct kinematic model can be built using homogenous transformation matrices (HTMs) [Roberts, 1966] and accommodating both link and motion error modeling. Srivastava [Srivastava et al., 1995] used this approach to model geometric and thermal errors in a five-axis machine tools. This modeling approach is used to model the machine tool in the present research as explained in details in chapter three (first article).
- **Non-rigid body** assumption may be applied where a heavy movable slide in a large size machine, for instance, produces deformations in the guideways of other slides. Chen et al. [Chen et al., 1992] compared two approaches, i.e. off-line multidimensional fitting and on-line identification to measure the non-rigid body kinematic effect using a laser

interferometer and then compensated it by compensation signals through digital I/O board.

- **D-H modeling** [Denavit, 1955]; using D-H modeling, Mahbubur et al. [Mahbubur et al., 1997] proposed a compensation strategy in which the nominal values of the rotary axes are derived from CL-data and then applied for correcting the tool path within the post-processor before generating the G-code. This modeling approach is mostly used to model the robots and not machine tools. This is due to the rules imposed in this method for the definition of the local reference frames.
- **Product of exponential (POE)** method is widely used in robotic and recently in machine tools. It represents the kinematics of an open-chain mechanism as the product of exponentials of twists. Using POE method, the problem of determining the joint angle given the end-effector location (inverse kinematic) can be solved compared to D-H modeling. Furthermore, the manipulator Jacobian and its singularities can be easily characterized. [Murray et al., 1994].

1.4 Error measurement and identification

1.4.1 Direct and indirect measurement

Several measurement instruments and techniques are applied to detect the geometric errors of the machine tool. The most suitable measuring method depends on the machine geometry and the errors to be measured or identified. In "direct" measurement methods, a specific geometric error of only one axis is measured and there is no need to simultaneously move other axes. Direct measurements can be divided into three subgroups [Sartori et al., 1995; Schwenke et al., 2008];

1. The material-based methods wherein standard artifacts such as straightedges, line scales or step gages and even multidimensional artifacts like ball plates are applied.
2. The laser-based methods which use laser light wavelength as a reference; Environmental factors like temperature and pressure have a relatively small effect on the laser wavelength characteristics but should be taken into consideration for calibration purposes. Yielding a high accuracy on short- and long-machine axes, the laser interferometer is commonly used for measurement of the positioning errors as shown in Figure 1-8.

3. The gravity-based method wherein local gravity of the earth is used to define the metrological reference to measure some errors such as angular errors around horizontal axes.

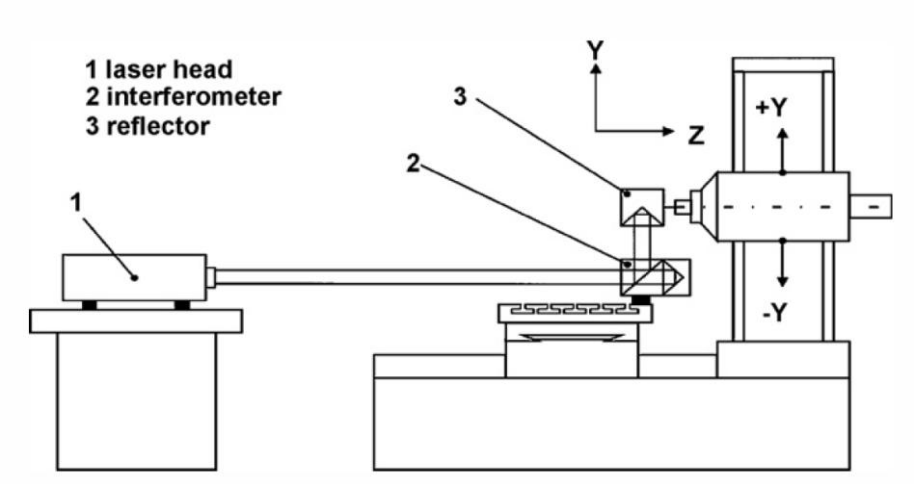

Figure 1-8 Laser interferometer for the measurement of Y-axis positioning error [Schwenke et al., 2008]

In contrast, "indirect" measurement techniques focus on superposed errors and thus, multi-axis motions are required. Either calibrated, partially calibrated or un-calibrated artifacts may be used in indirect methods. Contour measurement, multi-lateration measurement and chase-the-ball measurement are some examples of indirect measurement approaches. [Schwenke et al., 2008]. One of the most common indirect methods is the circular test using a ball bar as presented in ISO 230-4 [ISO230-4, 2005]. This method was established by Bryan [Bryan, 1982] and is applicable to check of contouring accuracy, backlash error and also the error motions of two orthogonal linear axes in machine tools. Other developed artifacts and measurement approaches are still the subject of much researches [Lei et al., 2002; Weikert, 2004; Zargarbashi et al., 2009; Erkan et al., 2011].

1.4.2 Error identification

The machine error to be identified must have a significant effect on the measurement results in order to its influence to be separated from any combination of other parameters. In other words, if, a geometric error parameter does not have a distinguished effect on the measurement result, its identification may be impossible. Error identification is done using analytical or best fit methods.

Regarding the measurement method applied, an appropriate identification approach is used. For example, the errors measured using calibrated artifacts or self-calibrated methods could be identified by analytical methods. While best fit methods are usually used in cases of multi-lateration or chase-the-ball measurement methods [Schwenke et al., 2008]. Another categorization for error identification approaches was reported by Lo [Lo, 1994], i.e. 1) grid calibration method 2) error synthesis method 3) designed artifact method 4) metrology frame method 5) finite element method. He found the error synthesis model as the only efficient method to correct the overall quasi-static error in his research on a four-axis turning center. In addition, an adaptive error identification method was developed [Mou et al., 1995] in which inverse kinematic were used to characterize the individual effect of machine error parameters on machined part geometric errors.

1.5 Error elimination and its categorizations

The efforts for accuracy improvement for machine tools are categorized in two main groups; "Error avoidance" and "error compensation".

1.5.1 Error avoidance

In "error avoidance", the source of the error or its effect is eliminated through refinement of the machine design or its environment. The machine accuracy is improved during both designing and manufacturing steps. Precise components, high stiffness, and low thermal distortion will result in machine accuracy enhancement. However, this approach basically needs high degree of investment especially to reach as accuracy beyond a certain level. As an example, to avoid the thermal induced errors in machine tools, three strategy are proposed [Ni, 1997]:

a) heat source reduction; control the environmental conditions through heat exchangers or enclosing the machine tool in temperature-controlled boxes.

b) heat flow control through passive control (such as blocking the heat flow using insulation pads) or active control (modifying the thermal-induced deformations of machine tool structure by using an external heat source to minimize the machine warm-up time etc.)

c) thermally robust structural design; that reduces the sensitivity of machine structure to thermal changes or symmetric design of heat sources etc.

1.5.2 Error compensation

The second approach is "error compensation" in which no attempt is made to avoid the error and involves lower costs compared to the former. In this approach, the errors in the machine are measured and then suitably compensated. In the literature, the strategy reported by Koliskor [Koliskor, 1971] based on the results of post-process inspection and also the software-based method developed by Donmez et al. [Donmez et al., 1986] for geometric error correction are two early researches on error compensation. The strategies for error compensation can be generally categorized as follow:

1.5.2.1 Real-time compensation and off-line compensation

If the machining process and measurement is repeatable enough, a “pre-calibrated” error compensation can be applied. Errors are measured after the machining process and used to subsequently change or calibrate the process (off-line). This method is suitable especially for cases involving with mass productions. The second and more accurate method is named "real-time active error compensation" (or “dynamic compensation” as it is named in [Ramesh et al., 2000]) wherein the process is altered or calibrated based on the error measurement results during the same operation. However, this is more expensive and time consuming compared to the former [Hocken, 1980].

Two real-time techniques are proposed as follow:

- **Feedback interception method** in which feedback signals from the servo loop are intercepted by a computer. The computer calculates the volumetric error and modifies the feedback signals before embedding back to the controller and this, leads to adjustment of the slide position [Yee et al., 1990]. Although, no modification in controller software is required, the electronic devices used for insertion of the quadrature signals in this technique need extreme caution to prevent inserted signals interfering with the machine tool error controls.
- **Origin-shift method** in which the computer sends compensation signals after calculating the volumetric error and without interception of the feedback signal from servo loop. This results in shifting the reference origins of the control system through an I/O interface as shown in Figure 1-9 [J.S. Chen, 1993].

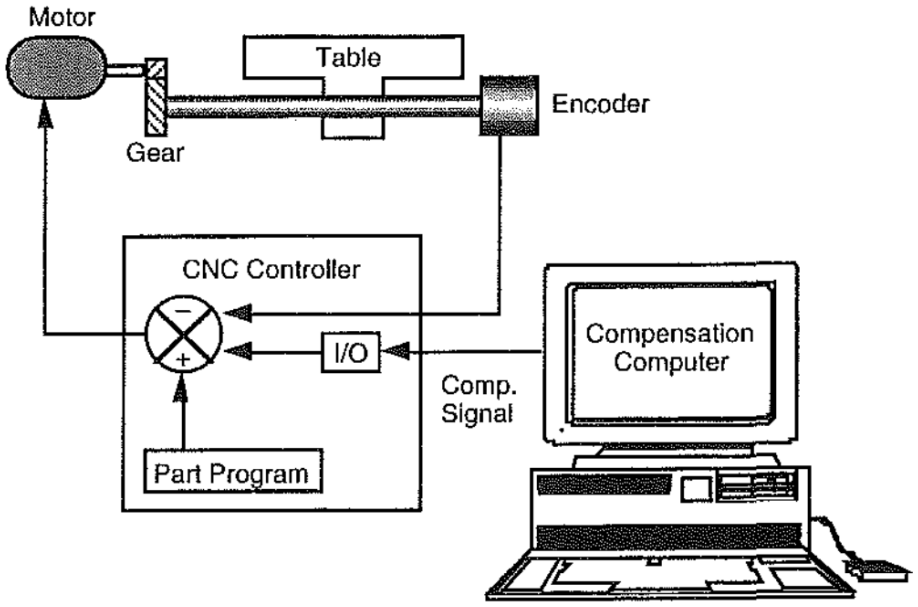

Figure 1-9 Compensation by shifting the origins of machine axes [Ni, 1997]

In real-time compensation usually the information on thermal-induced errors and force-induced errors are acquired using sensors mounted on the machine and so, a synthesis model of all positioning, thermal and force errors is used [Lo, 1994; Spaan, 1995]. Although, both systematic and random errors can be corrected, there are some difficulties in this approach. Firstly, finding the optimal location of the sensors (especially thermocouples) to be mounted is not easy and usually needs statistical analysis and several empirical (trial-and-error) processes. Secondly, characterization of the machine thermal behavior is time consuming since a considerable time is needed for machine to reach the thermal steady state and then to cool down to its original state. Robustness of the error model when modeling the thermal errors depends on several factors such as sensors mounting location, sudden change in the coolant or environmental temperature etc. [Ni, 1997].

1.5.2.2 Software (numerical) compensation and hardware compensation

Another categorization for the compensation techniques could be assumed; 1) hardware error compensation (similar to the error avoidance conceptm involves modifications in machine tool hardware and physical components and so, applicable only when errors are larger than a defined

range and 2) software error compensation. Hocken [Hocken, 1993] defines the term software correction as follows: “The use of per-process data, a machine model and indirect sensing of process parameters relevant to that model, in order to provide data to control system for the correction of a nominal tool position with respect to a nominal part during the machining process or measuring using the actuators normally supplied with the machine.” Software compensation is also called “numerical compensation” in some references.

For numerical compensation, the quantified information of machine errors through measurement methods is required. The compensation will be effective if the machining conditions and errors are time invariant and also have high repeatability. An absolute coordinate system is also required. Numerical compensation could maintain accuracy over the machine life time even when its geometry changes due to aging, wear, foundation stabilization, environment thermal condition, etc. However, the required motions for error compensation in the functional orientation in five-axis machine tools is not always available to the CNC and it may leads to highly accelerated motions of other axes. The thermal conditions of the machine and the object used for its calibration affect the numerical compensation results and should be considered as one of the limitations [ISO/TR16907, 2015].

Most modern industrial controllers provide useful tools to compensate specific geometric errors such as positioning errors of linear and rotary axes, backlash error, straightness error and some thermal induced errors. As discussed in ISO/TR 16907 [ISO/TR16907, 2015] and also [Sartori et al., 1995], there are four ways to store the error information (obtained from measurement) into the CNC controller;

- Error lattice; the error magnitudes are stored at points spread evenly in a working volume and used to directly compensate only translational deviations at those spatial points. Such error lattices are applicable only when the tool offset is fixed.
- Look-up tables; assuming positioning errors as a function of axis position, such tables contain nominal position and direction of the axis motion and the corresponding error value (which is a correction value to cancel the error effect). CNC controller may apply linear interpolation for intermediate points.
- Coefficient table; the coefficients of polynomials used for analytical error modeling are stored and employed for error compensation at working points.

- Spatial error grid tables; in which user is required to input translational and angular error values at all grid points of each linear or rotary axis. A model based software may calculate the spatial error grid both on modeled or un-modeled error motion of the machine tool. An example of such spatial error grid tables is shown in Table 1-6.

Table 1-6 A spatial error grid for rotary axes [ISO/TR16907, 2015]

Point No.	Sample points		Compensation value (error value)					
	A (or B)-axis	C-axis	ΔX (mm)	ΔY (mm)	ΔZ (mm)	ΔA (°)	ΔB (°)	ΔC (°)
1	0	0	0	0	0	0	0	0
2	0	5	0.001	-0.001	0.001	0	0	0.001
3	0	10	0.002	-0.002	0	0.002	-0.001	0.002
…	…	…	…	…	…	…	…	…

Correction of erroneous tool path prior to the inverse kinematic conversion to G-code is another software compensation strategy widely used in the literature. Uddin et al. [Uddin et al., 2009] employed this strategy in five-axis machining of a cone frustum as the case study (based on standard NAS979). In a similar strategy, a recursive compensation method was applied by Khan et al. [Khan et al., 2011] in which the nominal tool path is obtained from CAD/CAM software and the actual path is calculated through kinematic equations considering error information. Then, the correction vector is computed from the difference between the actual and nominal paths and is used to correct the actual path until an assigned tolerance limit is satisfied.

Some research focused on compensation of both translational and angular errors in presence of rotary axes in machine tools. As a recent case, Lei and Hsu [Lei et al., 2003] assumed a linear relation between differential changes in machine joint coordinates and the workpiece Cartesian coordinates and used a nominal machine Jacobian matrix to calculate the correction vector and then conduct real-time compensation. Due to some limitations of the proposed method, such as singular points of the machine, they, later applied a two-step process (decouple method) assuming that the motion of only rotary axes can compensate the tool orientation error. This

method first compensates the volumetric errors relevant to rotary axes and then, linear ones in real time [Hsu et al., 2007].

Khan et al. [Khan et al., 2011] grouped numerical (software) compensation techniques into four main classes as shown in Figure 1-10;

1. **Additional embedded software module** wherein the position signals are modified in an additional software module based on machine error information. This module could be either inside of the controller or get connected to it using I/O interface.
2. **Control parameter modification**: it is possible to calibrate some of the controller parameters before executing the NC program. The information of some errors such as pitch error, backlash error, temperature error, etc. can be uploaded in the CNC controller look-up or spatial grid tables. Siemens 840D and Heidenhain iTNC are some examples of controllers equipped with control systems to compensate sagging, lead screw, and even nonlinear behavior errors.
3. **Post-processor modification:** Post processor applies the cutter location (CL) data and machine geometry information to produce the NC program. If geometric error information is available, a compensated NC code can be produced, in principle.
4. **NC program modification**: In the cases that machine has a close-structure controller or the post processor does not cater for the all required error information, NC code modification after post processor step could be a strategy for compensation.

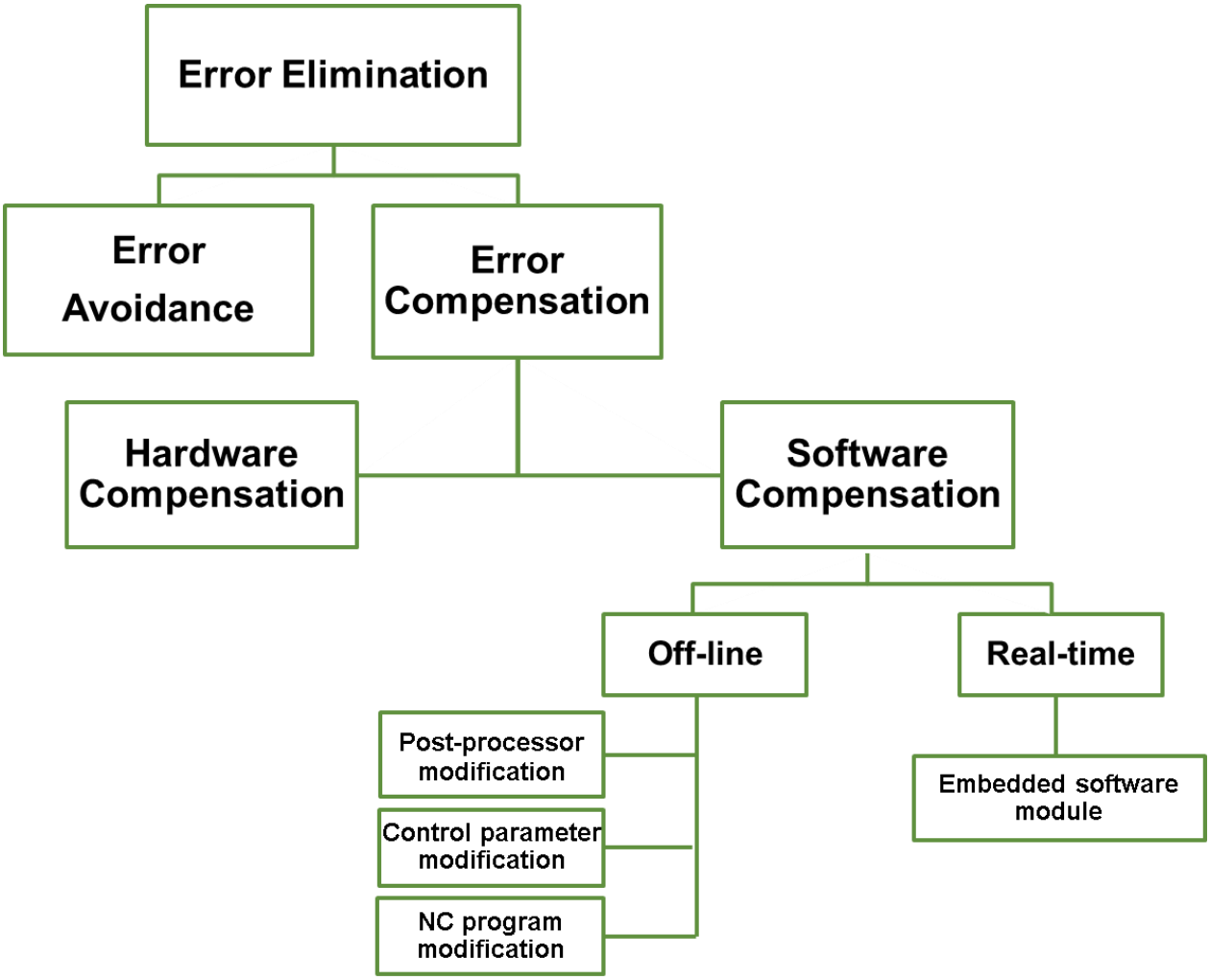

Figure 1-10 Error elimination categorization

CHAPTER 2 ORGANIZATION OF THE WORK

After an introduction to the thesis subject and objectives, the theory and a critical literature review were presented in the first chapter. In this chapter, the general organization of the work and the coherence of articles presented in the thesis are briefly described. Based on the defined objectives for the project, the three presented articles answer these questions, respectively:

1) How to compensate the errors?
2) How to validate the compensation strategy?
3) How to optimize the compensation?

Chapter three includes the first article entitled “volumetric error formulation and mismatch test for five-axis CNC machine compensation using differential kinematics and ephemeral G-code” which is published in the international journal of advanced manufacturing technology. It proposes an off-line strategy for error compensation in which original G-code is modified after the post-processing step and before being uploaded into the controller. First, the axis commands are extracted from the original G-code and used for volumetric error prediction. A general formulation for volumetric error twist is developed that solely relies on the axis commands and machine error parameters. Assuming a local linearization of the actual erroneous kinematic model in the form of a sensitivity Jacobian matrix, it is possible to mathematically relate the differential changes in volumetric error at the tool tip to small changes of the machine axes positions. Therefore, a correction vector cancelling the effect of the volumetric error is defined and then the required small changes of the machine axes position to produce such a correction vector at the tool tip are calculated. This provides a modified G-code in which the axes commands are adjusted before uploading to the CNC controller. For validation purpose, a new experimental procedure based on a surface mismatch producing machining test is introduced and performed on a HU40T CNC machine. The newly produced G-code is coined ‘ephemeral G-code’ because it must be regenerated as the machine geometry changes over time.

In the next article (chapter four) entitled “validation of volumetric error compensation for a five-axis machine using surface mismatch producing tests and on-machine touch probing”, published in the International Journal of Machine Tools and Manufacture, the idea of surface mismatch producing test is further developed for more machine axes indexations sets. Seven

series of machining patterns are proposed as a new validation strategy. In each proposed pattern, two-dimensional geometric features are milled, each using two different rotary axes indexation sets. Due to the machine geometric errors, a surface mismatch may appear in each feature that helps to verify the machine volumetric accuracy. The overall accuracy of the machine after implementation of the compensation strategy is checked using a touch probe and OMM (on-machine measurement) immediately after machining. The OMM is accurate enough and does not need to be compensated since the measurement is done in a small volume and using a single linear axis motion and in the same direction for each slot so that most error sources affecting the probing cancel out.

Finally, in the third article which is submitted to the the "CIRP Journal of Manufacturing Science and Technology", the optimization of the compensation is pursued and two new notions are introduced in five-axis machining. The "relevance" of the error indicates if the final dimension and accuracy of the machined part is affected by an error component or not. The irrelevant components of the volumetric error that have no effect on the machined part accuracy do not require compensation. A filtration matrix is defined for each machining process regarding the tool geometry and the feature to be machined. The second introduced notion is the "error compensability" which refers to the ability of the machine to cancel the effect of volumetric error. Due to the kinematic singularities of the machine tool, it may not be possible to compensate all error components by small adjustments in machine axes positions. In the proposed optimized compensation, first, the irrelevant errors are filtered out in compensation process and their reduction is not sought. Then, the uncompensable parts of the volumetric error are flagged using a compensability ratio and filtered out in the compensation process. As a case study, a designed workpiece containing four common features, i.e. hole, curved slot on a spherical surface, cone frustum and flat surface, is machined using uncompensated, compensated and optimized compensated G-code. This chapter also includes visual presentations and comparison of best fit residuals of the measured features before and after compensation.

Figure 2-1 shows the highlights of the mentioned articles in brief. A general discussion on the three articles is presented in the sixth chapter which is followed by the conclusions and recommendations. The thesis ends by the list of all bibliographical references used in this work.

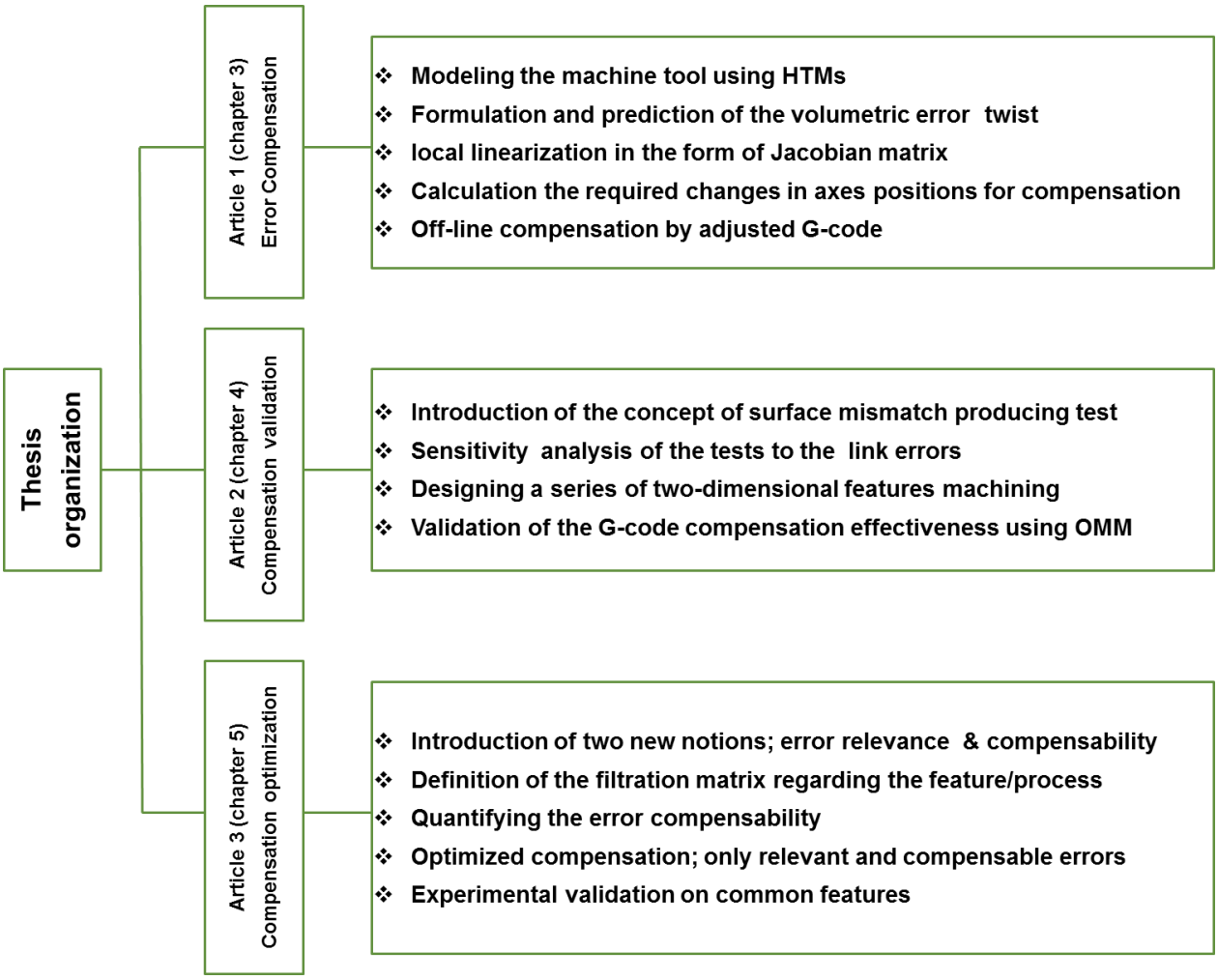

Figure 2-1 Thesis organization

CHAPTER 3 ARTICLE 1: VOLUMETRIC ERROR FORMULATION AND MISMATCH TEST FOR FIVE-AXIS CNC MACHINE COMPENSATION USING DIFFERENTIAL KINEMATICS AND EPHEMERAL G-CODE

Mehrdad Givi [1] and J.R.R Mayer [1]

[1] *Mechanical Engineering Department, Polytechnique Montréal, P.O. Box 6079, Station Downtown, Montréal (Qc), Canada, H3C 3A7*

*Based on the paper published in the International Journal of Advanced Manufacturing Technology: 1-9, 2014

3.1 Abstract

Machine tool kinematic errors directly impact on the accuracy of machined parts. A general volumetric error formulation effectively implementing ISO230-1:2012 definition and an off-line compensation scheme are proposed and partly tested to improve part accuracy on a five-axis CNC machine. Using rigid body kinematics and estimated machine error parameters, the machine position commands contained in a standard G-code are used to calculate the tool erroneous location. The Jacobian, expressing the differential joint space to Cartesian space relationship, is also developed and used to calculate minute joint command modifications so that the effect of inter-axis link errors and intra-axis error motions, for example, can be canceled by making small changes directly to the G-code. Finally, a simple case of a machining sequence producing a surface mismatch in the presence of particular machine deviations is used to illustrate the usefulness of the analytical tools presented. A graphical representation of the volumetric errors assists in understanding the impact of each error source for this particular application. The measurement results are compatible with the predicted volumetric error values and show an accuracy improvement of about 90 % after compensation.

Keywords: Volumetric error; Five-axis machine; Off-line compensation; G-code; Mismatch test

3.2 Introduction

Five-axis CNC machine tools are widely used to machine complex parts with high accuracy. On the other hand, the added complexity of these machines due, in part, to the rotary axes causes the machine to have potentially significant volumetric errors. The machine errors are often classified as geometric, thermal and force-induced errors [Schwenke et al., 2008]. Geometric error sources can be further separated in two subgroups, the intra-axis joint kinematic errors (positioning errors, straightness errors, etc.) and the inter-axis link geometric errors (or simply link errors such as out-of-squareness). These errors are then propagated to the tool tip using rigid body kinematics [Paul et al., 1981; Abbaszadeh-Mir et al., 2002]. The relative location of the tool frame and workpiece frame is commonly assumed as the volumetric error in actual five-axis [Srivastava et al., 1995] or lathe machine tools [Donmez et al., 1986].

Prediction, avoidance, and compensation of volumetric errors are actively sought. Early research work on error compensation techniques was reported by Koliskor [Koliskor, 1971] based on results from post-process inspection of a machined part and then, correcting the tool path trajectory for the subsequent parts. Direct tool path correction in Cartesian space is an approach applied by many researchers to compensate the volumetric error in multi-axis machine tools. Srivastava et al. [Srivastava et al., 1995], applied homogeneous transformation matrices (HTMs) for modeling the erroneous machine and calculated the volumetric error at the tool tip considering the time-varying geometric errors and thermal errors and then, compensated the tool path. Using the Denavit-Hartenberg [Denavit, 1955] modeling method, a numerical compensation algorithm was proposed by Rahman et al.[Mahbubur et al., 1997] where the nominal values of the rotary axes are derived from CL-data and then applied for correcting the tool path within the post-processor before generating the G-code. An automatic tool path correction was developed by Wang et al. [Wang et al., 2002] for static/quasi-static error compensation where a non-rigid body kinematics was assumed and the shape function theory used for mathematical modeling and error prediction in a three-axis machine tool. Three CCD cameras and a standard gage with evenly distributed holes were used by Wang et al. [Wang et al., 2013] in order to measure the axes positioning errors in a three-axis micro machine tool. The volumetric error in some points in the work space was calculated based on the measurement results and then a recursive compensation

method was applied to modify the machining trajectory (tool path) and improve the accuracy in the micro machine tool.

Uddin et al. [Uddin et al., 2009] corrected the erroneous tool path prior to the inverse kinematic conversion to G-code in five-axis machining of a cone frustum, as the case study (based on standard NAS979), to compensate the geometric errors. In a similar strategy, a recursive compensation method was applied by Khan et al. [Khan et al., 2011] in which the nominal tool path is obtained from CAD/CAM software and the actual path is calculated through kinematic equations considering error information. Then, the correction vector is computed from the difference between the actual and nominal paths and is used to correct the actual path until an assigned tolerance limit is satisfied.

Another compensation approach is to modify the axes position in real time through a digital I/O interface [Donmez et al., 1986]. Real-time compensation is an appropriate strategy especially when thermal errors are considered [Lo, 1994]. Lei and Hsu [Lei et al., 2003] assumed a linear relation between differential changes in machine joint coordinates and the workpiece Cartesian coordinates and used a nominal machine Jacobian matrix to calculate the correction vector and then conduct real-time compensation. Due to some limitations of the proposed method, such as singular points of the machine, Lei [Hsu et al., 2007] applied a two-step process (decouple method) assuming that the motion of only rotary axes can compensate the tool orientation error. This method first compensates the volumetric errors relevant to rotary axes and then, linear ones in real time.

G-code program modification after the post-processing step and before being loaded into the controller is another compensation approach. Jing et al. [Jing, 2006] and Lu et al. [Lu, 2011] proposed this method for compensating linear and circular interpolation movements for a three-axis machine tool. In this paper, first, the volumetric error is defined as deviation of the actual tool location in tool branch compared to the desired tool location in workpiece branch. An “exact model” formulation is presented, without any small angular error approximation, and then a formal definition of volumetric error is proposed to calculate the six volumetric error components. The workpiece is taken out of the loop since in practice, in the machine tool controller, it has neither relevance nor existence. This leads to the definition of a desired cutter location (DCL) defined in the last workpiece branch frame. This formulation of the volumetric

error solely relies on the axes commands extracted from the G-code which facilitates implementing the off-line compensation strategy. The compensation uses a local linearization of the actual erroneous kinematic model in the form of a Jacobian matrix as part of an iterative Gauss-Newton procedure to calculate exact small joint coordinate adjustment for the original G-code. Then, a new experimental procedure based on a surface mismatch producing machining test is described in which a one-dimensional slot machining sensitive to link geometric errors is machined. Finally, the results obtained on a HU40T CNC machine with a significant cross-axis distance error between its B and C rotary axes are presented.

3.3 Machine Modeling

A five-axis machine tool generally has three prismatic and two rotary joints or axes in two serial open kinematic branches from its foundation bed (Figure 3-1). One holds the workpiece, the other the tool. As an example, let us take a machine with a topology WCBXFZYSt.

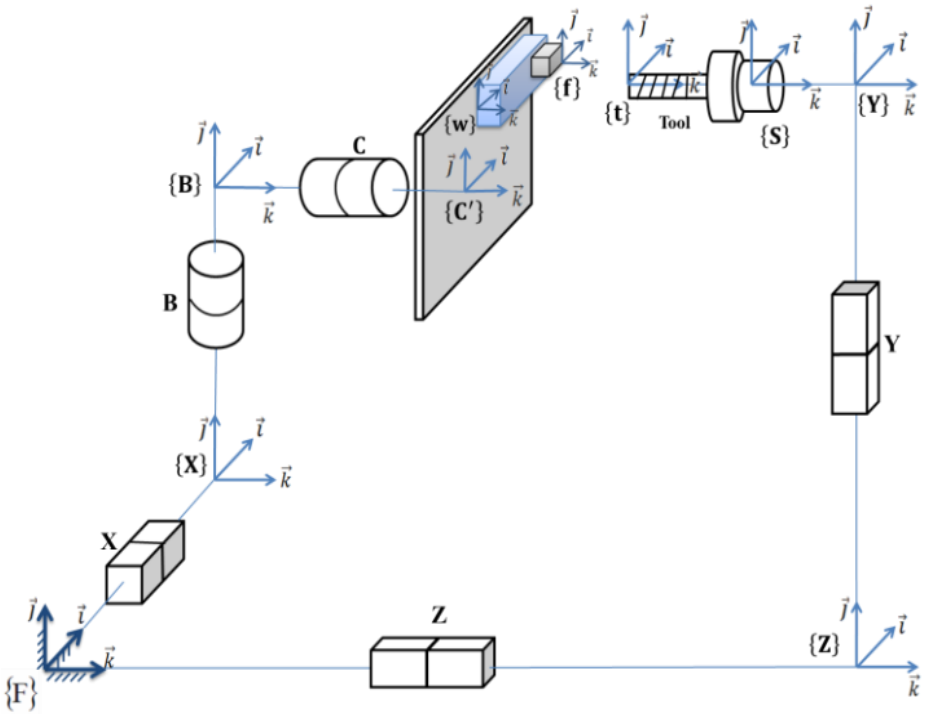

Figure 3-1 Five-axis machine tool (WCBXFZYSt) as a kinematic chain

Assuming a perfect machine, the nominal foundation frame origin {F} can be uniquely defined at the intersection point of the two rotary joints, B and C, with its $\hat{\imath}_F$, $\hat{\jmath}_F$ and $\hat{k}_F$ direction cosines parallel to the nominal X, Y and Z prismatic joints of the machine. Based on the rigid body

assumption, the tool and feature frame poses relative to the foundation frame for a perfect machine are calculated by multiplying the relevant homogeneous transformation matrices (HTMs) as follows:

$$ {}^{\mathrm{F}}T_{\mathrm{f}}^{\mathrm{nominal}} = {}^{\mathrm{F}}T_{\mathrm{X}}\ {}^{\mathrm{X}}T_{\mathrm{B}}\ {}^{\mathrm{B}}T_{\mathrm{C}}\ {}^{\mathrm{C}}T_{\mathrm{W}}\ {}^{\mathrm{W}}T_{\mathrm{f}} \tag{3-1} $$

$$ {}^{\mathrm{F}}T_{\mathrm{t}}^{\mathrm{nominal}} = {}^{\mathrm{F}}T_{\mathrm{Z}}\ {}^{\mathrm{Z}}T_{\mathrm{Y}}\ {}^{\mathrm{Y}}T_{\mathrm{S}}\ {}^{\mathrm{S}}T_{\mathrm{t}} \tag{3-2} $$

where indices $\mathrm{F, X, B, C, W, f, Z, Y, S}$ and t represent the foundation, X-joint, B-joint, C-joint, workpiece, feature, Z-joint, Y-joint, spindle and tool frames, respectively. Note that neither the links nor joint kinematic errors are considered in the perfect nominal machine model. Therefore, the tool versus feature location HTM, ${}^{\mathrm{f}}T_{\mathrm{t}}$ is given by:

$$ {}^{\mathrm{f}}T_{\mathrm{t}}^{\mathrm{nominal}} = \left({}^{\mathrm{F}}T_{\mathrm{f}}\right)^{-1}\ {}^{\mathrm{F}}T_{\mathrm{t}} \tag{3-3} $$

3.4 Definition of desired cutter location

A frame is added to the workpiece side of the kinematic chain, named desired cutter location (DCL). The DCL frame is attached to the feature frame and its HTM, ${}^{\mathrm{f}}T_{\mathrm{DCL}}$ represents the desired relative location of the tool and feature. Often, the DCL frame coincides with the feature frame during machining and therefore, ${}^{\mathrm{f}}T_{\mathrm{DCL}}$ is the identity matrix. However, in some machining operations, it may be different. For example, in milling of a curved surface with a bull-nose end tool, the tool orientation is not necessarily the same as the feature orientation. For a perfect machine ${}^{\mathrm{f}}T_{\mathrm{DCL}} \equiv {}^{\mathrm{f}}T_{\mathrm{t}}^{\mathrm{nominal}}$ and the HTM, ${}^{\mathrm{DCL}}T_{\mathrm{t}}^{\mathrm{nominal}}$ is a 4×4 identity matrix.

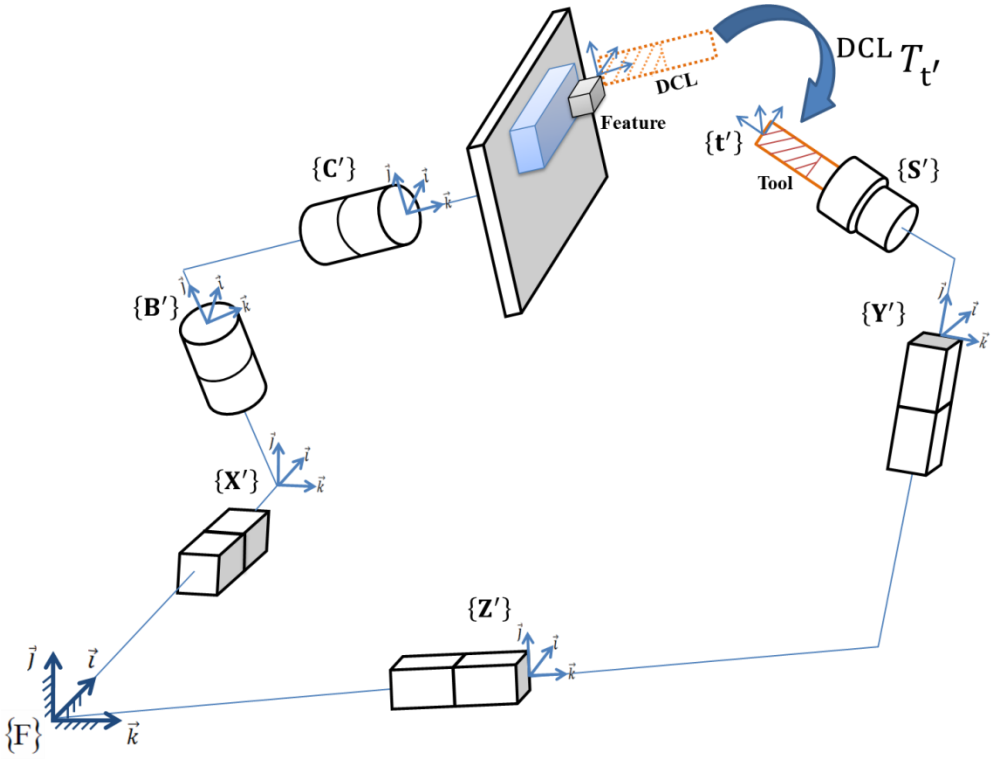

Figure 3-2 Volumetric error

Let us now consider the actual erroneous machine kinematic model illustrated in Figure 3-2 where the errors are exaggerated for a better understanding of the volumetric error definition. A geometrically erroneous machine tool (considering all possible link geometric errors, joint kinematic errors, workpiece setup errors, spindle misalignments and tool deviations) can be modeled as follows:

$$
{}^{F}T_{DCL}^{actual} =
$$

$$
{}^{F}T_{X_0}\,{}^{X_0}T_{X_0'}\,{}^{X_0'}T_{X}\;{}^{X}T_{X'}\;{}^{X'}T_{B_0}\,{}^{B_0}T_{B_0'}\,{}^{B_0'}T_{B}\;{}^{B}T_{B'}\;{}^{B'}T_{C_0}\;{}^{C_0}T_{C_0'}\,{}^{C_0'}T_{C}\;\;{}^{C}T_{C'}\,{}^{C'}T_{W}\,{}^{W}T_{W'}\,{}^{W'}T_{f}\;\;{}^{f}T_{DCL} \tag{3-4}
$$

$$
{}^{F}T_{t'}^{actual} = {}^{F}T_{Z_0}\,{}^{Z_0}T_{Z_0'}\,{}^{Z_0'}T_{Z}\;{}^{Z}T_{Z'}\,{}^{Z'}T_{Y_0}\,{}^{Y_0}T_{Y_0'}\,{}^{Y_0'}T_{Y}\,{}^{Y}T_{Y'}\,{}^{Y'}T_{S}\;{}^{S}T_{S'}\,{}^{S'}T_{t}\;\;{}^{t}T_{t'} \tag{3-5}
$$

and therefore,

$$
{}^{DCL}T_{t'}^{actual} = \left({}^{F}T_{DCL}^{actual}\right)^{-1}\;{}^{F}T_{t'}^{actual} \tag{3-6}
$$

where W, t, S, X_0 , Y_0 , Z_0 , B_0 and C_0 are the nominal joint frames, X_0', Y_0', Z_0', $B_0'$and C_0' are the actual joint frames before motion, X, Y, Z, B and C are the nominal motion frames assuming a joint has moved perfectly relative to its erroneous predecessor and, $W', t', S', X', Y', Z', B'$and C' are the actual frames of the moved joints accounting for the motion errors. Note that both the link geometric errors (such as the X-Z out-of-squareness, BOZ) and the joint kinematic errors (such as the X-direction out-of-straightness error of axis Z, EXZ) are included in this exact model. For example, for the Z-joint,

$$ {}^{F}T_{Z_0} = \begin{bmatrix} 1 & 0 & 0 & 0 \\ 0 & 1 & 0 & 0 \\ 0 & 0 & 1 & 0 \\ 0 & 0 & 0 & 1 \end{bmatrix} \tag{3-7} $$

$$ {}^{z_0}T_{Z_0'} = \begin{bmatrix} & R_{0y} & & 0 \\ & & & 0 \\ & & & 0 \\ 0 & 0 & 0 & 1 \end{bmatrix} \tag{3-8} $$

$$ {}^{z_0'}T_{Z} = \begin{bmatrix} 1 & 0 & 0 & 0 \\ 0 & 1 & 0 & 0 \\ 0 & 0 & 1 & Z \\ 0 & 0 & 0 & 1 \end{bmatrix} \tag{3-9} $$

$$ {}^{z}T_{Z'} = \begin{bmatrix} & & & EXZ \\ R_z & R_y & R_x & EYZ \\ & & & EZZ \\ 0 & 0 & 0 & 1 \end{bmatrix} \tag{3-10} $$

where R_{0y} is the rotation matrix associated with the angular axis location error of the Z link around local Y axis (EBOZ) and R_x, R_y and R_z are the rotation matrices associated with the angular errors of the Z motion (EAZ, EBZ, ECZ) around local axes. The error notation is based on [Schultschik, 1977] and [ISO230-1, 2012]. On the basis of the proposed structure which includes the DCL frame, the volumetric error matrix ${}^{DCL}T_{t'}^{actual}$ can be interpreted as the difference between the tool's nominal and actual poses (Figure 3-2). The three positional volumetric error components (E_{XV} , E_{YV} , E_{ZV}) and the three orientation volumetric error components (E_{AV}, E_{BV}, E_{CV}) can be extracted from this matrix:

${}^{DCL}T_{t'}{}^{actual} =$

$$\begin{bmatrix} \mathrm{C}\,E_{\mathrm{BV}}.\mathrm{C}\,E_{\mathrm{CV}} & \mathrm{C}\,E_{\mathrm{CV}}.\mathrm{S}\,E_{\mathrm{BV}}.\mathrm{S}\,E_{\mathrm{AV}} - \mathrm{S}\,E_{\mathrm{CV}}.\mathrm{C}\,E_{\mathrm{AV}} & \mathrm{C}\,E_{\mathrm{CV}}.\mathrm{S}\,E_{\mathrm{BV}}.\mathrm{C}\,E_{\mathrm{AV}} + \mathrm{S}\,E_{\mathrm{AV}}.\mathrm{S}\,E_{\mathrm{CV}} & E_{\mathrm{XV}} \\ \mathrm{C}\,E_{\mathrm{BV}}.\mathrm{S}\,E_{\mathrm{CV}} & \mathrm{S}\,E_{\mathrm{BV}}.\mathrm{S}\,E_{\mathrm{AV}}.\mathrm{S}\,E_{\mathrm{CV}} + \mathrm{C}\,E_{\mathrm{AV}}.\mathrm{C}\,E_{\mathrm{CV}} & \mathrm{C}\,E_{\mathrm{AV}}.\mathrm{S}\,E_{\mathrm{BV}}.\mathrm{S}\,E_{\mathrm{CV}} - \mathrm{S}\,E_{\mathrm{AV}}.\mathrm{C}\,E_{\mathrm{CV}} & E_{\mathrm{YV}} \\ -\mathrm{S}\,\mathrm{E}_{\mathrm{BV}} & \mathrm{C}\,E_{\mathrm{BV}}.\mathrm{S}\,E_{\mathrm{AV}} & \mathrm{C}\,E_{\mathrm{BV}}.\mathrm{C}\,E_{\mathrm{AV}} & E_{\mathrm{ZV}} \\ 0 & 0 & 0 & 1 \end{bmatrix} \tag{3-11}$$

where C and S represent cosine and sine, respectively. So, in the form of a twist,

$${}^{\{\mathrm{DCL}\},\mathrm{DCL}}\boldsymbol{\tau}^{\mathrm{V}}{}_{\mathrm{t}'} = [\,E_{\mathrm{XV}} \quad E_{\mathrm{YV}} \quad E_{\mathrm{ZV}} \quad E_{\mathrm{AV}} \quad E_{\mathrm{BV}} \quad E_{\mathrm{CV}}]^{\mathrm{T}} \tag{3-12}$$

Usually, machine errors are sufficiently small so that a small angular error assumption allows approximating Eq. 3-11 by

$${}^{\mathrm{DCL}}T_{\mathrm{t}'}{}^{\mathrm{actual}} = \begin{bmatrix} 1 & -E_{\mathrm{CV}} & E_{\mathrm{BV}} & E_{\mathrm{XV}} \\ E_{\mathrm{CV}} & 1 & -E_{\mathrm{AV}} & E_{\mathrm{YV}} \\ -E_{\mathrm{BV}} & E_{\mathrm{AV}} & 1 & E_{\mathrm{ZV}} \\ 0 & 0 & 0 & 1 \end{bmatrix} \tag{3-13}$$

which facilitates the extraction of the six volumetric error component twist. The volumetric error vector calculated using this definition, will be graphically shown for a particular case in the experimental verification section. This definition of volumetric error also helps to compute the "correction twist", (${}^{\mathrm{t}'}\boldsymbol{\tau}^{\mathrm{C}}{}_{\mathrm{DCL}}$), by extraction from the inverse of the volumetric error matrix:

$${}^{\mathrm{t}'}T_{\mathrm{DCL}} = ({}^{\mathrm{DCL}}T_{\mathrm{t}'})^{-1} \tag{3-14}$$

The correction twist contains the small variations in tool pose required to compensate the combined effect of all geometric errors and so bring the actual cutting tool (t') back at the desired location (DCL). For small errors, the correction twist can be approximated as:

$${}^{\{\mathrm{t}'\},\mathrm{t}'}\boldsymbol{\tau}^{\mathrm{C}}{}_{\mathrm{DCL}} \approx -{}^{\{\mathrm{DCL}\},\mathrm{DCL}}\boldsymbol{\tau}^{\mathrm{V}}{}_{\mathrm{t}'} \tag{3-15}$$

3.5 Error compensation

3.5.1 Compensation model

The Jacobian matrix, ${}^{\{\mathrm{t}'\},\mathrm{DCL}}J_{\mathrm{t}'}$, expresses the effect of small motions in axes (Δaxis) on the tool to DCL relative location [Paul et al., 1981; Abbaszadeh-Mir et al., 2002; Lei et al., 2003]:

$$^{\{t'\},DCL}\delta\tau_{t'}{}_{6\times1} = {}^{\{t'\},DCL}J_{t'}{}_{6\times5}\ \Delta\text{axis}_{5\times1} \tag{3-16}$$

where $^{\{t'\},DCL}\delta\tau_{t'}$ is the volumetric error twist as defined in the previous section that expressed in the actual tool frame. Eq. 3-16 can be solved for Δaxis by replacing the volumetric error twist with the correction error twist as follows:

$$\Delta\text{axis}_{5\times1} = \left({}^{\{t'\},DCL}J_{t'}{}_{6\times5}\right)^{\dagger}{}_{5\times6}.\left({}^{\{t'\},t'}\tau^{C}{}_{DCL}\right)_{6\times1} \tag{3-17}$$

Δaxis has five terms for a five-axis machines ($[\Delta x\ \Delta y\ \Delta z\ \Delta b\ \Delta c]^{T}$) and expresses the required adjustments in machine axes positions to produce the correction vector and so compensate the volumetric error. Since a linear system is assumed for the machine tool, an iterative approach (Gauss-Newton method) is applied to find a numerically exact solution for Δaxis when large machine errors are present. The calculated Δaxis, after the first iteration, is used for calculating the new volumetric error HTM and twist and then the second iteration is done to obtain the new value for Δaxis.

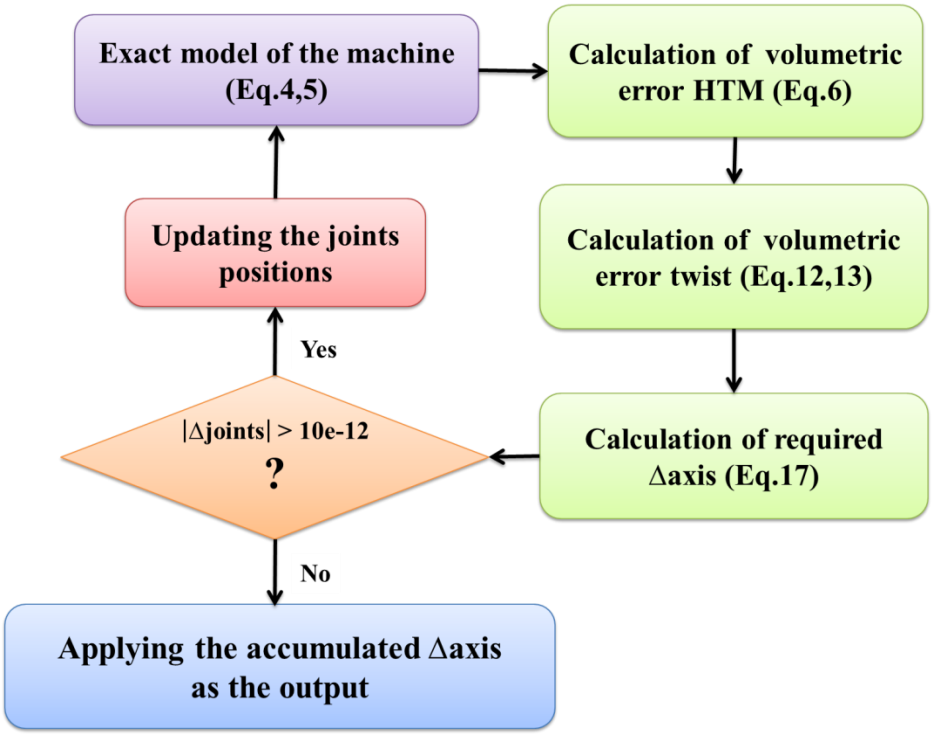

Figure 3-3 Gauss-Newton method for iteration

This cycle is repeated until the required Δaxis to cancel the remained volumetric error is negligible. The accumulated Δaxis at the end, is applied to modify the original G-code before loading to the machine (Figure 3-3).

3.5.2 Ephemeral G-code

An off-line scheme in now described in which the compensation is performed using an original G-code as input, so after post-processing, but before the CNC controller (Figure 3-4). It involves modifying the original G-code offline to produce an ephemeral (used once and then discarded) G-code. The original axes commands are explicit in the original G-code lines. These axes commands, tool length and the current machine geometric errors are used to compute the volumetric error matrix (${}^{\mathrm{DCL}}T_{t'}{}^{\mathrm{actual}}$) using Eq. 3-6 and then, the required Δaxis with Eq. 3-17.

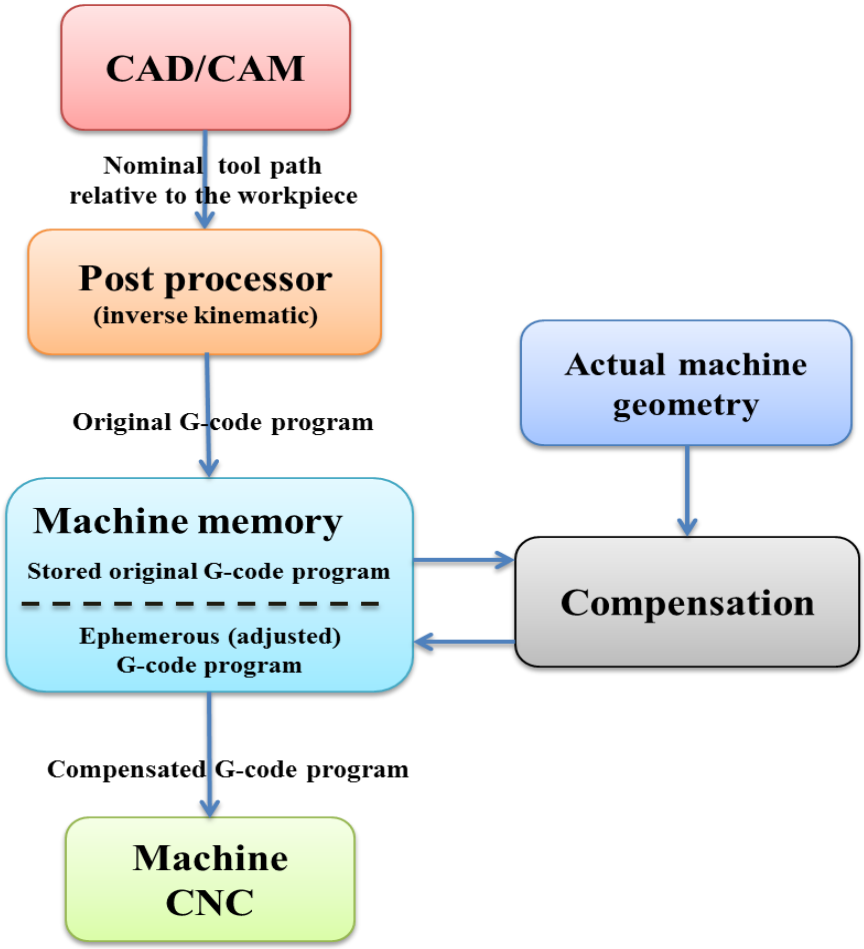

Figure 3-4 Error compensation strategy

3.6 Experimental verification

A simple test was performed to compare the machining accuracy before and after compensation. The idea is to machine each half of a slot using different indexations of the rotary axes. This causes a particular link error associated with rotary axes to produce a mismatch between the two halves. The test is designed to be particularly sensitive to the laboratory machine's significant BC cross-axis distance error (XOC) by causing a surface mismatch twice as big. A rectangular parallelipipedic aluminum part was selected as the workpiece and mounted on the table. The compensation aims at eliminating the "surface mismatch" error on the machined part.

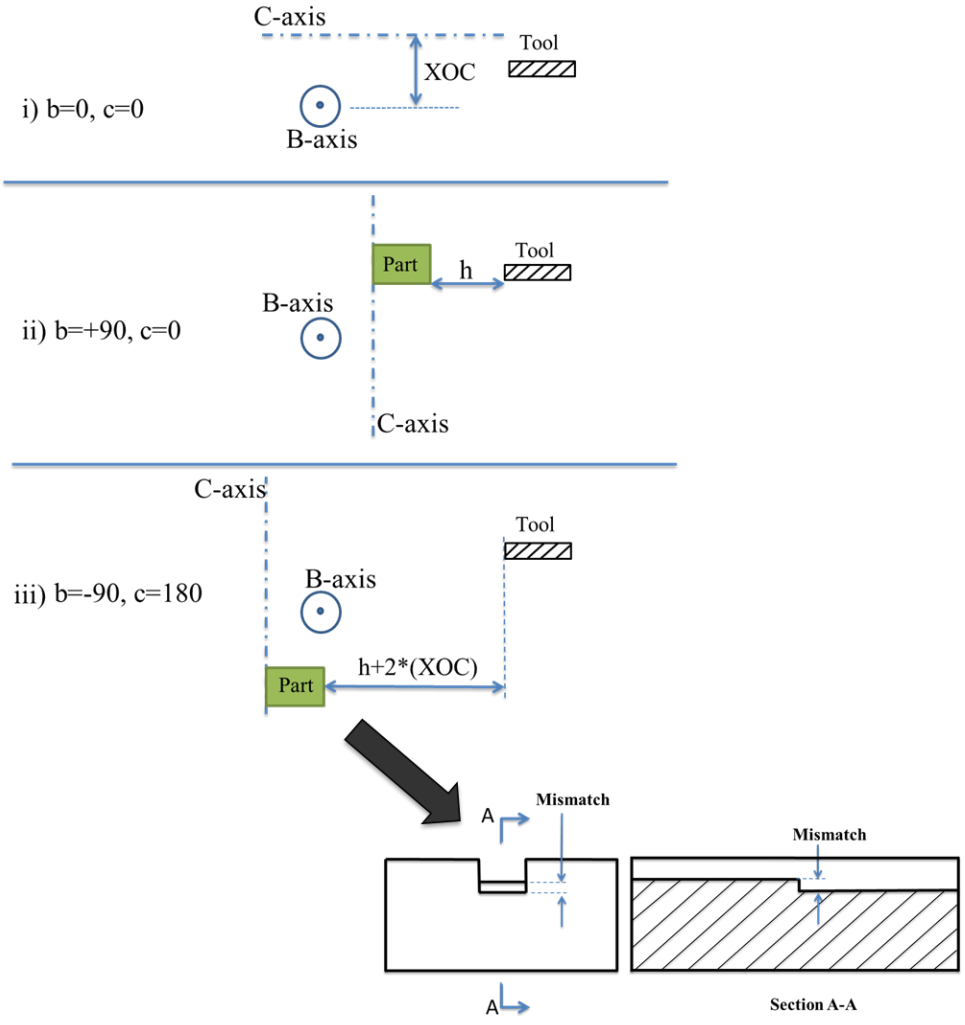

Figure 3-5 Top view of the machine tool, BC cross-axis distance error (XOC) causes a mismatch on the part when the same point is reached by the tool using two different rotary axes indexations.

Table 3-1 Test steps

Step	Title	Indexation	Compensation
1a	Machining one half of the first reference slot	B = 90º C = 0	No
1b	Machining the other half of the first reference slot	B = 90º C = 0	No
2	Machining one half of the uncompensated slot	B = 90º C = 0	No
3	Machining the other half of the uncompensated slot	B = -90 º C = 180 º	No
4	Machining one half of the compensated slot	B = 90 º C = 0	Yes
5	Machining the other half of the compensated slot	B = -90 º C =180 º	Yes
6a	Machining one half of the second reference slot	B = 90º C = 0	Yes
6b	Machining the other half of the second reference slot	B = 90º C = 0	Yes

Let us set the B-axis to 90º and the C-axis to 0º and the relative horizontal distance between tool tip and the part surface is h (Figure 3-5). If the Z-axis is kept fixed at the initial command and both B and C-axes rotate 180º (B=-90º and C=180º), the relative distance of the tool tip and the part should be the same (h) after rotations if there is no B-C distance error.

Any XOC error results in a "mismatch" which is easily measured with a comparator and also, can be felt to the touch. Spindle speed, tool length, tool diameter and depth of cut were set to 4000 rpm, 157.3 mm, 19.0 mm and 2.0 mm, respectively. The machining steps are summarized in Table 3-1 and Figure 3-6 and machining setup is shown in Figure 3-7.

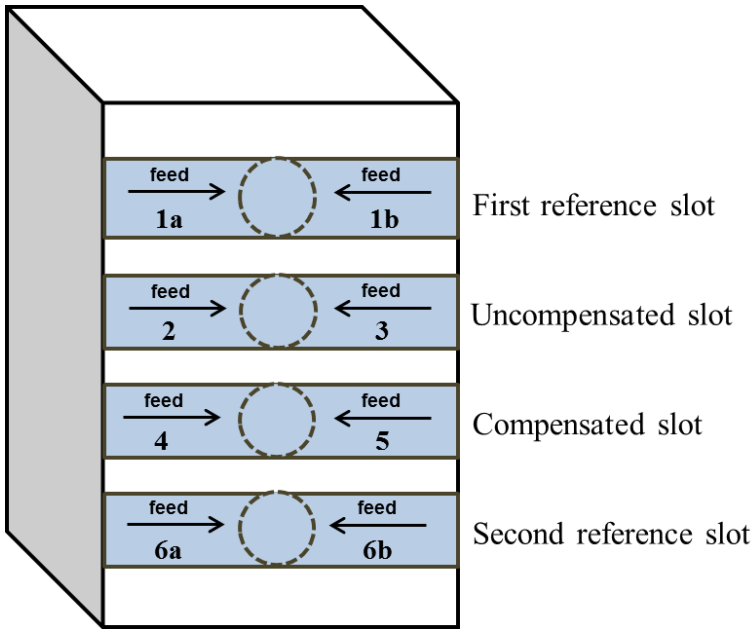

Figure 3-6 Test steps and machined slots according to Table 3-1

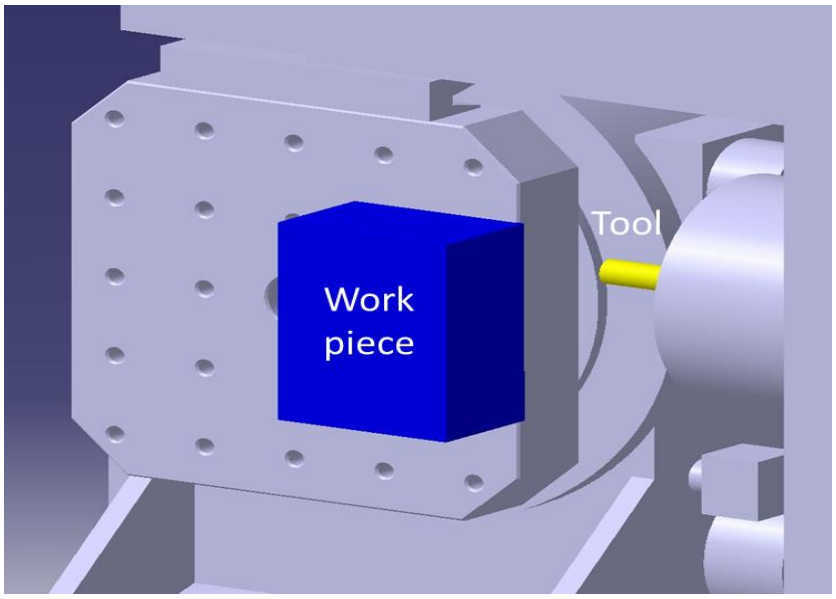

Figure 3-7 Machining setup

Four NC programs are used for the validation test. The first and last NC program codes produce a full reference slot before and after compensation, respectively, but without any rotary axes indexation changes, and therefore, no mismatch is expected. This validates that the process itself, does not generate a significant mismatch. The second program machines one half of the slot before and then the other half after indexation changes of the rotary axes. The mismatch between these two half slots is attributed to the link errors especially the most significant error, i.e. XOC in this case. The third program uses a compensated G-code. The original G-code (the second program) provides the input axes commands as the inputs of the compensation function. For this experiment, eight link errors, estimated using the SAMBA method [Mayer, 2012], are fed to the function while other sources of errors are neglected (Table 3-2).

Table 3-2 The machine link errors used to calculate the volumetric error and the compensation Jacobian

Error description	Symbol (μrad or μm)	First value	Second value
Out-of-squareness of the B-axis relative to the Z-axis	AOB	4	-1
Out-of-squareness of the B-axis relative to the X-axis	COB	-3	1
Distance between the B and C axis	XOC	-103	-102
Out-of-squareness of the C-axis relative to the B-axis	AOC	4	20
Out-of-squareness of the C-axis relative to the X-axis	BOC	23	4
Out-of-squareness of the Z-axis relative to the X-axis	BOZ	-30	-38
Out-of-squareness of the Y-axis relative to the Z-axis	AOY	1	24
Out-of-squareness of the Y-axis relative to the X-axis	COY	26	-9

The SAMBA test was repeated twice, at a few months interval providing two sets of link error values. The compensation validation was performed for both sets of link error values. In order to

achieve a better compensation, intermediate points are added along the slot and corrected. Table 3-3 illustrates the original and the ephemeral modified G-code program before and after compensation for the test with the first sets of link error values.

Table 3-3 Original G-code and compensated ephemeral G-code

Original G-code for the first slot's half (B=90 and C=0)	**Compensated ephemeral G-code for the first slot's half (B=90 and C=0)**
G54 G0 B90. C0.;	G54 G0 B90.00573 C0.;
X18.926 Y-15.;	X19.0228 Y-15.0157 ;
G43 Z261. H5;	G43 Z261. H5;
Z251.;	Z251.;
G94 G1 Z201. F1000.;	G94 G1 X19.0228 Y-15.0139 Z200.8985 B90.00573 C0. F1000.;
X-33.574;	X11.0968 Y-15.0139 Z200.8982 B90.00573 C0. F1000.;
Z251.;	X3.09680 Y-15.0139 Z200.8979 B90.00573 C0. F1000.;
G0 Z261.;	X-4.9032 Y-15.0139 Z200.8976 B90.00573 C0. F1000.;
	X-12.9032 Y-15.0140 Z200.8973 B90.00573 C0. F1000.;
	X-20.9032 Y-15.0140 Z200.8970 B90.00573 C0. F1000.;
	X-28.9032 Y-15.0140 Z200.8967 B90.00573 C0. F1000.;
	X-33.4772 Y-15.0140 Z200.8965 B90.00573 C0. F1000.;
	X-33.4772 Y-15.0136 Z250.8965 B90.00573 C0. F1000.;
	G94 G0 Z261.;

3.7 Results and discussion

As mentioned in section 3, the volumetric error HTM (${}^{\mathrm{DCL}}T_{\mathrm{t}'}{}^{\mathrm{actual}}$) can be predicted considering the second set of values for machine link errors in Table 3-2 and then the six volumetric error twist components can be extracted. The three positional components of the volumetric error form a vector in 3D workspace. Examples of such error vectors are shown in Figure 3-8 for some arbitrary positions in the workpiece table frame. The volumetric error vector at the test point located at the interaction of both halves of the machined slot is also shown in bold. Given the significant XOC error on the laboratory machine tool, the volumetric error vector is mainly in the z direction (mismatch depth direction) as expected. The vectors length and orientation look almost similar for each indexation since the rotary axes positions are the same for all these points.

However, because each point is reached using two different rotary axes indexations as explained in Table 3-1, the calculated components of the volumetric error may not be the same for the two indexations. The positional components values (in μm) of the volumetric error for the test point for the first and second indexations are (-4.8, 1.0, -98.9) and (-4.8, 0.5, 98.9) respectively. As illustrated in Figure 3-8, the E_{ZV} component of the volumetric error at each point has opposite direction for each indexation and so the effect of this error on the surface mismatch is expected to be doubled. For example, for the test point the predicted mismatch depth would be around $2 \times 98.9 = 198$ μm. The other error components in the x and y direction are negligible compared to this component. Note that the vector length is magnified to be observable compared to the working volume dimensions in Figure 3-8. Figure 3-9 shows the machined slots on the part mounted on the machine table. The part was later measured on a granite table where a comparator was used to measure the variation between the depths of the two halves of each slot (mismatch). The measurement results of both tests are shown in Table 3-4.

For the second test using the second set of link error values, for example, the reference slots had mismatches of around 5 μm which shows that the process itself causes an insignificant mismatch.

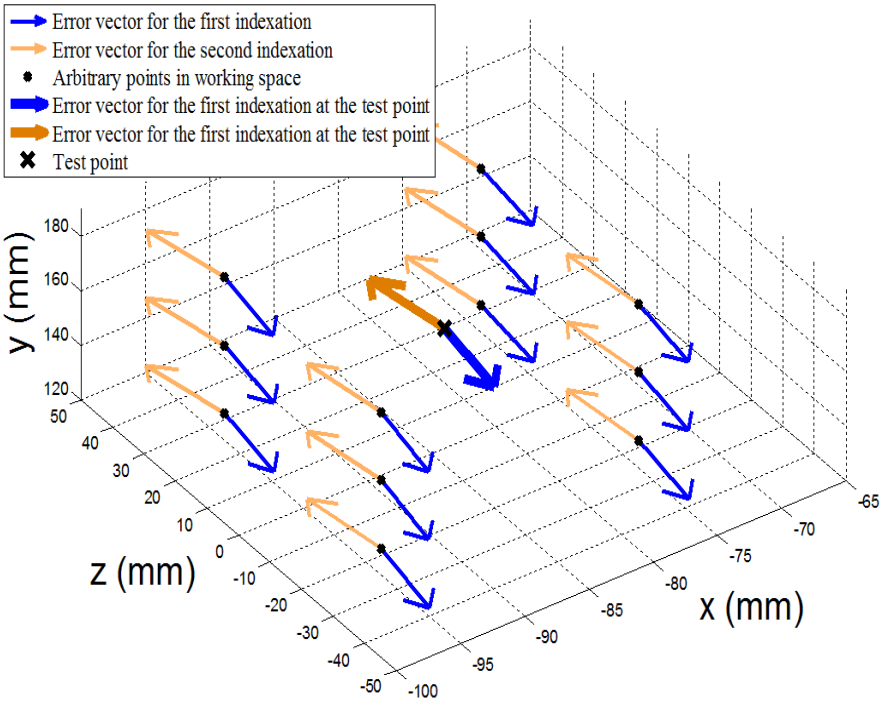

Figure 3-8 Volumetric error vector projected in the foundation frame, calculated at arbitrary working points and at the test point on the machined slot, magnified 200X.

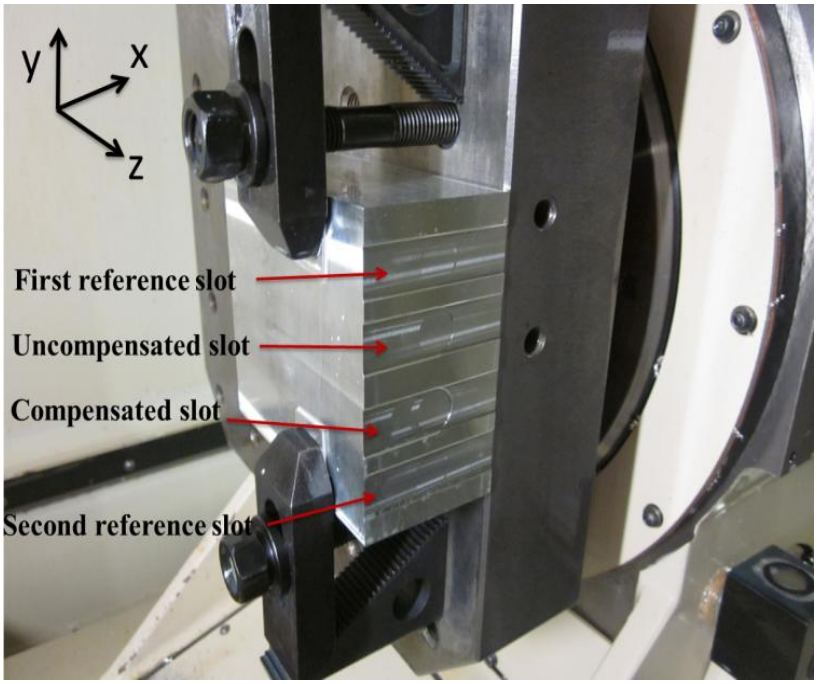

Figure 3-9 Machined slots for original and ephemeral G-code programs

Table 3-4 Measurement results

Mismatch measurement results	First test	Second test
The first reference slot (μm)	5	5
The second reference slot (μm)	5	5
Mismatch depth before compensation (μm)	220	210
Mismatch depth after compensation (μm)	20	25
Percentage of accuracy improvement (%)	91	88

Before compensation, there was a large mismatch of 210 μm, which is approximately $2 \times$ XOC, as expected. The small difference between the measured mismatch depth (in Table 3-4) and the predicted one (198 μm) may be due to other error sources of the machine tool such as thermal, force-induced and motion errors that were not taken into account for mismatch depth calculation. After compensation, a mismatch of 25 μm is measured for an 88% improvement.

3.8 Conclusion

Rigid body kinematics and HTMs are used to calculate the complete and general position and orientation components of the volumetric error of a five-axis machine tool in accordance with the proposed formulation based on the concept of desired cutter location in the workpiece branch. Then, joint coordinate corrections are obtained by iteratively solving a linear system of equations built around the locally linearized variational error model (Jacobian matrix) between small changes in machine joints (axes) coordinates and consequent differential changes in the machine volumetric error.

The compensation scheme requires, as input, the original G-code and the estimated machine geometric error parameters to produce a corrected ephemeral G-code that is executed by the machine and then discarded.

The capability of this compensation algorithm for a five-axis machine was verified for one-dimensional slots machining. The effect of the large cross-axis distance between the B and C axes (XOC) of the test machine, which was a source of significant mismatch, was compensated by around 90%.

3.9 Acknowledgements

The authors greatly appreciated the support of CNC machine technician, Guy Gironne, during the experimental validations. This research work was performed with the financial support of an NSERC-CANRIMT Strategic Network grant.

3.10 References

Abbaszadeh-Mir, Y., et al.; "Theory and simulation for the identification of the link geometric errors for a five-axis machine tool using a telescoping magnetic ball-bar." International Journal of Production Research 40(Compendex): 4781-4797, 2002.

Denavit, J.; "A kinematic notation for lower-pair mechanisms based on matrices." Trans. of the ASME. Journal of Applied Mechanics 22: 215-221, 1955.

Donmez, M. A., et al.; "A general methodology for machine tool accuracy enhancement by error compensation." Precision Engineering 8(4): 187-196, 1986.

Hsu, Y. Y., et al.; "A new compensation method for geometry errors of five-axis machine tools." International Journal of Machine Tools and Manufacture 47(2): 352-360, 2007.

ISO230-1; "Test code for machine tools-part 1 : geometric accuracy of machines operating under no-load or quasi-static conditions.", 2012.

Jing, H. J., Yao, Y. X., Chen, S. D., & Wang, X. P.; "Machining accuracy enhancement by modifying NC program." Advances in machining and manufacturing technology eighth: 71-75, 2006.

Khan, A., et al.; "A methodology for systematic geometric error compensation in five-axis machine tools." The International Journal of Advanced Manufacturing Technology 53(5): 615-628, 2011.

Koliskor, A.; "Compensating for automatic-cycle machining errors." Machines and Tooling 5(41(1)): 1–14, 1971.

Lei, W. T., et al.; "Accuracy enhancement of five-axis CNC machines through real-time error compensation." International Journal of Machine Tools and Manufacture 43(9): 871-877, 2003.

Lu, Y., Li, J.G., Gao, D., Zhou, F.; "Reconstructing NC program-based geometrical error compensation for heavy-duty NC machine tool." Advanced Materials Research 314: 2082-2086, 2011.

Mahbubur, R. M. D., et al.; "Positioning accuracy improvement in five-axis milling by post processing." International Journal of Machine Tools and Manufacture 37(2): 223-236, 1997.

Mayer, J. R. R.; "Five-axis machine tool calibration by probing a scale enriched reconfigurable uncalibrated master balls artefact." CIRP Annals - Manufacturing Technology 61(1): 515-518, 2012.

Paul, R. P., et al.; "Differential kinematic control equations for simple manipulators." Systems, Man and Cybernetics, IEEE Transactions 11(6): 456-460, 1981.

Schultschik, R.; "The components of the volumetric accuracy." Annals of CIRP 25, No.1: 223-227, 1977.

Schwenke, H., et al.; "Geometric error measurement and compensation of machines—an update." CIRP Annals - Manufacturing Technology 57(2): 660-675, 2008.

Srivastava, A. K., et al.; "Modelling geometric and thermal errors in a five-axis cnc machine tool." International Journal of Machine Tools and Manufacture 35(9): 1321-1337, 1995.

Uddin, M. S., et al.; "Prediction and compensation of machining geometric errors of five-axis machining centers with kinematic errors." Precision Engineering 33(2): 194-201, 2009.

Wang, S.-M. and J.-J. Lin (2013); "On-machine volumetric-error measurement and compensation methods for micro machine tools." *International Journal of Precision Engineering and Manufacturing* 14(6): 989-994.

Wang, S.-M., Y.-L. Liu and Y. Kang (2002); "An efficient error compensation system for CNC multi-axis machines." *International Journal of Machine Tools and Manufacture* 42(11): 1235-1245.

CHAPTER 4 ARTICLE 2: VALIDATION OF VOLUMETRIC ERROR COMPENSATION FOR A FIVE-AXIS MACHINE USING SURFACE MISMATCH PRODUCING TESTS AND ON-MACHINE TOUCH PROBING

Mehrdad Givi [1] and J.R.R Mayer [1]

[1] *Mechanical Engineering Department, Polytechnique Montréal, P.O. Box 6079, Station Downtown, Montréal (Qc), Canada, H3C 3A7*

*Based on the paper published in the International Journal of Machine Tools and Manufacture, 87(0): 89-95, 2014

4.1 Abstract

In order to validate volumetric error compensation methods for five-axis machine tools, the machining of test parts have been proposed. For such tests, a coordinate measuring machine (CMM) or other external measurement, outside of the machine tool, are required to measure the accuracy of the machined part. In this paper, a series of machining tests are proposed to validate a compensation strategy and compare the machining accuracy before and after the compensation using only on-machine measurements. The basis of the tests is to machine slots, each completed using two different rotary axes indexations of the CNC machine tool. Using directional derivatives of the volumetric errors, it is possible to verify that a surface mismatch is produced between the two halves of the same slot in the presence of specific machine geometric errors. The mismatch at the both sides of the slot, which materialize the machine volumetric errors are measured using touch probing by the erroneous machine itself and with high accuracy since the measurement of both slot halves can be conducted using a single set of rotary axes indexation and in a volumetric region of a few millimetres. The effect of a compensation strategy is then validated by comparing the surface mismatch value for compensated and uncompensated slots. A compensation effectiveness of about 65% to 99 % was observed using the proposed strategy.

Keywords: Error compensation validation, surface mismatch, on-machine probing, five-axis machining

4.2 Literature review

A number of error compensation strategies have been proposed to increase the accuracy of industrial parts machined by five-axis machine tools [Donmez et al., 1986; Mahbubur et al., 1997; Wang et al., 2002]. Compensation efficiency must be verified experimentally. To do so, the geometric accuracy of a machined part, before and after the implementation of the compensation, can be measured using coordinate measuring machine (CMM) and then compared. Different workpieces have been used as case studies for such purpose. Semi-spherical surfaces [Lei et al., 2003], a cone frustum as described in standard NAS979 [Uddin et al., 2009] and two-dimensional contouring path [Zhu et al., 2012] were proposed. In ISO10791-1 [ISO10791-7, 1998] a composite test piece in which there are some features (central hole, square, diamond, circle, sloping faces and bored holes) is introduced for accuracy check in five-axis machining centres. In the same standard, a cone frustum and a truncated square pyramid are also proposed. The machining setup and stipulations of these two artefacts were discussed and then the measurement results of the finished parts were compared in [S.P. Moylan, 2011]. Khan et al. [Khan et al., 2011] machined a standard workpiece with additional features like step portions, circle, diamond and cylindrical parts and also, a spherical surface to verify the compensation method effectiveness for different geometric errors. In all of the above mentioned cases, a CMM was used to inspect the machined part to compare the uncompensated and compensated part dimensions against the desired geometry. This approach requires an accurate CMM, additional setups and part handling.

Takeshima et al. [Takeshima, 2009] mounted an LVDT sensor on the machine tool for measuring purpose. They proposed a cubic box (containing a square hole) whose inside and outside surfaces were machined using a ball-end mill and simultaneous five-axis motion and then, measured the squareness, flatness and dimensions of the flat surfaces using only linear axes machine motion.

On-machine measurement (OMM) was used to verify the five-axis machining where a semi-sphere was machined with and without tool path compensation and then, measured with a touch probe [Jung et al., 2006]. However, the OMM accuracy needed to be compensated based on mathematical model of the machine and some diagonal measurements before the machining process.

Ibaraki et al. [Ibaraki et al., 2010] proposed a series of simple machining patterns to identify the kinematic errors associated with rotary axes in five-axis machine tools. The geometric errors of the workpiece are measured using a CMM and then, the sensitivity of the machined part geometry to the above mentioned kinematic errors is analysed. Although, the proposed method was applied solely for error identification, it illustrates the use of multiple axes indexations to produce related part surfaces and doing so materialize the machine volumetric errors.

In this paper, two-dimensional geometric features are milled, each using two different rotary axes indexation sets. Due to the machine geometric errors, a surface mismatch may appear in each feature that helps to verify the machine volumetric accuracy. In total, seven machining patterns are proposed to check the overall accuracy of the machine tool after compensation. There is no need for independent measurement device like a CMM as the validation process can be done using a touch probe and OMM immediately after machining. The OMM is accurate enough and does not need to be compensated since, in this case, the measurement is done in a small volume and using a single linear axis motion and in the same direction for each slot. The paper begins by presenting the mathematical model of the machine and the effect of the geometric errors using a sensitivity Jacobian in section 2. Then, in section 3, the surface mismatch concept and the proposed machining patterns are described while section 4 details the machining procedure. This is followed by a sensitivity analysis of each machined pattern to the machine link geometric errors in section 5. Section 6 presents the results followed by a discussion and conclusion in sections 7 and 8.

4.3 Machine modeling

A five-axis machine tool is modelled as an open kinematic chain made of prismatic and rotary joints as shown in Figure 4-1. Assuming a perfect machine, the nominal foundation frame {F} can be located at the intersection point of the two rotary axes (B and C) with its $\hat{\imath}_F$, $\hat{\jmath}_F$ and $\hat{k}_F$ directions cosines parallel to the nominal X-, Y- and Z-axis of the machine. Assuming rigid body kinematics, homogenous transformation matrices (HTMs) can be applied to model the five-axis machine tool. On a real machine, geometric errors occur as link error affecting the position and orientation of each axis with respect to its predecessor in the chain. So, for example, the z-axis

HTM, ${}^{\mathrm{F}}T_{\mathrm{Z}}$ can be decomposed as a nominal link ${}^{\mathrm{F}}T_{\mathrm{Z_0}}$, a link error ${}^{\mathrm{Z_0}}T_{\mathrm{Z_0}'}$, and a nominal motion ${}^{\mathrm{Z_0}'}T_{\mathrm{Z}}$, so that

$$ {}^{\mathrm{F}}T_{\mathrm{Z}} = {}^{\mathrm{F}}T_{\mathrm{Z_0}}\,{}^{\mathrm{Z_0}}T_{\mathrm{Z_0}'}\,{}^{\mathrm{Z_0}'}T_{\mathrm{Z}} . \tag{4-1} $$

where F is the foundation frame, $\mathrm{Z_0}$ is the nominal joint frame, $\mathrm{Z_0}'$ is the actual joint frame before motion and Z is the joint frame after nominal motion.

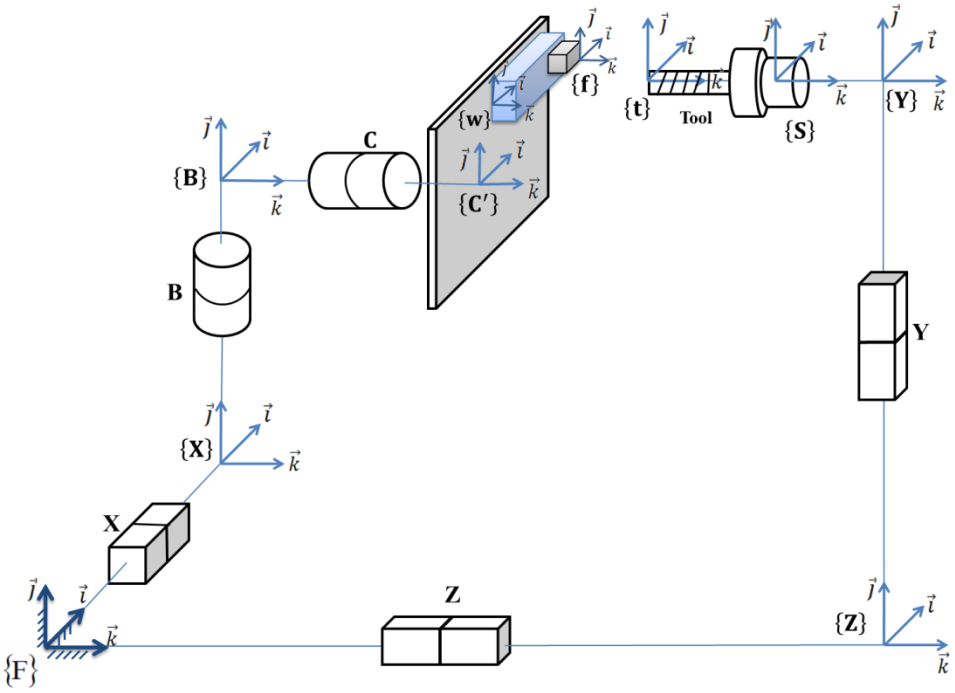

Figure 4-1 Five-axis machine tool (WCBXFZYSt) as a kinematic chain

Assuming small errors, a small angle approximation ($\sin\theta \approx \theta$, $\cos\theta \approx 1$) is used and a linear relationship results between small changes in machine link errors and the consequent variations in feature-tool relative location. A nominal Jacobian matrix is generated that expresses the effect of the link geometric errors ($\boldsymbol{E}_{\mathrm{p}}$) on differential changes in volumetric errors at the tool tip relative to feature frame projected in the tool frame [Paul et al., 1981; Abbaszadeh-Mir et al., 2002]:

$$ {}^{\{t\},f}\boldsymbol{E}_{\mathbf{v_t}} = {}^{\{t\},f}J_{\,t}\;\boldsymbol{E}_{\mathrm{p}} \tag{4-2} $$

where ${}^{\{t\},f}\boldsymbol{E}_{\mathbf{V}_t}$ is the 6×1 volumetric error twist of the tool (subscript t) relative to the feature (f) expressed in tool frame, {t}, and has six error components, $[\,E_{XV}\;\; E_{YV}\;\; E_{ZV}\;\; E_{AV}\;\; E_{BV}\;\; E_{CV}]^T$.

According to Abbaszadeh-Mir et al. [Abbaszadeh-Mir et al., 2002] and ISO-231 standard [ISO230-1, 2012], only eight machine error parameters are sufficient to fully characterize a five-axis machine tool link errors. So, in this research, only these eight components are considered:

$$\boldsymbol{E}_p = [E_{AOB}\;\; E_{COB}\;\; E_{XOC}\;\; E_{AOC}\;\; E_{BOC}\;\; E_{BOZ}\;\; E_{AOY}\;\; E_{COY}]^T \tag{4-3}$$

The error notations are based on ISO230-1 [ISO230-1, 2012].

4.4 Surface mismatch concept

If one specific machining point in the workpiece space can be reached using two different rotary axes indexations, there exist two different Jacobian matrices, one for each configuration. The idea of the surface mismatch producing tests is to machine a linear slot in two steps. In each step, one half of the slot is completed using a distinct rotary axes indexation set. For the perfect machine, there is no mismatch between the machined halves of the slot. In the actual machine, a depth lateral surface mismatch may appear caused by the machine errors (see Figure 4-2).

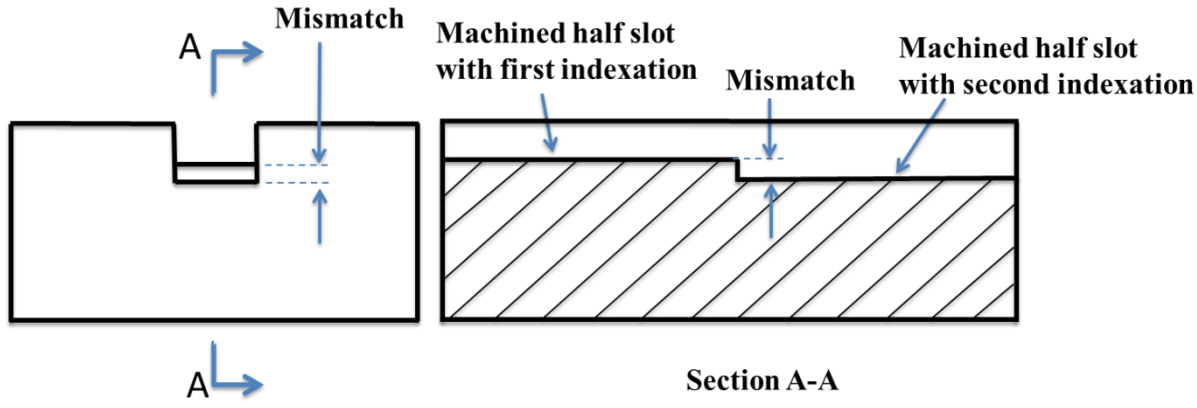

Figure 4-2 Depth mismatch between two halves of the machined slot

This can be mathematically explained based on the Jacobian matrix. To study the effect of the errors on a mismatch produced in the feature frame, the Jacobian matrix is projected in the

feature frame to yield the directional derivatives of the volumetric error along the $\hat{\imath}$, $\hat{\jmath}$ and $\hat{k}$ axes of the slot feature frame {f} as a set of the machine link errors ${}^{\{f\},f}\Delta J_t$. Let us assume the Jacobian matrix at the two halve slots meeting point for one set of indexation is J_1 and the Jacobian matrix at the same point but, for the other half of the slot, reached using a different rotary axes indexation set, is J_2 .Then, the differential directional Jacobian which models the two halves of the same slot is calculated as follows:

$$ {}^{\{f\},f}\Delta J_t = {}^{f}H_t \cdot ({}^{\{t\},f}J_{2_t} - {}^{\{t\},f}J_{1_t}) \tag{4-4} $$

where ${}^{f}H_t$ is a projection matrix (6×6) projecting the Jacobian from tool to feature frame so that the effect on the slot feature can be readily quantified. The first three lines of the Jacobian relate to the translational volumetric errors and the last three lines of the Jacobian relate to the angular volumetric errors. The translational and angular sets are projected separately so the projection matrix takes the form of Eq. 4-5:

$$ {}^{f}H_t = \begin{bmatrix} R_{3\times3} & 0 \\ 0 & R_{3\times3} \end{bmatrix} \tag{4-5} $$

where

$$ R_{3\times3} = \begin{bmatrix} {}^{t}\hat{\imath}_f^T \\ {}^{t}\hat{\jmath}_f^T \\ {}^{t}\hat{k}_f^T \end{bmatrix} \tag{4-6} $$

where, ${}^{t}\hat{\imath}_f$, ${}^{t}\hat{\jmath}_f$ and ${}^{t}\hat{k}_f$ are the slot frame unit vectors projected in the tool frame. Using Eq. 4-2 and substituting J with ΔJ, it becomes possible to predict the volumetric error twist during the machining of the slot halves:

$$ {}^{\{f\},f}\boldsymbol{\delta E}_{\mathbf{v}_t} = {}^{\{f\},f}\Delta J_t \ \boldsymbol{E}_p \tag{4-7} $$

where ${}^{\{f\},f}\boldsymbol{\delta E}_{\mathbf{v}_t}$ is the differential volumetric error twist, $[\,\delta E_{XV} \ \ \delta E_{YV} \ \ \delta E_{ZV} \ \ \delta E_{AV} \ \ \delta E_{BV} \ \ \delta E_{CV}]^T$, expressed in feature frame with for example, δE_{ZV}, the depth mismatch between the two slots halves. The other error components in the feature frame are as illustrated in Figure 4-3.

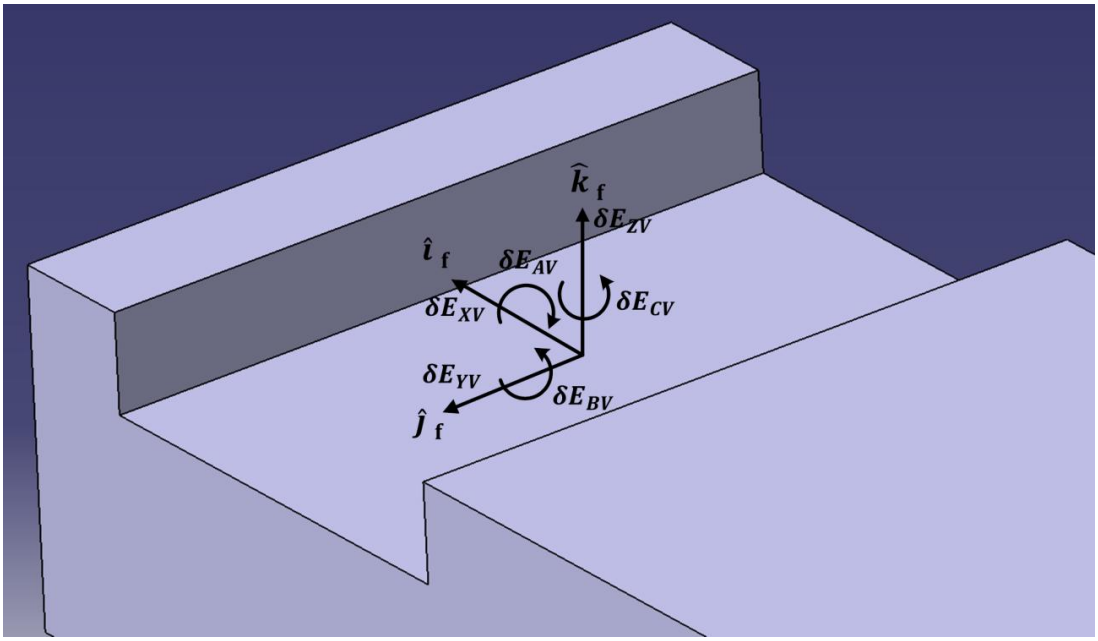

Figure 4-3 Coordinate system and error components on the machined slot

Therefore, a machining process can be mathematically shown to be mismatch producing in the presence of machine tool geometric errors and then selected and used for validating a compensation strategy.

Although it is believed that the mismatch producing test can be used to validate any compensation strategy, in this research, a G-code modification method is applied for volumetric error compensation in a five-axis machine tool. In this strategy, first, the original axes commands (that are explicit in the original G-code lines), tool length and the current machine geometric errors are used as inputs to compute the volumetric error twist using Eq. 4-7. Then, the required adjustments in the original axes positions to cancel the volumetric error are calculated assuming a local linearization of the erroneous kinematic model. A Jacobian matrix mathematically relates the differential changes in volumetric error at the tool tip (E_V) and the small changes in machine axes positions (Δaxis) as shown in Eq. 4-8 [Lei et al., 2003] :

$$\boldsymbol{E}_{\mathbf{V}} = J \,.\, \Delta\text{axis} \qquad (4\text{-}8)$$

So, an ephemeral G-code is generated substituting the adjusted axes commands for the original ones.

4.5 Machining procedure

Seven machining patterns are proposed. In each machining pattern, as illustrated in Figure 4-4, two halves of three slots are machined; Slot R) reference slot without any change in rotary axes positions, slot U) uncompensated slot, and slot C) compensated slot using modified G-code.

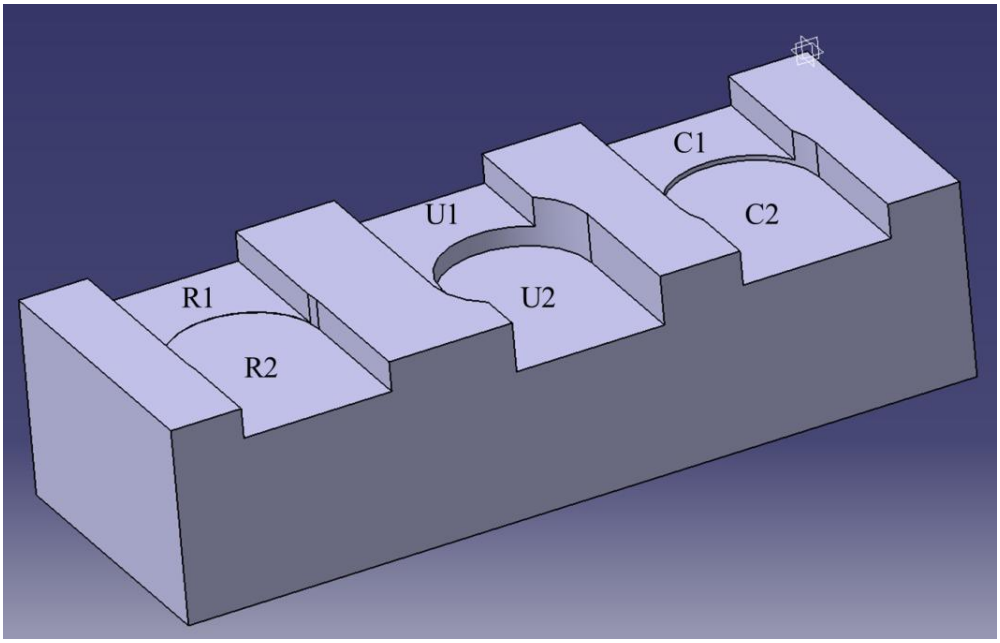

Figure 4-4 Reference (R), uncompensated (U) and compensated (C) machined slots in each pattern

Table 4-1 lists the proposed seven machining patterns illustrated in Figure 4-5. For machining patterns 1 to 5, slots are machined using a flat end-mill cutter tool. The slots are wide enough to allow touch probing both its bottom and side surfaces. In order to minimize the effect of the forced induced errors, the machining of each slot is done in two steps. The slots are rough machined using an end-mill with diameter 7.938 mm and then, the mentioned procedure for patterns is applied only for the finishing pass using a tool with diameter 9.525 mm. Spindle speed, tool length, and depth of cut (for finishing step) are 5000 rpm, 137.9 mm and 0.8 mm, respectively.

For patterns 6 and 7 a flank mill with diameter 9.525 mm is used for one-step flank milling process with the machine Y-axis motion. In these cases, the mismatch depth is measured in only

one direction (E_{ZV}). Spindle speed, tool length, and depth of cut are 5000 rpm, 212.48 mm and 1.00 mm, respectively.

Table 4-1 Applied rotary axes indexations for machining patterns

Pattern number	B- and C-axis indexation			
	First half of the slot (step 1)		Second half of the slot (step 2)	
	B	C	b	C
1	-90	-45	90	135
2	-45	-45	45	135
3	-90	0	90	180
4	-45	0	45	180
5	-90	-90	90	90
6	-90	0	-90	180
7	-90	0	90	0

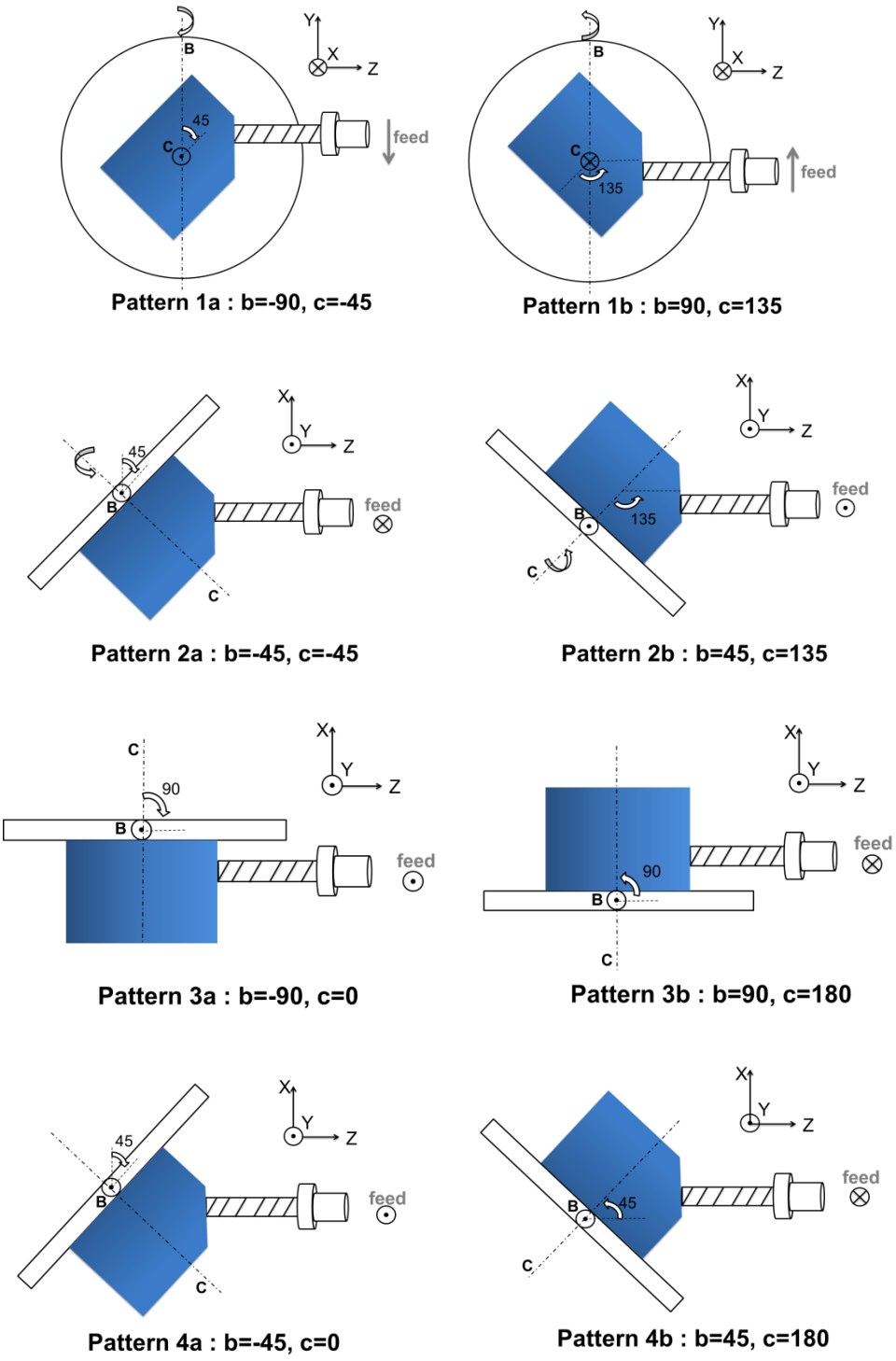

Figure 4-5 Proposed patterns for machining the slots

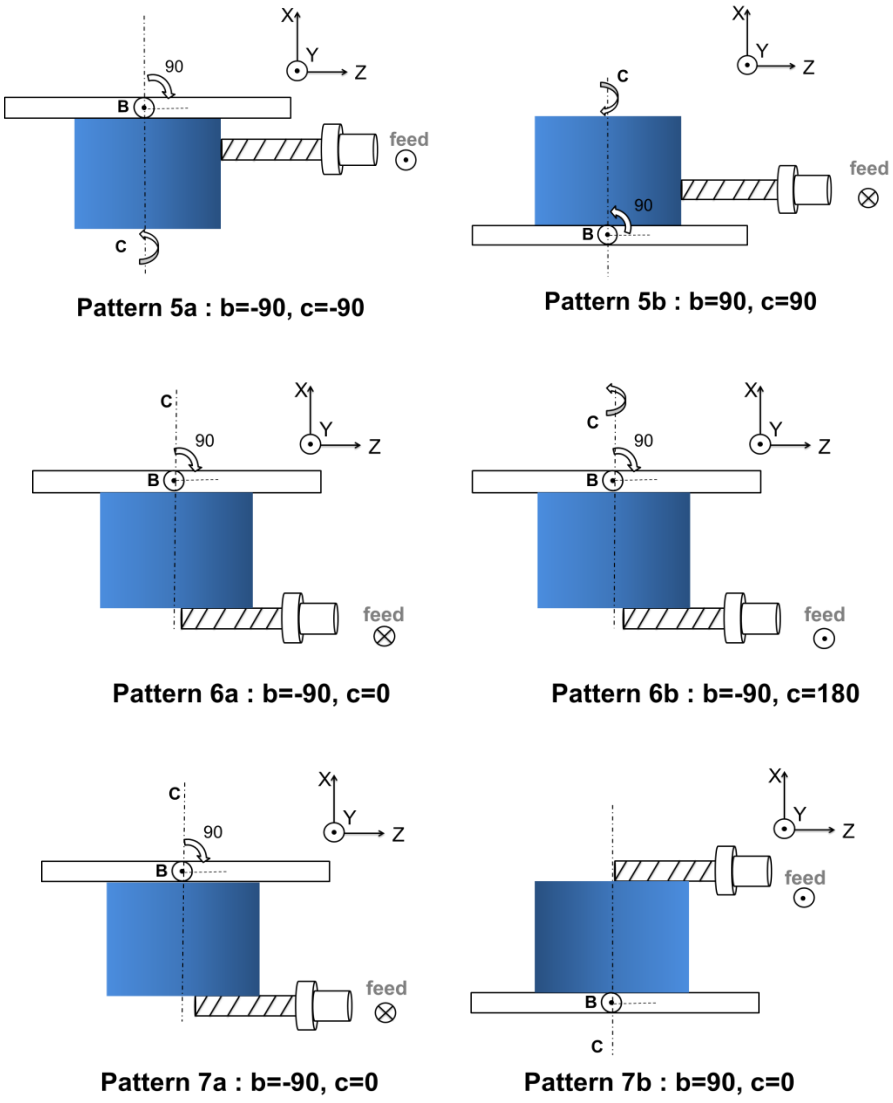

Figure 4-5 (cont.) Proposed patterns for machining the slots

An aluminium pre-machined part provides the required planes to perform the machining patterns (Figure 4-6).

A numerical solid model of the nominal workpiece after performing the seven machining patterns is shown in Figure 4-7. The labels indicate the two machining steps of the compensated slot in each pattern.Figure 4-8 illustrates the machined workpiece on the machine table.

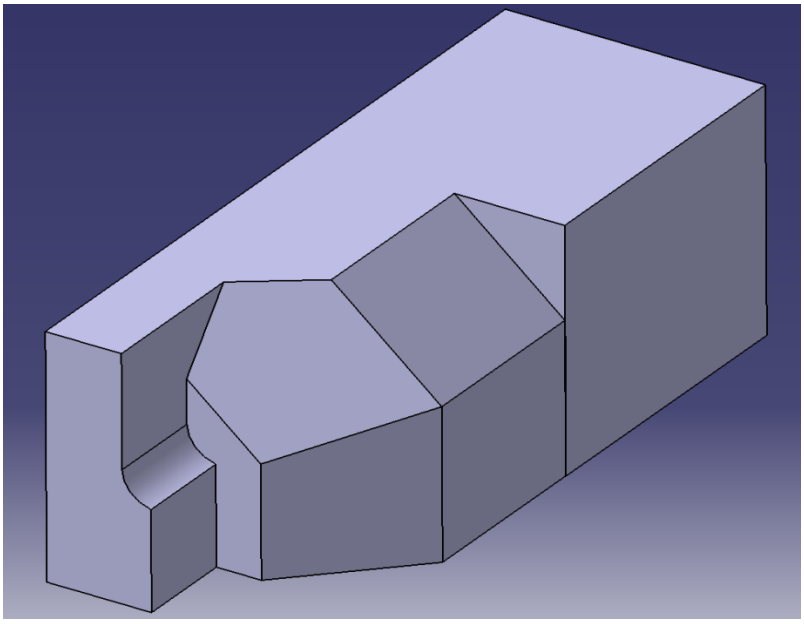

Figure 4-6 Workpiece with pre-machined planes

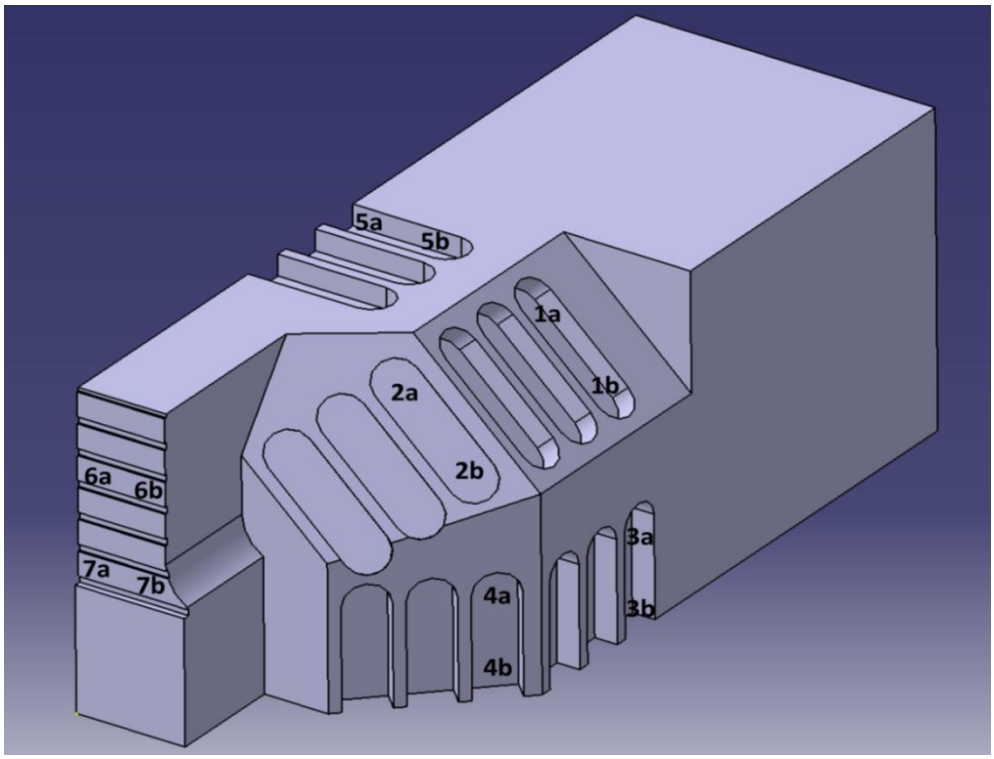

Figure 4-7 Numerical solid model of the nominal machined workpiece

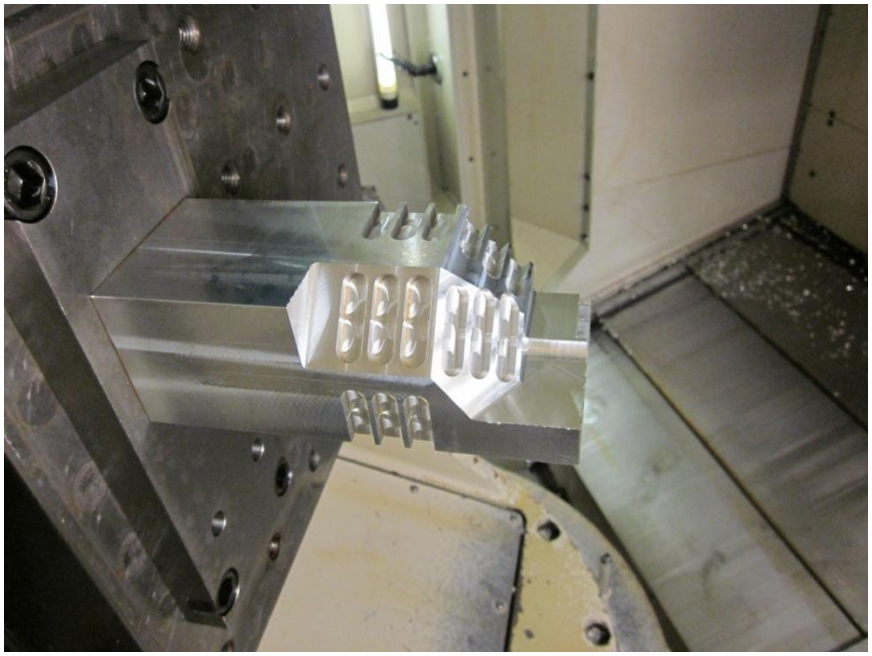

Figure 4-8 Machined workpiece on the machine table

4.6 Sensitivity analysis to link errors

In order to assess the sensitivity of the surface mismatch to the machine link errors, the differential directional Jacobian matrix of tool to feature volumetric error expressed in feature frame, ${}^{\{f\},f}\Delta J_t$, is calculated for each pattern using Eq. 4-4. As a numerical example, the calculation of differential Jacobian matrix for pattern 3 is as below:

$$\left({}^{\{f\},f}\Delta J_t\right)_{p3} = \begin{bmatrix} -0.0023 & -97.1715 & 0 & 97.1715 & 108.0371 & -107.93 & -0.0044 & 97.17 \\ -20.5148 & -121.729 & 0 & 121.7295 & 0 & 0.0005 & 215.9492 & 0.0016 \\ 97.1693 & -0.0004 & 1 & 0 & 121.7295 & -0.001 & -97.1717 & -0.001 \\ -1 & 0 & 0 & 0 & 0 & 0 & 1 & 0 \\ 0 & 0 & 0 & 0 & -1 & 1 & 0.0001 & 0 \\ 0 & -1 & 0 & 1 & 0 & 0 & 0 & 1 \end{bmatrix}$$

$$- \begin{bmatrix} 0.0023 & 93.1654 & 0 & 93.1654 & 107.8229 & -107.93 & -0.0103 & -93.17 \\ -107.931 & 121.7354 & 0 & 121.7349 & 0 & -0.0033 & 215.9507 & -0.0048 \\ 93.1676 & 0.0004 & -1 & 0 & -121.735 & 0.003 & 93.1683 & 0.0009 \\ -1 & 0 & 0 & 0 & 0 & 0 & 1 & 0 \\ 0 & 0 & 0 & 0 & -1 & 1 & 0.0001 & 0 \\ 0 & -1 & 0 & -1 & 0 & 0 & 0 & 1 \end{bmatrix}$$

$$= \begin{bmatrix} -0.046 & -190.3368 & 0 & 4.0061 & 0.2142 & 0 & 0.0059 & 190.34 \\ 0.0015 & -243.4644 & 0 & -0.0054 & 0 & 0.0038 & -0.015 & 0.0064 \\ 190.3368 & -0.0008 & 2 & 0 & 243.4644 & -0.004 & -190.34 & -0.0019 \\ 0 & 0 & 0 & 0 & 0 & 0 & 0 & 0 \\ 0 & 0 & 0 & 0 & 0 & 0 & 0 & 0 \\ 0 & 0 & 0 & 2 & 0 & 0 & 0 & 0 \end{bmatrix}$$

where the columns correspond to the link errors as in Table 4-2, with the same units, and the rows correspond to the translational and then rotational volumetric error twist components as previously described. Then, the first and third rows of the resultant matrix, which correspond to the first and third components of volumetric error (i.e. E_{XV} and E_{ZV} as shown in Figure 4-3), are extracted and listed in Table 4-2 and Table 4-3 separately. E_{XV} represents the mismatch depth on the lateral walls of the slots and E_{ZV} represents the mismatch depth at the bottom surface of the slots.

According to the sensitivity tables, each test pattern is affected by some of the link errors. Since multiple error parameters affect the volumetric error value, the produced mismatch in each pattern can be predicted by multiplying the corresponding row by a link error column matrix using Eq. 4-7.

Table 4-2 The sensitivity of the mismatch depth in the x direction (E_{XV}) to the link errors

Machining pattern	$\frac{\partial E_{\mathrm{XV}}}{\partial E_{\mathrm{AOB}}}$ (mm/rad)	$\frac{\partial E_{\mathrm{XV}}}{\partial E_{\mathrm{COB}}}$ (mm/rad)	$\frac{\partial E_{\mathrm{XV}}}{\partial E_{\mathrm{XOC}}}$ (mm/mm)	$\frac{\partial E_{\mathrm{XV}}}{\partial E_{\mathrm{AOC}}}$ (mm/rad)	$\frac{\partial E_{\mathrm{XV}}}{\partial E_{\mathrm{BOC}}}$ (mm/rad)	$\frac{\partial E_{\mathrm{XV}}}{\partial E_{\mathrm{BOZ}}}$ (mm/rad)	$\frac{\partial E_{\mathrm{XV}}}{\partial E_{\mathrm{AOY}}}$ (mm/rad)	$\frac{\partial E_{\mathrm{XV}}}{\partial E_{\mathrm{COY}}}$ (mm/rad)
1	-0.002	-61.9528	0	4.0052	0.2152	0	0.0072	61.956
2	-0.0001	-65.3361	0	2.8284	0.1535	0	0.0048	65.336
3	-0.0046	-190.3368	0	4.0061	0.2142	0	0.0059	190.34
4	-0.0016	-190.3391	0	2.8289	0.1538	0	0.0036	190.34
5	-0.0018	117.9632	0	4.0054	0.2166	0	0.009	-117.96

Table 4-3 The sensitivity of the mismatch depth in the z direction (E_{ZV}) to the link errors

Machining pattern	$\frac{\partial E_{ZV}}{\partial E_{AOB}}$ (mm/rad)	$\frac{\partial E_{ZV}}{\partial E_{COB}}$ (mm/rad)	$\frac{\partial E_{ZV}}{\partial E_{XOC}}$ (mm/mm)	$\frac{\partial E_{ZV}}{\partial E_{AOC}}$ (mm/rad)	$\frac{\partial E_{ZV}}{\partial E_{BOC}}$ (mm/rad)	$\frac{\partial E_{ZV}}{\partial E_{BOZ}}$ (mm/rad)	$\frac{\partial E_{ZV}}{\partial E_{AOY}}$ (mm/rad)	$\frac{\partial E_{ZV}}{\partial E_{COY}}$ (mm/rad)
1	61.9528	-0.0002	2	0	243.46	-0.0013	-61.956	-0.0006
2	65.3361	-0.0001	1.4142	46.1996	-9.0738	-0.0014	-65.336	-0.0007
3	190.3368	-0.0008	2	0	243.4644	-0.004	-190.34	-0.0019
4	190.3391	-0.0017	1.4142	134.59	73.0064	-0.004	-190.34	-0.0019
5	-117.9632	0.0005	2	0	243.4539	0.0025	117.96	0.0012
6	271.6409	-0.0011	0	0	0.013	-0.0046	-271.64	-0.0027
7	-0.0045	0	2	0	419.691	0.0011	0	0

4.7 Mismatch measurement

After performing the tests, the improvement in overall accuracy of the five-axis machining is measured prior to removing the part from the machine by on-machine touch probing using a 6 mm stylus tip diameter.

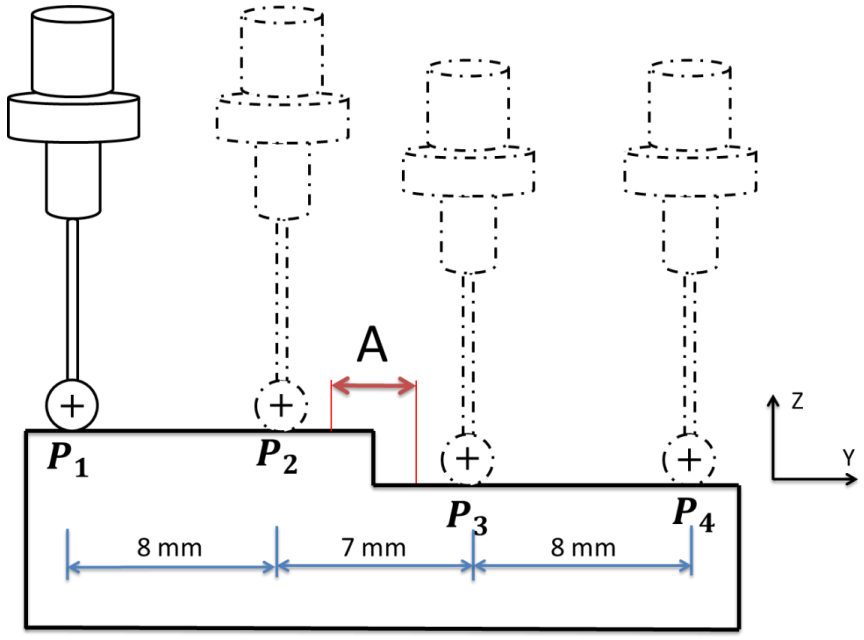

Figure 4-9 Probing the machined surfaces to acquire the points coordinates in each half slot

As shown in Figure 4-9, two points are touched on each half slot surface and the averages of the relevant acquired coordinates is compared to the ones of the other half slot in order to calculate the surface mismatch (with the assumption of parallelism of the surfaces of two halves). For example, for the slot bottom mismatch:

$$E_{\mathrm{ZV}} = \left(\frac{\boldsymbol{P}_{1,\mathrm{z}}+\boldsymbol{P}_{2,\mathrm{z}}}{2} - \frac{\boldsymbol{P}_{3,\mathrm{z}}+\boldsymbol{P}_{4,\mathrm{z}}}{2}\right)_{\text{Compensated slot}} - \left(\frac{\boldsymbol{P}_{1,\mathrm{z}}+\boldsymbol{P}_{2,\mathrm{z}}}{2} - \frac{\boldsymbol{P}_{3,\mathrm{z}}+\boldsymbol{P}_{4,\mathrm{z}}}{2}\right)_{\text{Reference slot}} \quad (4\text{-}8)$$

The specified area (A) in Figure 4-9 may not be used for measurement since the forces are not stable in this area and machining conditions for the two halves of the slot are not the same. This is because when the tool reaches this area when machining the second slot half, the first slot half having been machined there is not the same amount of material to be machined compared to the machining of the first half. So, the machining forces vary in this area and may affect the volumetric error (mismatch dimensions). Therefore, measurement in this area is avoided for surface mismatch comparison. The accuracy of the on-machine probing measurement (using single linear axis motion) is high since the measurement volume, in this case, is in the range of a few millimetres (for each specific pattern) and motion kinematic errors of the machine do not significantly affect the measurement accuracy in such small volume [Zargarbashi et al., 2009; Andolfatto et al., 2011]. In addition, all form probing is done with the same approach direction for any one slot. For validation purpose, the mismatch depth measurement results were confirmed for all patterns using a sine table, a surface plate and a dial indicator. This is repeated for all three (reference, uncompensated and compensated) slots for every pattern (Figure 4-10 and Figure 4-11) and the results of mismatch measurement for the x and z directions, are shown in Table 4-4 and Table 4-5.

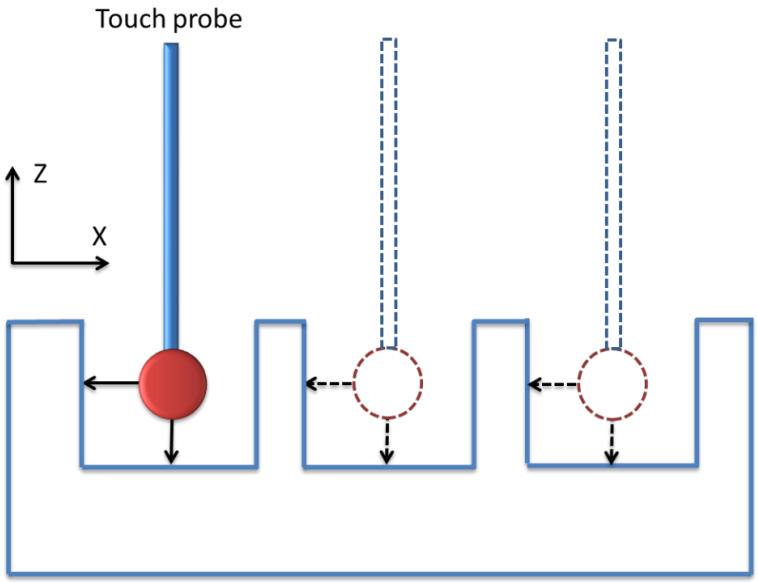

Figure 4-10 Probing on bottom surface and side surface of the three machined slots of each pattern

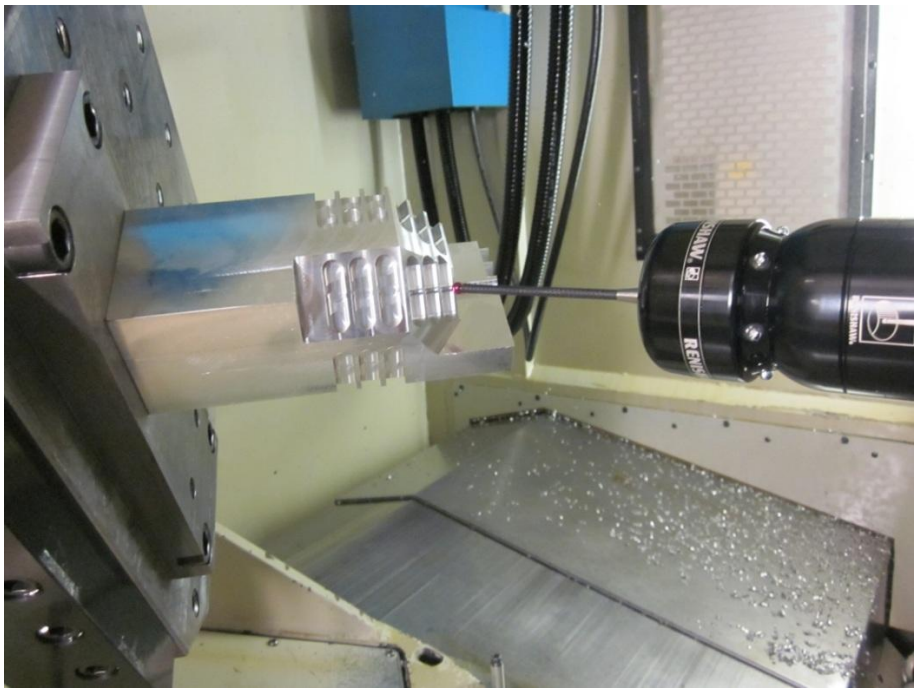

Figure 4-11 On-machine measurement of the mismatches using a Renishaw MP700 touch trigger probe

Table 4-4 Measurement results using touch trigger probe

Pattern no.	Mismatch depth in x direction			Approximate accuracy improvement (%)
	reference slot (μm)	uncompensated slot (μm)	compensated slot (μm)	
1	1	175	32	82
2	1	50	6	88
3	1	185	37	80
4	1	44	13	70
5	1	184	18	90

Table 4-5 Measurement results using touch trigger probe

Pattern no.	Mismatch depth in z direction			Approximate accuracy improvement (%)
	reference slot (μm)	uncompensated slot (μm)	compensated slot (μm)	
1	1	210	3	99
2	2	152	3	98
3	1	107	3	97
4	3	155	3	98
5	3	230	6	98
6	1	20	7	65
7	1	172	38	78

To better illustrate the mismatch depth reduction in the x and y directions, the measurement results are presented graphically in Figure 4-12 and Figure 4-13 respectively.

4.8 Discussion

Regarding Table 4-4 and Table 4-5, for the reference slot (the first columns of the tables), the mismatch is close to zero showing that despite the fact that the two slot halves are machined in opposite feed directions, the process itself causes insignificant errors. It also supports the measurement procedure. In addition, the measurement values demonstrate a significant reduction (around from 65% to 99%) in surface mismatch depth after compensation using the modified G-code. The accuracy improvement in the cases of pattern 6 and 7 (flank machining) are lower compared to other patterns. Regarding Table 4-2 and Table 4-3, at each machining point, the effect of multiple machine geometric error parameters combines to produce a volumetric error on the machined part. So, some of them may cancel each other. Therefore, this method is proposed to assess the "overall" accuracy improvement of the machine but not to find the effect of each error source separately. Also, regarding the sensitivity analysis tables, none of the proposed machining patterns can sensitively detect the E_{BOZ} link error. Thus, work is underway to imagine a pattern sensitive to this remained link error. In general, the mismatch depth is not the result of only one link error, but of several other geometric errors as well as error motions of each individual axis, thermal errors and force induced errors amongst many. In this research, the effect of the force errors can be neglected because of the relatively small value for slot depth (depth of cut) in finishing passes as observed in the reference slot. However, if the measurement of each slot is done over a short time but the slot machining is conducted by machining all first halves of the slots and then all second halves, then, the effect of machine thermal drift could be brought to zero.

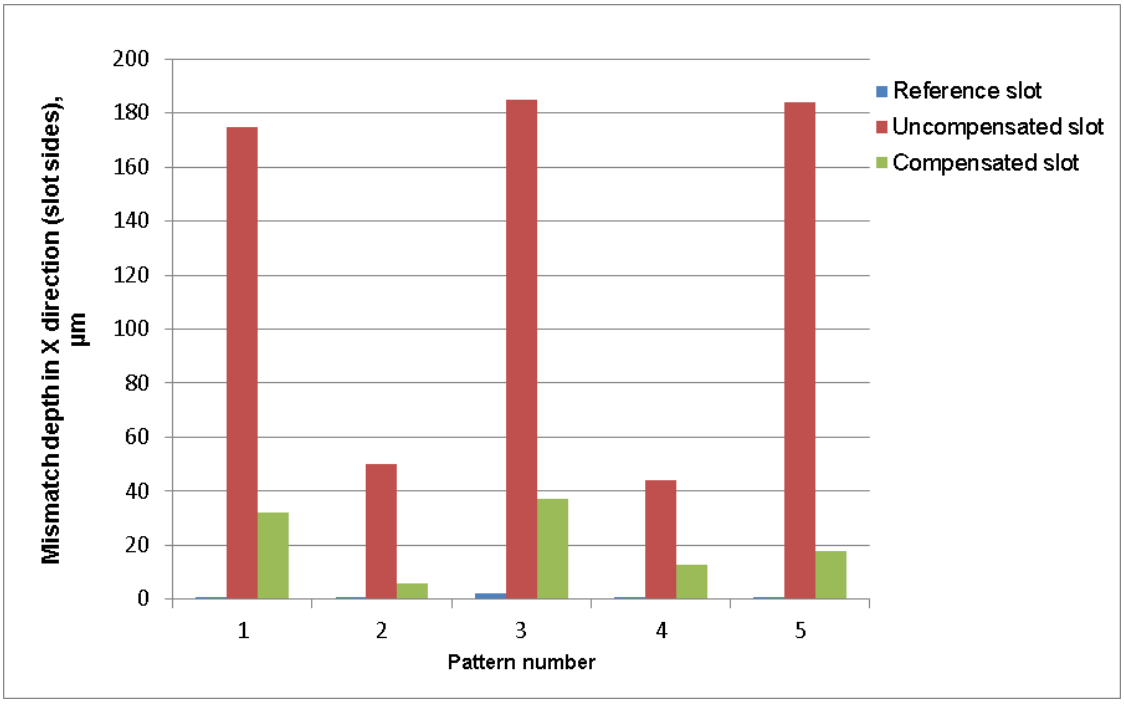

Figure 4-12 Mismatch depth comparison in x direction for three slots of each pattern

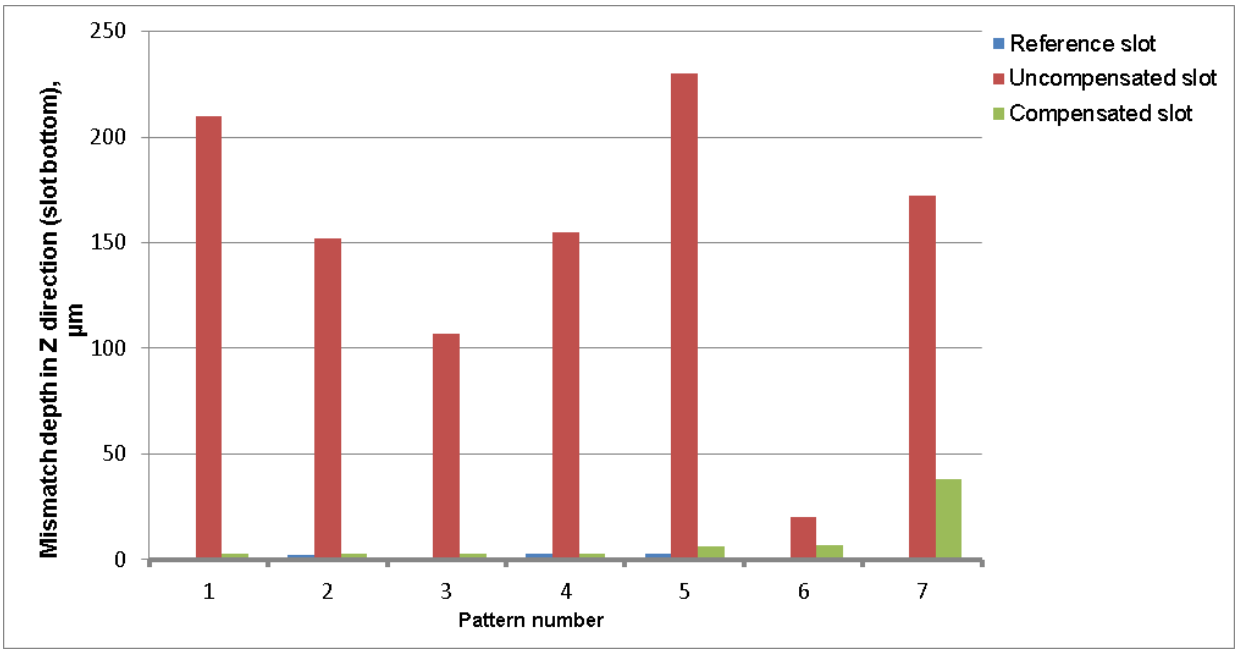

Figure 4-13 Mismatch depth comparison in y direction for three slots of each pattern

4.9 Conclusion

The paper proposes an “all on-machine” fully automated experimental validation of the effectiveness of volumetric error compensation on a machined part. A series of simple two-dimensional cutting patterns were performed in the form of two halves of one slot produced using different rotary axes indexations. Due to the machine errors, a mismatch may appear on each slot’s surface. The concept of differential directional Jacobian of the volumetric error is proposed and applied to analyse the effect of the machine geometric link errors on the machined slot mismatch. For each pattern, three slots were produced, one with uncompensated G-code, another one with compensated G-code to see the effect of error compensation on the mismatch depth and a third slot without indexation change nor compensation used as a reference. The mismatch is measured by the erroneous machine itself using on-machine touch probing in a small volume and using unidirectional probing to avoid machine tool errors. The reference slot showed that the machining process and measurement produced no significant mismatch readings. A compensation effectiveness of about 65% to 99 % was observed. This strategy simplifies the validation of the compensation process in five-axis machine tools in a machining situation.

4.10 Acknowledgements

This research work was performed with the support of an NSERC-CANRIMT strategic network GRANTS.

4.11 References

Abbaszadeh-Mir, Y., et al.; "Theory and simulation for the identification of the link geometric errors for a five-axis machine tool using a telescoping magnetic ball-bar." *International Journal of Production Research* 40(Compendex): 4781-4797, 2002.

Andolfatto, L. L., S. Mayer, J. R. R.; "Evaluation of servo, geometric and dynamic error sources on five-axis high-speed machine tool." *International Journal of Machine Tools and Manufacture* 51(10-11): 787-796, 2011.

Donmez, M. A., et al.; "A general methodology for machine tool accuracy enhancement by error compensation." *Precision Engineering* 8(4): 187-196, 1986.

Ibaraki, S., et al.; "Machining tests to identify kinematic errors on five-axis machine tools." *Precision Engineering* 34(3): 387-398, 2010.

ISO230-1 (2012). Test code for machine tools-part 1 : geometric accuracy of machines operating under no-load or quasi-static conditions.

ISO10791-7 (1998). ISO 10791-7: Test conditions for machining centres -- Part 7: Accuracy of a finished test piece.

Jung, J.-H., et al.; "Machining accuracy enhancement by compensating for volumetric errors of a machine tool and on-machine measurement." *Journal of Materials Processing Technology* 174(1–3): 56-66, 2006.

Khan, A., et al.; "A methodology for systematic geometric error compensation in five-axis machine tools." *The International Journal of Advanced Manufacturing Technology* 53(5): 615-628, 2011.

Lei, W. T., et al.; "Accuracy enhancement of five-axis CNC machines through real-time error compensation." *International Journal of Machine Tools and Manufacture* 43(9): 871-877, 2003.

Mahbubur, R. M. D., et al.; "Positioning accuracy improvement in five-axis milling by post processing." *International Journal of Machine Tools and Manufacture* 37(2): 223-236, 1997.

Paul, R. P., et al.; "Differential kinematic control equations for simple manipulators." *Systems, Man and Cybernetics, IEEE Transactions* 11(6): 456-460, 1981.

S.P. Moylan, D. B., M.L. McGlauflin, R.R. Fesperman, and M.A. Donmez; "Evaluation of Proposed Test Artifacts for Five-Axis Machine Tools". *the 26th ASPE Annual Meeting*. 2011.

Takeshima, H., & Ihara, Y. ; "Finished Test Piece Example for Fiveaxis Machining Centers". *The 5th Int. Conf. on Leading Edge Manufacturing in 21st century (LEM21)*, Osaka, Japan. 2009.

Uddin, M. S., et al.; "Prediction and compensation of machining geometric errors of five-axis machining centers with kinematic errors." *Precision Engineering* 33(2): 194-201, 2009.

Wang, S.-M., et al.; "An efficient error compensation system for CNC multi-axis machines." *International Journal of Machine Tools and Manufacture* 42(11): 1235-1245, 2002.

Zargarbashi, S. H. H., et al.; "Single setup estimation of a five-axis machine tool eight link errors by programmed end point constraint and on the fly measurement with Capball sensor." *International Journal of Machine Tools and Manufacture* 49(10): 759-766, 2009.

Zhu, S., et al.; "Integrated geometric error modeling, identification and compensation of CNC machine tools." *International Journal of Machine Tools and Manufacture* 52(1): 24-29, 2012.

CHAPTER 5 ARTICLE 3: OPTIMIZED VOLUMETRIC ERROR COMPENSATION FOR FIVE-AXIS MACHINE TOOLS CONSIDERING RELEVANCE AND COMPENSABILITY

Mehrdad Givi [1] and J.R.R Mayer [1]

[1] *Mechanical Engineering Department, Polytechnique Montréal, P.O. Box 6079, Station Downtown, Montréal (Qc), Canada, H3C 3A7*

*Based on the paper submitted to the CIRP Journal of Manufacturing Science and Technology

5.1 Abstract

Compensation of a machine tool's volumetric errors can be achieved by adjustment of the axes original commands. Depending on the machine topology, the volumetric errors and the axes commands, a full compensation may not be achieved due to kinematic singularities. Furthermore, corrections of volumetric errors which do not affect part quality, by virtue of the machining process and machined feature, may lead to excessive corrections causing surface degradation. The paper addresses these problems through the introduction of two notions, error relevance and error compensability, leading to an optimized compensation in which minimal but effective command modifications are made. Mathematical definitions are presented together with application examples for different processes. A specially designed test part containing four common features, i.e. hole, curved slot on a spherical surface, cone frustum and flat surface is machined, using up to five-axis simultaneous machining, for the experimental validation. Three parts are machined using uncompensated G-code, compensated G-code and optimized compensated G-code, respectively, which are then measured on a coordinate measuring machine. Simulation results show a reduction (up to 75%) in the 1-norm of the linear and angular compensations while the relevant errors are effectively corrected by the proposed optimized strategy.

Keywords: Machining, Compensation, Volumetric error, Error compensability, Error relevance

5.2 Introduction

Various approaches have been proposed to compensate multi-axis machine tool volumetric errors in order to increase the machined part accuracy such as tool path correction before generating the G-code [Srivastava et al., 1995], off-line G-code modification [Jing, 2006], and real time compensation [Donmez et al., 1986]. Most effort have been directed to the question "how to compensate?" and less attention has been paid to "what to compensate?". As briefly mentioned in ISO 230-1 standard [ISO230-1, 2012], in machining processes some machine errors may not produce significant defect on the feature surface. Such irrelevant volumetric errors that have no effect on the machined part accuracy do not require compensation [Schwenke et al., 2008]. In numerical error compensation for machine tools, it may happen that some axes, which nominally are not programmed to move, are required to move for the sake of error correction. For example, when milling a flat surface in the XY plane, straightness errors of both the X and Y axes in the Z-direction could be compensated by programming small Z-axis movements. This may result in some additional errors (such as reversal errors when the Z-axis motion direction changes) [ISO/TR16907, 2015]. Furthermore, if such Z-axis changes are significant relative to the programmed depth of cut, undesirable surface effects may result for example by approaching the minimum chip thickness limit.

In addition, in a machine tool with a specific configuration, some components of the volumetric error may not be compensable. If uncompensable components are known, no attempt should be made to compensate them and the situation should simply be flagged.

In the robotic field, the terms "observability" and "controllability" are used for almost similar concepts. For example, some observability indices were proposed and compared to find the relevant kinematic parameters for robot calibration purpose [Yu et al., 2008]. Liebrich et al. [Liebrich et al., 2009] proposed a measurement procedure to minimize the effect of a CMM geometric errors on the calibration of a 3D-ball plate. It was found that some geometric error parameters of the CMM were "non-compensable".

This paper defines and explores the concepts of "error relevance" and "error compensability" and applies them in five-axis machining. First, the compensation strategy used in this work is reviewed and then a new mathematical tool called the "filtration matrix" is proposed to filter out any irrelevant volumetric error components. In section 5, the error compensability concept is

described in details and the inability of the machine tool to correct uncompensable errors at a singular position, for example, is graphically illustrated. Consideration of these two notions leads to an optimized compensation which is practically implemented in machining a specially designed workpiece containing four common features as a case study in section 7. It discusses the implementation of the optimized strategy using the proposed concepts. Off-line measurements are performed for all three parts using a coordinate measuring machine (CMM) in order to compare the part accuracy when no compensation, regular compensation and optimized compensation are applied. The measurement results are presented and compared in section 7 and followed by a conclusion in section 8.

5.3 Error compensation strategy

The volumetric error at each working location and axis commands consists of six components twist i.e. three positioning errors and three angular errors of the tool with respect to its desired location. The volumetric error twist is here taken as the difference between the actual and desired tool location as follows [Givi et al., 2014].

$$^{\{DCL\},DCL}\boldsymbol{\tau}^{v}{}_{t'} = [\, E_{XV} \quad E_{YV} \quad E_{ZV} \quad E_{AV} \quad E_{BV} \quad E_{CV}]^{T} \tag{5-1}$$

where $^{\{\mathrm{DCL}\},\mathrm{DCL}}\boldsymbol{\tau}^{\mathrm{v}}{}_{\mathrm{t}'}$ is the volumetric error twist of the actual tool frame (t') relative to desired cutter location (DCL) and projected in DCL frame ({DCL}). Assuming the error components are known, their compensation is sought through changes to the machine axis commands which could, for example, be achieved through off-line modification of the G-code using a locally linearized model [Lei et al., 2003; Givi et al., 2014]. This linear relation between small axis motions (Δaxis) and a volumetric error twist ($\delta\tau$) can be expressed using the Jacobian matrix (J) [Paul et al., 1981; Abbaszadeh-Mir et al., 2002] :

$$\delta\tau = J\,\Delta axis. \tag{5-2}$$

Solving Eq. 2 for Δaxis provides the required changes in machine axis commands to cancel the volumetric error twist$\delta\tau$. Therefore, the compensation formula is

$$\Delta axis = J^{-1}\,\delta\tau. \tag{5-3}$$

Since a linear system is assumed for the modeled machine, an iterative method is applied to obtain an exact solution for Δaxis as explained in [Givi et al., 2014].

5.4 Error relevance

In some machining operations, one or more error components of the volumetric error may not be relevant for the accuracy of the machined feature. For instance, in face milling, if the surface normal is the z direction, the translational errors in the x or y directions of the tool tip (δx and δy) are irrelevant. Figure 5-1 shows four common machining processes and the relevant components of the deviation of the actual cutter related to its desired location (volumetric error) in each case.

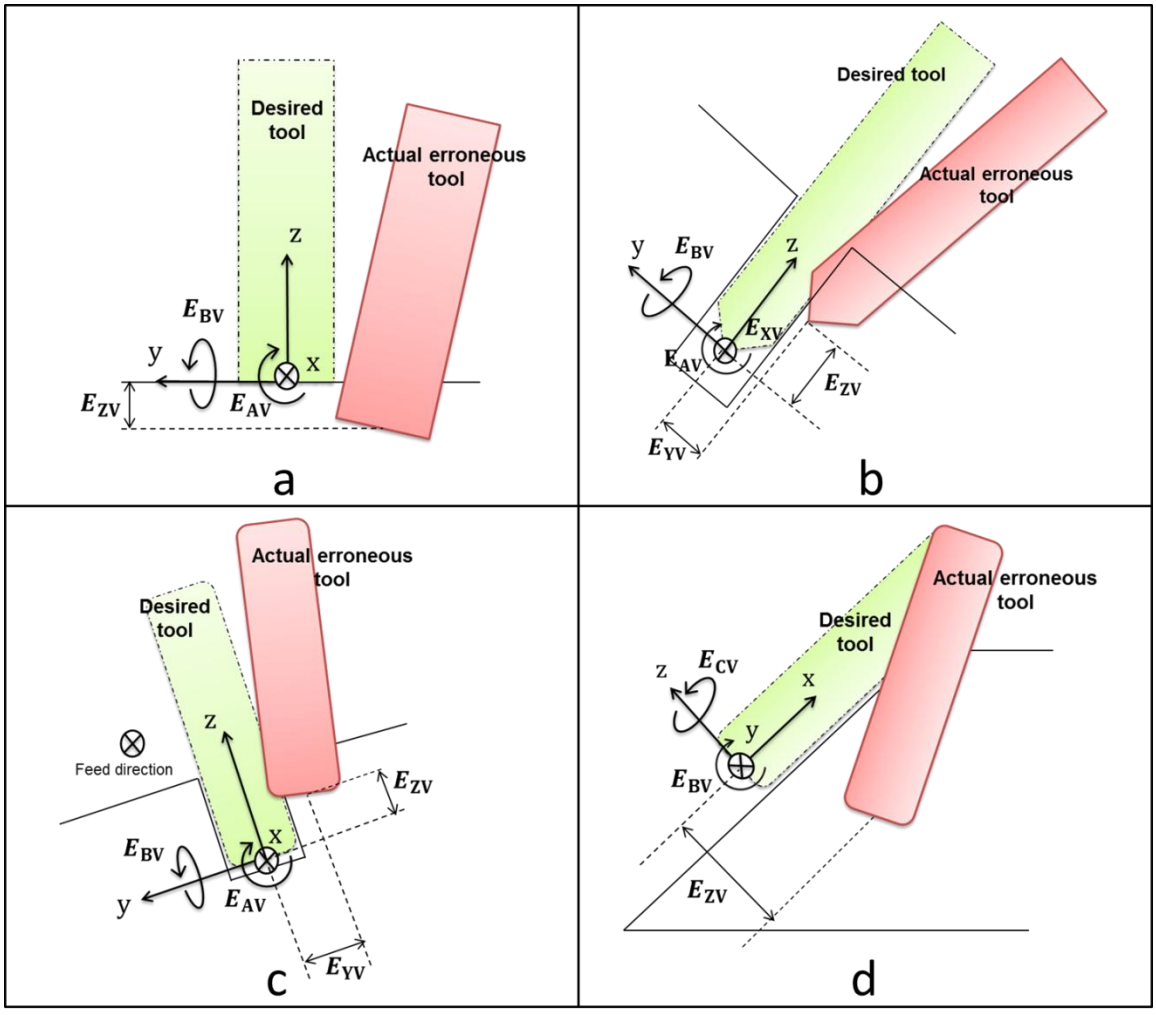

Figure 5-1 Relevant components of the volumetric error in common machining processes a) face milling b) hole drilling c) slot milling d) flank milling a conical surface

Based on the machining process, feature and tool geometry, the relevant errors can be isolated for the calculation of the compensation. A "filtration matrix" pre-multiplies the volumetric error twist in order to filter out (eliminate) the irrelevant errors as shown in Eq. 5-4

$$\boldsymbol{\tau}^{rv} = F\,\boldsymbol{\tau}^{v} = F\,[\,E_{XV} \quad E_{YV} \quad E_{ZV} \quad E_{AV} \quad E_{BV} \quad E_{CV}]^{T} \tag{5-4}$$

where $\boldsymbol{\tau}^{\mathrm{v}}$ and $\boldsymbol{\tau}^{\mathrm{rv}}$ represent the whole and relevant volumetric error twists defined in feature frame respectively and F is the filtration matrix. Filtration matrices for the cases shown in Figure 5-1, and also relevant and irrelevant error components for each one are listed in Table 5-1.

Table 5-1 Filtration matrix for common machining processes illustrated in Figure 5-1

Feature	Machining process	Tool type	Relevant components (in feature frame)	Irrelevant components (in feature frame)	Filtration matrix
a) Flat surface	Face milling	Flat-end mill	E_{ZV}, E_{AV}, E_{BV}	E_{XV} , E_{YV} , E_{CV}	$\begin{bmatrix}0&0&1&0&0&0\\0&0&0&1&0&0\\0&0&0&0&1&0\end{bmatrix}$
b) Hole	Drilling	Twist drill	E_{XV} , E_{YV} , E_{ZV}, E_{AV} , E_{BV}	E_{CV}	$\begin{bmatrix}1&0&0&0&0&0\\0&1&0&0&0&0\\0&0&1&0&0&0\\0&0&0&1&0&0\\0&0&0&0&1&0\end{bmatrix}$
c) Slot on spherical surface	Curve milling	Ball-end mill	E_{YV} , E_{ZV} , E_{AV} , E_{BV}	E_{XV} , E_{CV}	$\begin{bmatrix}0&1&0&0&0&0\\0&0&1&0&0&0\\0&0&0&1&0&0\\0&0&0&0&1&0\end{bmatrix}$
d) Cone frustum	Flank milling	Flank mill	E_{ZV} , E_{BV} , E_{CV}	E_{XV} , E_{YV} , E_{AV}	$\begin{bmatrix}0&0&1&0&0&0\\0&0&0&0&1&0\\0&0&0&0&0&1\end{bmatrix}$

To obtain the volumetric error in feature frame, the volumetric error in actual tool frame can be simply calculated using Eq. 5-5 and 5-6 as explained in [Givi et al., 2014].

$$ {}^{\mathrm{t}'}T_{\mathrm{DCL}} = \left({}^{\mathrm{F}}T_{\mathrm{t}'} \right)^{-1} . \, {}^{\mathrm{F}}T_{\mathrm{DCL}}^{\mathrm{actual}} \tag{5-5} $$

and in the form of twist vector:

$$ {}^{\{\mathrm{t}'\},\mathrm{t}'}\boldsymbol{\tau}^{v}{}_{\mathrm{DCL}} = [\, E_{XV} \quad E_{YV} \quad E_{ZV} \quad E_{AV} \quad E_{BV} \quad E_{CV}]^{T} \tag{5-6} $$

Then, the volumetric error is projected in the feature frame applying a projection matrix as follows:

$$ {}^{\{f\},t'}\boldsymbol{\tau}^{v}{}_{DCL} = {}^{f}H_{t'} . \, {}^{\{t'\},t'}\boldsymbol{\tau}^{v}{}_{DCL} \tag{5-7} $$

where ${}^{\mathrm{f}}H_{\mathrm{t}'}$ is a projection matrix (6×6) projecting the error twist from actual tool to feature frame. The translational and angular error components are projected separately so the projection matrix takes the form:

$$ {}^{\mathrm{f}}H_{\mathrm{t}'} = \begin{bmatrix} R_{3\times3} & 0_{3\times3} \\ 0_{3\times3} & R_{3\times3} \end{bmatrix} \tag{5-8} $$

where

$$ R_{3\times3} = \begin{bmatrix} {}^{\mathrm{t}'}\hat{\imath}_{\mathrm{f}}{}^{\mathrm{T}} \\ {}^{\mathrm{t}'}\hat{\jmath}_{\mathrm{f}}{}^{\mathrm{T}} \\ {}^{\mathrm{t}'}\hat{k}_{\mathrm{f}}{}^{\mathrm{T}} \end{bmatrix} \tag{5-9} $$

where, ${}^{\mathrm{t}'}\hat{\imath}_{\mathrm{f}}$, ${}^{\mathrm{t}'}\hat{\jmath}_{\mathrm{f}}$ and ${}^{\mathrm{t}'}\hat{k}_{\mathrm{f}}$ are the feature frame orthonormal basis projected in the tool frame. Finally, the filtration matrix ($F_{\mathrm{n}\times6}$) is applied in this step to filter out the irrelevant errors:

$$ {}^{\{\mathrm{f}\}}\boldsymbol{\tau}^{\mathrm{rv}} = FH \, {}^{\{\mathrm{t}'\},\mathrm{t}'}\boldsymbol{\tau}^{v}{}_{\mathrm{DCL}} \tag{5-10} $$

The number of rows n of the F matrix is the number of relevant error components for each machining case. Multiplying the matrices F and H in both sides of the Eq.5-2 and replacing the relevant volumetric error from Eq. 5-10 leads to:

$$^{\{f\}}\boldsymbol{\tau}^{rv} = F\ H\ ^{\{t'\},DCL}J_{t'}\quad \Delta axis \tag{5-11}$$

which is solved for $\Delta axis$

$$\Delta axis_{\,5\times1} = \left(F\ H\ ^{\{t'\},DCL}J_{t'}\right)^{\dagger}_{5\times n}\left(^{\{f\}}\boldsymbol{\tau}^{rv}\right)_{n\times1} \tag{5-12}$$

For example, in case of a cone frustum as mentioned in Table 5-1, the filtration matrix is:

$$F = \begin{bmatrix} 0 & 0 & 1 & 0 & 0 & 0 \\ 0 & 0 & 0 & 0 & 1 & 0 \\ 0 & 0 & 0 & 0 & 0 & 1 \end{bmatrix}_{3\times6} \tag{5-13}$$

which has three rows since only three volumetric error components are relevant. If the number of rows of relevant volumetric errors is less than the number of controllable axes, a solution can be found for the equation using underdetermined least square approach [Press, 1992].

5.5 Compensability ratio

Due to the machine tool configuration, it may not be possible to compensate all of the relevant error components. For example, when the target five-axis machine tool, with topology WCBXbZYt (as shown in Figure 5-2) is in its singular position (b=0), it is not possible to compensate a pure angular error around the X-axis (E_{AV}). In this case, the volumetric error component cannot be cancelled with minute adjustments in axes command.

This can be mathematically explained when Eq. 5-2 is rewritten with each matrix details:

$$\begin{bmatrix} E_{XV} \\ E_{YV} \\ E_{ZV} \\ E_{AV} \\ E_{BV} \\ E_{CV} \end{bmatrix} = \begin{bmatrix} a_{11} & a_{12} & a_{13} & a_{14} & a_{15} \\ a_{21} & a_{22} & a_{23} & a_{24} & a_{25} \\ a_{31} & a_{32} & a_{33} & a_{34} & a_{35} \\ 0 & 0 & 0 & 0 & 0 \\ a_{51} & a_{52} & a_{53} & a_{54} & a_{55} \\ a_{61} & a_{62} & a_{63} & a_{64} & a_{65} \end{bmatrix} \cdot \begin{bmatrix} \Delta x \\ \Delta y \\ \Delta z \\ \Delta b \\ \Delta c \end{bmatrix} \tag{5-14}$$

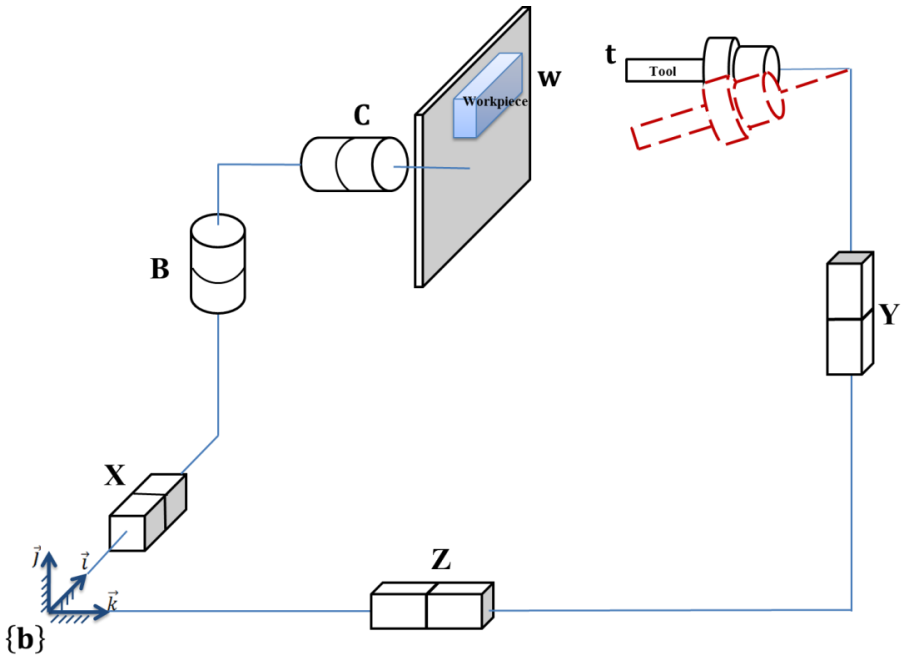

Figure 5-2 Five-axis machine tool with the topology WCBXFZYt and and a pure angular error in the tool frame

At this singular position (b=0), all elements of the fourth line of the Jacobian matrix have zero value and none of the axes is able to affect the fourth component of the volumetric error twist (E_{AV}). So, this component is not compensable using axis command adjustment.

It may be possible to resolve such conditions in the presence of kinematic singularities [Press, 1992] and find a solution to cancel all the error components but only with relatively large changes in axes positions. It means large motions in machine axes, but such modifications are not desirable in machining. As mentioned in [ISO/TR16907, 2015] the rotary axis which is nominally parallel to the spindle axis is considered as kinematic pole (singularity) of a five-axis machine tool. In the vicinity of kinematic poles, the required motions to compensate the errors in the functional orientation may not be directly available to the CNC and it could lead to highly accelerated motions of other axes.

A metric so-called ‘compensability ratio’ between the volumetric error and the Δaxis components is proposed considering linear and angular portions as two separate vectors that can be compared:

$$\Delta axis_{\,linear} = [\Delta x, \Delta y, \Delta z] \tag{5-15}$$

$$\Delta axis_{\,angular} = [\Delta b, \Delta c] \tag{5-16}$$

$$\boldsymbol{\tau}^{v}_{linear} = [E_{XV} \;\; E_{YV} \;\; E_{ZV}] \tag{5-17}$$

$$\boldsymbol{\tau}^{v}_{angular} = [E_{AV} \;\; E_{BV} \;\; E_{CV}] \tag{5-18}$$

So, the compensability ratio can be calculated using the following ratios of the vectors' 1-norms:

$$R_{linear} = \frac{\left|\Delta axis_{\,linear}\right|}{\left|\boldsymbol{E}^{v}_{linear}\right|} = \frac{|\Delta x| + |\Delta y| + |\Delta z|}{|E_{XV}| + |E_{YV}| + |\,E_{ZV}|} \tag{5-19}$$

$$R_{angular} = \frac{\left|\Delta axis_{\,angular}\right|}{\left|\boldsymbol{E}^{v}_{angular}\right|} = \frac{|\Delta b| + |\Delta c|}{|E_{AV}| + |E_{BV}| + |\,E_{CV}|} \tag{5-20}$$

As an example, assume the five-axis machine tool is in an arbitrary position, (e.g., x=100 mm, y=200 mm, z=300 mm and c=30°) and that the estimated values for the inter-axis geometric errors in [Mayer, 2012] are used in the compensation procedure. The required $\Delta axis$ is calculated using Eq. 5-3 and for different B-axis positions. When B-axis moves toward zero (a singularity point), the compensability ratios dramatically increase. Especially for values of b less than 0.01 rad, the volumetric error and $\Delta axis$ components are not commensurate anymore which could indicate an uncompensability of the volumetric errors. (Figure 5-3 and Figure 5-4). Note that all of the six volumetric error components are assumed to be relevant in this section.

In practice, when the compensability ratio reaches too high values (out of the commensurability range), the residual volumetric errors after compensation and the absolute value of the required motions in the machine axes may be checked separately and in details and also compared to the related machining conditions such as depth of cut before declaration of the compensability of volumetric error components in such critical areas. On the other hands, too small compensability ratios could be critical too. This situation could happen either when the volumetric error is too large or when the required axes motion is too small. Therefore, a minimum threshold for the ratio value can be assumed regarding the machining conditions such as depth of cut and least input or

command increment of the CNC machine tool. Significant changes to the depth of cut could be largely avoided by also introducing compensation at the semi-finishing step, if an, since the compensation values are likely to be very similar.

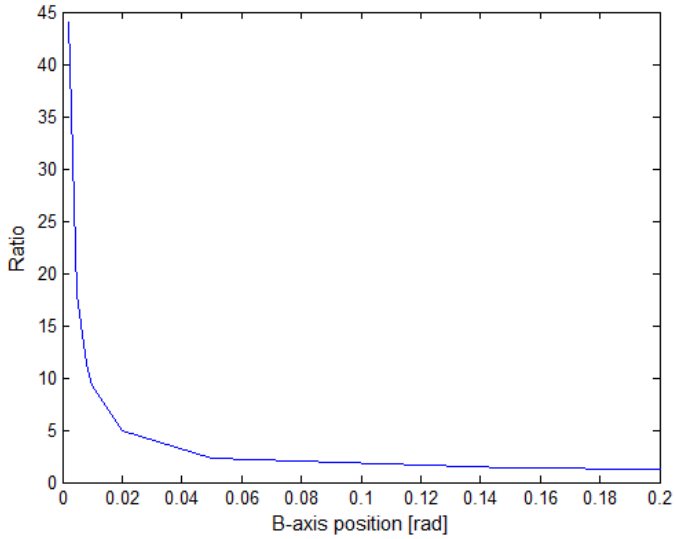

Figure 5-3 Changes of R_{linear} with B-axis position

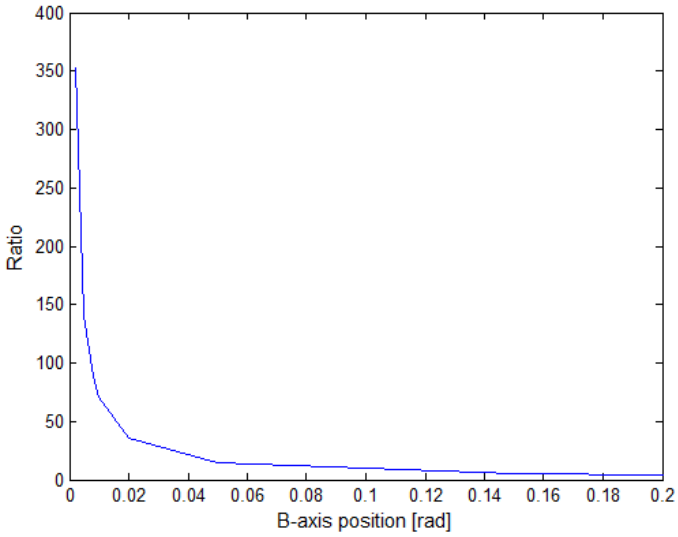

Figure 5-4 Changes of $R_{angular}$ with B-axis position

5.6 Compensation optimization

The optimization process consists in applying both the relevance concept and compensability ratio in order to only compensate what needs to be and refrain from causing excessive corrective axis motions (Figure 5-5).

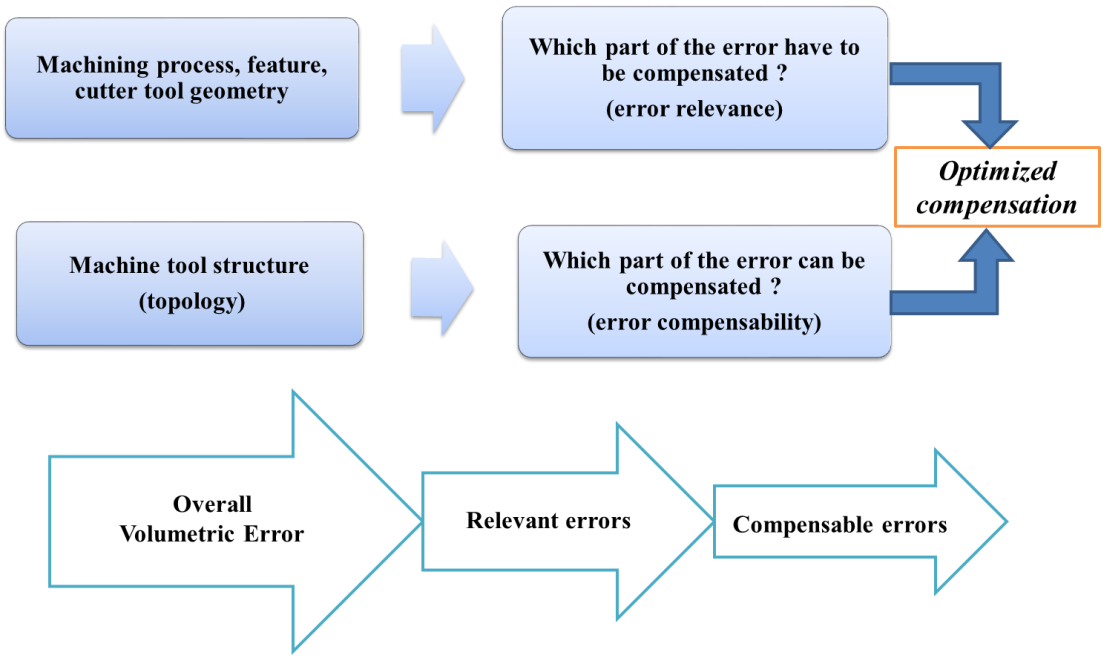

Figure 5-5 Relevant and compensable errors

5.7 Case study

5.7.1 Design of the test piece

A test piece containing four common features, as introduced in Table 5-1 , is designed to verify the effectiveness of the compensation based on the proposed concepts. The test piece is a hemispherical aluminum part contain with a flat surface, three holes, a curved slot on the hemisphere surface and also a tilted cone frustum as a standard feature in five-axis machining [NAS979, 1969; ISO10791-7, 2014]. The CAD model of the part is shown in Figure 5-6.

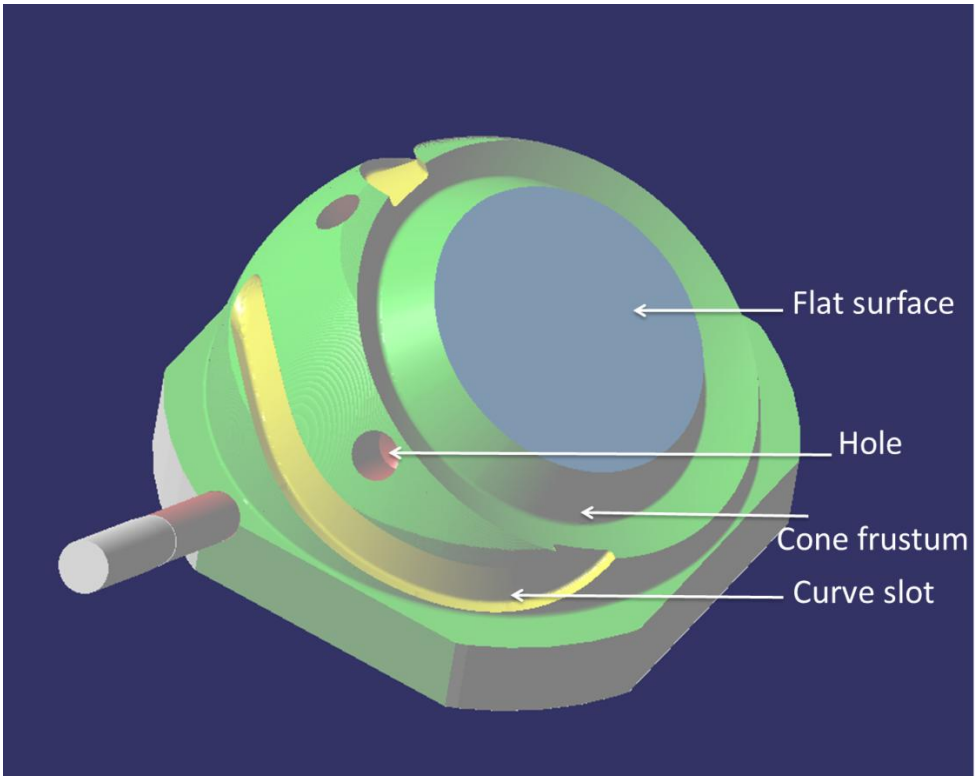

Figure 5-6 Test piece with four features to be machined

To study the error relevance and find the relevant errors, the feature frame orientation must be defined for each feature. For all features, except the cone frustum in which flank milling is used, the normal vector of the machined surface can be defined as the same direction of the tool axis. In other words, the feature frame origin and orientation can be defined as the tool frame.

5.7.2 Feature frame definition for tilted cone frustum

To make the process of cone frustum machining sensitive to the machine geometric errors, the largest possible motions for rotary axes are sought. The required range of the rotary axes motions directly depends on the tilt and taper angles of the cone [Ihara, 2005; Hong et al., 2011] and the geometry of the other features of the test piece.

For a tilted cone frustum, a feature frame origin can be defined at the tool tip and its $\widehat{\imath}_{\mathrm{f}}$ basis vector (surface normal) can be aligned with the tool axis. To find the orientation of the feature frame, imagine the flank milling process of the tilted cone frustum as shown in Figure 5-7. The subscripts t, f, C and cone represent tool, feature, C-axis and cone frame respectively.

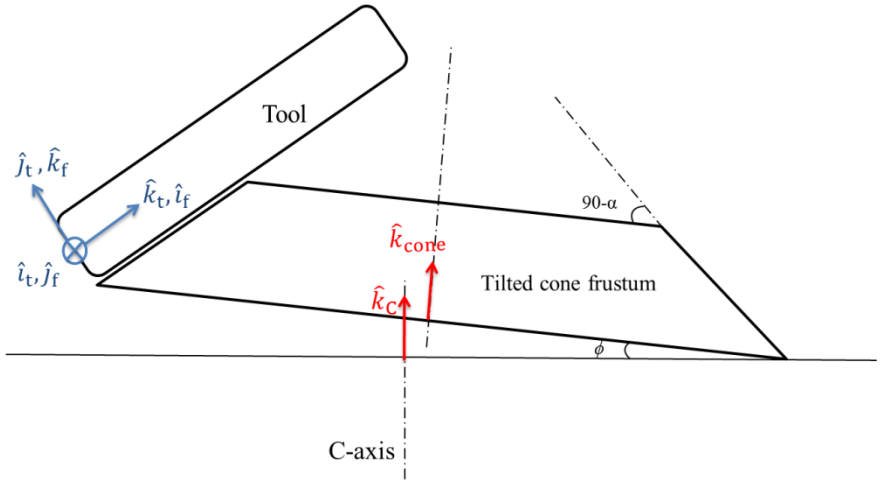

Figure 5-7 Machining of a cone frustum

The position of the feature frame origin can be defined at the tip of the tool and expressed in the C-axis frame:

$$^{\{C\},C}P_f = {}^{\{C\},C}P_t \tag{5-21}$$

In terms of orientation of the feature frame, let assume the k direction of the C-axis as shown in Figure 5-7:

$$^{C}\hat{k}_C = [0\ 0\ 1]^{\mathrm{T}} \tag{5-22}$$

The direction of $^{\mathrm{C}}\hat{k}_{\mathrm{cone}}$ is also calculated by rotating the $^{\mathrm{C}}\hat{k}_{\mathrm{C}}$ in direction of the cone tilt angle (ϕ). The direction of the $^{\mathrm{C}}\hat{k}_{\mathrm{t}}$ is obtained from the HTM, $^{\mathrm{C}}T_{\mathrm{t}}$. As illustrated in Figure 5-7, $^{\mathrm{C}}\hat{\jmath}_{\mathrm{f}}$ is perpendicular to both $^{\mathrm{C}}\hat{k}_{\mathrm{cone}}$ and $^{\mathrm{C}}\hat{k}_{\mathrm{t}}$ and so, can be calculated using cross product of these two vectors:

$$^{C}\hat{\jmath}_f = {}^{C}\hat{k}_{cone} \times {}^{C}\hat{k}_t \tag{5-23}$$

Furthermore, $^{\mathrm{C}}\hat{\imath}_{\mathrm{f}}$ can be defined in the same direction as tool axis ($^{\mathrm{C}}\hat{k}_{\mathrm{t}}$). Finally the $^{\mathrm{C}}\hat{k}_{\mathrm{f}}$ can be obtained by cross product of $^{\mathrm{C}}\hat{\imath}_{\mathrm{f}}$ and $^{\mathrm{C}}\hat{\jmath}_{\mathrm{f}}$:

$$^{C}\hat{k}_f = {}^{C}\hat{\imath}_f \times {}^{C}\hat{\jmath}_f \tag{5-24}$$

So, the feature frame HTM becomes

$$ {}^{C}T_f = \left[{}^{C}\hat{\imath}_f \quad {}^{C}\hat{\jmath}_f \quad {}^{C}\hat{k}_f \quad {}^{\{C\},C}P_f \right]_{4\times4} \tag{5-25} $$

5.7.3 Experimental procedure

Table 5-2 shows the cutting tool type, depth of cut (hole depth in hole drilling case) and spindle speed for each feature at the finishing step.

Table 5-2 Machining conditions for each feature

No.	Feature	Cutting tool	Depth of cut (mm)	Spindle speed (rpm)
1	Cone frustum	Flank mill, Ø19.05	1.5	5000
2	Curved slot on the hemisphere surface	Bull-end mill, Ø19.05	4	70
3	Hole	Drill, Ø15.875 mm	18.6 (hole depth)	3000
4	Flat surface	Face mill, Ø62 mm	1	3500

Three test pieces are rough-machined with the same G-code and are then finished with three different G-codes i.e. 1) original G-code without compensation, 2) regular compensated G-code and 3) optimized compensated G-code. As an example, in case of cone frustum machining, the original G-code is shown in Figure 5-8 while the regular compensated G-code and optimized compensated G-code for the same feature are shown side by side in Figure 5-9. The required changes of the axes positions for all working points (corresponding to the G-code lines) are graphically shown and compared between regular and optimized compensation in next section.

```
N59 X-33.679 Y37.823 Z171.866 B54.303 C23.051 F2636.311;
N60 X-34.719 Y39.788 Z171.483 B54.467 C22.533 F2109.089;
N61 X-35.546 Y41.359 Z171.165 B54.596 C22.118 F2636.337;
N62 X-36.571 Y43.322 Z170.752 B54.754 C21.599 F2109.081;
N63 X-37.384 Y44.891 Z170.411 B54.878 C21.184 F2636.322;
N64 X-38.389 Y46.851 Z169.97 B55.029 C20.664 F2109.081;
N65 X-39.387 Y48.809 Z169.514 B55.177 C20.144 F2109.094;
N66 X-40.373 Y50.765 Z169.042 B55.321 C19.623 F2109.085;
N67 X-41.156 Y52.331 Z168.652 B55.434 C19.205 F2636.33;
N68 X-42.126 Y54.284 Z168.151 B55.572 C18.683 F2109.087;
N69 X-42.892 Y55.844 Z167.74 B55.679 C18.265 F2636.331;
N70 X-43.842 Y57.792 Z167.213 B55.81 C17.742 F2109.086;
N71 X-44.598 Y59.349 Z166.778 B55.913 C17.323 F2636.339;
N72 X-45.528 Y61.292 Z166.224 B56.037 C16.799 F2109.073;
N73 X-46.424 Y63.176 Z165.67 B56.155 C16.29 F2170.361;
N74 X-47.308 Y65.059 Z165.103 B56.268 C15.779 F2170.347;
N75 X-48.184 Y66.937 Z164.521 B56.379 C15.269 F2170.346;
N76 X-49.047 Y68.811 Z163.927 B56.485 C14.758 F2170.352;
N77 X-49.904 Y70.683 Z163.317 B56.589 C14.246 F2170.339;
N78 X-50.747 Y72.55 Z162.696 B56.688 C13.734 F2170.363;
N79 X-51.581 Y74.411 Z162.061 B56.784 C13.222 F2170.355;
N80 X-52.407 Y76.27 Z161.412 B56.877 C12.709 F2170.336;
N81 X-53.221 Y78.122 Z160.75 B56.966 C12.196 F2170.362;
N82 X-54.023 Y79.97 Z160.077 B57.051 C11.683 F2170.334;
N83 X-54.817 Y81.813 Z159.39 B57.133 C11.169 F2170.372;
```

Figure 5-8 Original G-code for machining the cone frustum

```
N59 X-33.6068 Y37.7942 Z171.78 B54.3 C23.0503 F2636.311;
N60 X-34.6465 Y39.7592 Z171.3968 B54.464 C22.5323 F2109.089;
N61 X-35.4733 Y41.3302 Z171.0787 B54.593 C22.1173 F2636.337;
N62 X-36.498 Y43.2932 Z170.6656 B54.751 C21.5983 F2109.081;
N63 X-37.3107 Y44.8622 Z170.3245 B54.875 C21.1833 F2636.322;
N64 X-38.3154 Y46.8222 Z169.8834 B55.026 C20.6633 F2109.081;
N65 X-39.3132 Y48.7802 Z169.4273 B55.174 C20.1434 F2109.094;
N66 X-40.2989 Y50.7362 Z168.9551 B55.318 C19.6224 F2109.085;
N67 X-41.0817 Y52.3023 Z168.5651 B55.431 C19.2044 F2636.33;
N68 X-42.0514 Y54.2553 Z168.0639 B55.569 C18.6824 F2109.087;
N69 X-42.8172 Y55.8153 Z167.6529 B55.676 C18.2644 F2636.331;
N70 X-43.7669 Y57.7633 Z167.1258 B55.807 C17.7414 F2109.086;
N71 X-44.5227 Y59.3203 Z166.6907 B55.91 C17.3224 F2636.339;
N72 X-45.4525 Y61.2633 Z166.1366 B56.034 C16.7984 F2109.073;
N73 X-46.3482 Y63.1473 Z165.5825 B56.152 C16.2894 F2170.361;
N74 X-47.232 Y65.0303 Z165.0154 B56.265 C15.7784 F2170.347;
N75 X-48.1078 Y66.9083 Z164.4333 B56.376 C15.2684 F2170.346;
N76 X-48.9705 Y68.7823 Z163.8392 B56.482 C14.7574 F2170.352;
N77 X-49.8273 Y70.6543 Z163.2292 B56.586 C14.2454 F2170.339;
N78 X-50.6701 Y72.5213 Z162.6081 B56.685 C13.7334 F2170.363;
N79 X-51.5039 Y74.3823 Z161.973 B56.781 C13.2214 F2170.355;
N80 X-52.3297 Y76.2413 Z161.324 B56.874 C12.7084 F2170.336;
N81 X-53.1435 Y78.0933 Z160.6619 B56.963 C12.1954 F2170.362;
N82 X-53.9453 Y79.9413 Z159.9888 B57.048 C11.6824 F2170.334;
N83 X-54.7391 Y81.7843 Z159.3018 B57.13 C11.1684 F2170.372;
```

a

```
N59 X-33.6254 Y37.8442 Z171.866 B54.3 C23.0517 F2636.311;
N60 X-34.6645 Y39.809 Z171.483 B54.464 C22.5337 F2109.089;
N61 X-35.4908 Y41.3799 Z171.165 B54.593 C22.1187 F2636.337;
N62 X-36.5149 Y43.3427 Z170.752 B54.751 C21.5997 F2109.081;
N63 X-37.3272 Y44.9115 Z170.411 B54.875 C21.1847 F2636.322;
N64 X-38.3314 Y46.8712 Z169.97 B55.026 C20.6647 F2109.081;
N65 X-39.3285 Y48.829 Z169.514 B55.174 C20.1447 F2109.094;
N66 X-40.3137 Y50.7847 Z169.042 B55.318 C19.6237 F2109.085;
N67 X-41.096 Y52.3505 Z168.652 B55.431 C19.2057 F2636.33;
N68 X-42.0652 Y54.3032 Z168.151 B55.569 C18.6837 F2109.087;
N69 X-42.8306 Y55.8629 Z167.74 B55.676 C18.2657 F2636.331;
N70 X-43.7797 Y57.8106 Z167.213 B55.807 C17.7426 F2109.086;
N71 X-44.5351 Y59.3673 Z166.778 B55.91 C17.3236 F2636.339;
N72 X-45.4643 Y61.31 Z166.224 B56.034 C16.7996 F2109.073;
N73 X-46.3596 Y63.1936 Z165.67 B56.152 C16.2906 F2170.361;
N74 X-47.2428 Y65.0762 Z165.103 B56.265 C15.7796 F2170.347;
N75 X-48.1181 Y66.9538 Z164.521 B56.376 C15.2696 F2170.346;
N76 X-48.9803 Y68.8274 Z163.927 B56.482 C14.7586 F2170.352;
N77 X-49.8366 Y70.699 Z163.317 B56.586 C14.2466 F2170.339;
N78 X-50.6789 Y72.5656 Z162.696 B56.685 C13.7346 F2170.363;
N79 X-51.5122 Y74.4261 Z162.061 B56.781 C13.2226 F2170.355;
N80 X-52.3375 Y76.2847 Z161.412 B56.874 C12.7096 F2170.336;
N81 X-53.1508 Y78.1362 Z160.75 B56.963 C12.1966 F2170.362;
N82 X-53.9522 Y79.9837 Z160.077 B57.048 C11.6836 F2170.334;
N83 X-54.7455 Y81.8262 Z159.39 B57.13 C11.1696 F2170.372;
```

b

Figure 5-9 a) compensated G-code b) optimized compensated G-code for machining the cone frustum

5.7.4 Discussion on simulation results

a) Compensability ratio comparison

The compensability ratios defined in Eq. 5-19 and Eq. 5-20, are calculated at each programmed point (different B-axis positions) for the cone frustum machining and curve slot machining and

are shown in Figure 5-10 and Figure 5-11 respectively. Relatively higher ratios (up to 5 for cone frustum and up to 14 for the curve slot) are observed when B-axis approaches zero. Such values are still proportional and show the commensurability between the required axes motions and volumetric error values. However, the remained volumetric error after compensation may be calculated for such critical points using the mathematical model and all relevant error components checked to be fully compensated.

b)

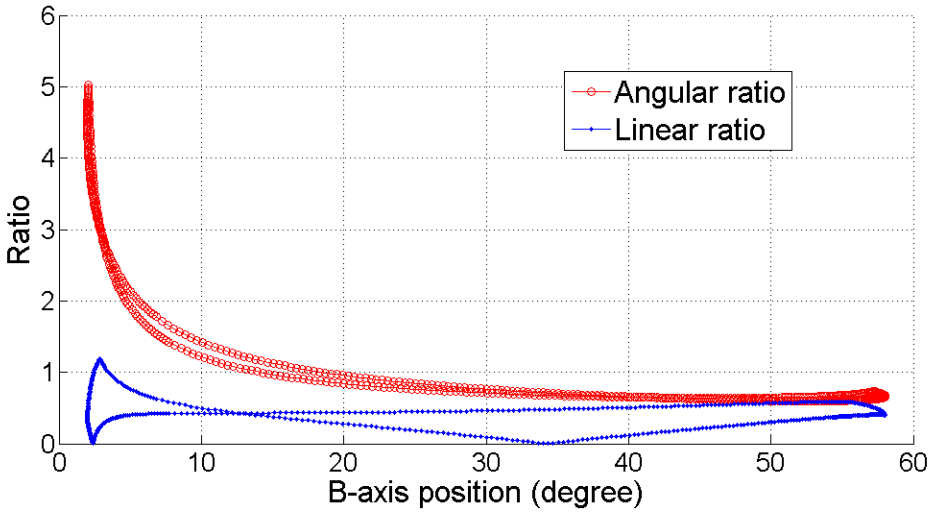

Figure 5-10 Compensability ratio at working points of the cone frustum machining trajectory

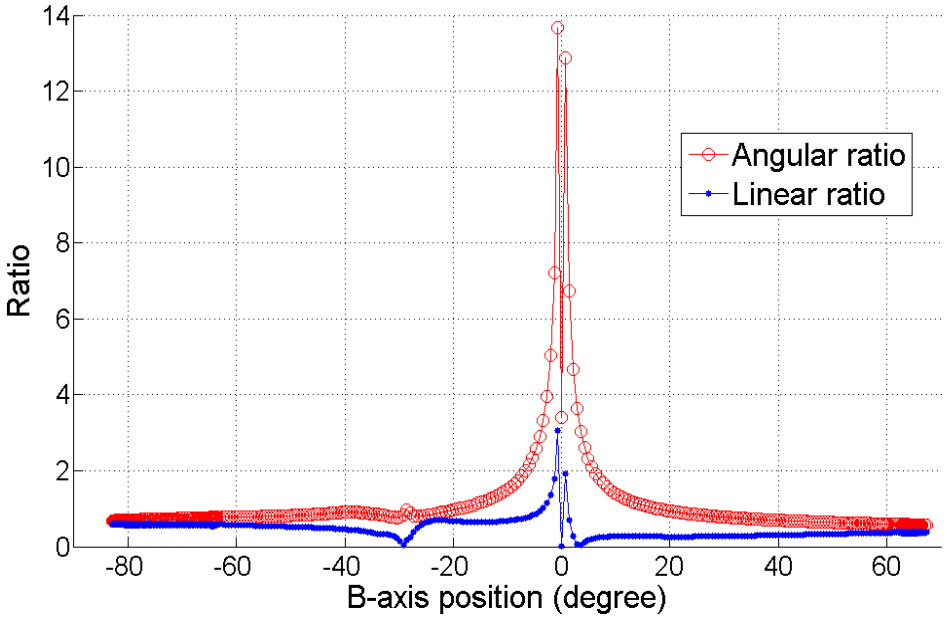

Figure 5-11 Compensability ratio at working points of the curve slot machining trajectory

c) Required axes movement for compensation

If the required modifications in axes positions are calculated and compared for the two compensation strategies (regular and optimized), it is expected that less axis movement modifications are required with the optimized compensation. Figure 5-12 illustrates the axis motion 1-norm (sum of the absolute values of the axes motions modifications at different B-axis positions) during machining of the cone for the two compensation strategies. This comparison is made separately for linear axes and rotary axes motions since the corresponding units are different.

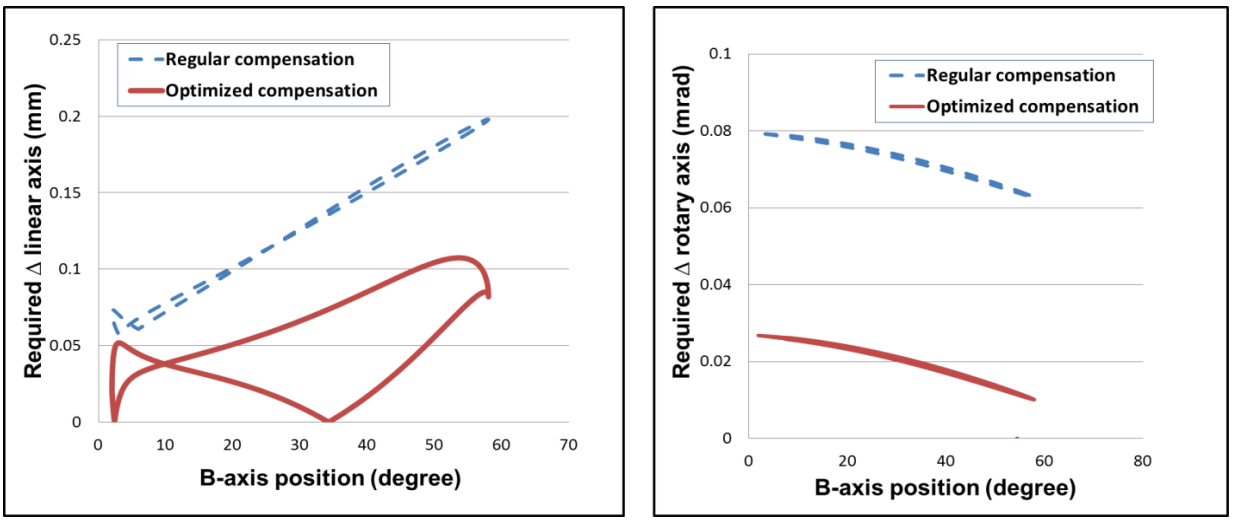

Figure 5-12 Required a) linear b) rotary axes movement for regular and optimized compensation of cone frustum machining

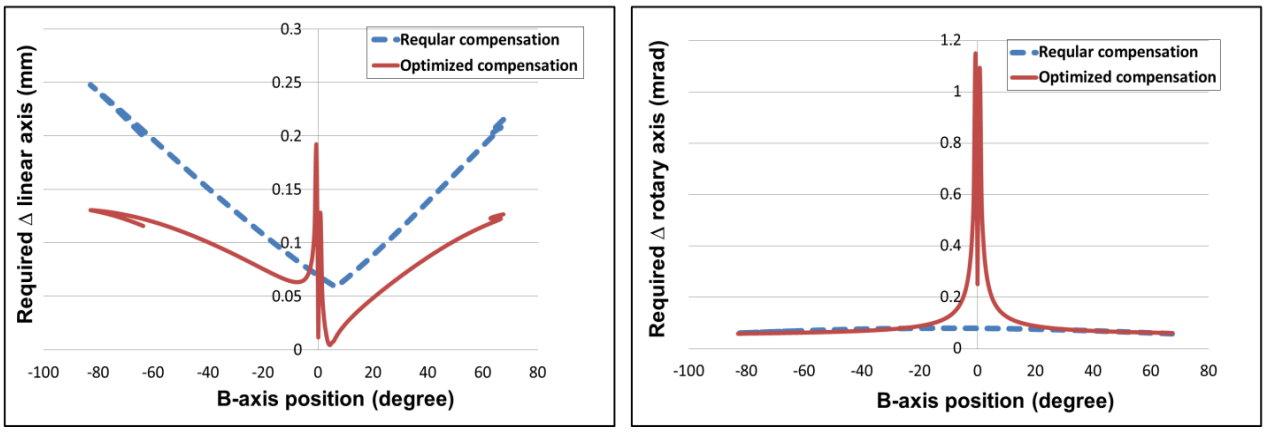

Figure 5-13 Required a) linear b) rotary axes movement for regular and optimized compensation of curve machining

The same comparison is made for machining of the curved slot. Figure 5-13 reveals less required changes in the axes command for optimized compensation. An unexpected increase in the required axes motion occurs at a few working points (when B-axis approaches zero) in which the compensability ratio is relatively higher but still indicating commensurability between Δaxis and volumetric error, as explained in the last section (Figure 5-11). The required axes motion goes up to 0.2 mm for linear axes and up to 1.15 mrad for rotary axes that could be explained regarding the less constraints for optimized compensation. Since, in optimized compensation, the irrelevant errors are not controlled, the constraints imposed to the machine axes are released.

Comparing the components of volumetric error values before and after compensation indicates the error compensability in such critical area. Table 5-3 illustrates the values for the linear and angular ratios, Δlinear axis and also Δrotary axis for six programmed points located close to the singularity area of the machine tool (b=0) and with the highest ratios. The sum of the linear and angular components of the volumetric error before and after (both regular and optimized) compensation at the same critical points is calculated using the mathematical model of the machine and listed in Table 5-4 as well. As seen in Table 5-3, relatively higher changes in linear and rotary axes commands are required for optimized compensation compared to the regular one especially at the points 2 and 5. However, Table 5-4 shows negligible residual volumetric error after compensation in these two points.

The fact is that angular error components can be corrected only with rotary axes motions and so extra translational errors may be produced and added to the original linear error components. This explains the relatively larger changes in linear axes commands. Based on Table 5-4, the linear error components at all critical points can be cancelled after either regular or optimized compensation, but the angular components cannot be fully compensated using regular strategy. Except two singular points of the machine (points 3 and 4 in which b=0), the angular components are effectively compensated using optimized compensation. A residual value for angular error component (around 13 μrad) is observed in such singular points that could be flagged as an uncompensable error in the curve slot machining.

Table 5-3 Compensability ratio and required Δaxis at critical points in curve slot machining

Working point	b value (degree)	Linear ratio	Angular ratio	Required Δ linear axis (mm)		Required Δ rotary axis (mrad)	
				Reg.	Opt.	Reg.	Opt.
1	-1.412	0.93	6.18	0.067	0.054	0.079	0.572
2	-0.707	2.15	11.80	0.068	0.128	0.079	1.090
3	0	0.18	2.73	0.069	0.011	0.079	0.252
4	0	0.18	2.73	0.069	0.011	0.079	0.252
5	0.671	3.07	12.46	0.070	0.190	0.079	1.150
6	1.341	1.82	6.50	0.071	0.115	0.079	0.599

Table 5-4 Comparison of the predicted volumetric error before and after compensation at critical points in curve slot machining

Working point	b value (degree)	Linear error component (mm)			Angular error component (mrad)		
		Before	Reg. comp.	Opt. comp.	Before	Reg. comp.	Opt. comp.
1	-1.412	0.058	0.000	0.000	0.092	0.012	0.000
2	-0.707	0.060	0.000	0.000	0.092	0.013	0.000
3	0	0.061	0.000	0.000	0.092	0.013	0.013
4	0	0.061	0.000	0.000	0.092	0.013	0.013
5	0.671	0.062	0.000	0.000	0.092	0.013	0.000
6	1.341	0.063	0.000	0.000	0.092	0.012	0.000

The direction of the axes motions are also checked for all working points in the case of cone frustum and curve slot machining and no change in motion direction is observed. Note that the positioning accuracy characteristics of the axes such as backlash errors may differ upon a direction change and this would affect the accuracy improvement in compensation process. The ability of the machine to correctly accomplish small movements is not considered in this work.

5.7.5 Measurements results and discussion

The features on the three test pieces (uncompensated, regular compensated and optimized compensated) are measured on the CMM using a probe stylus tip with diameter Ø=4 mm.

a) Holes

The measurement results for the holes are summarized in Table 5-5. Comparing the circularity error of the machined holes shows a small variation (less than a few micrometers) in all cases. Such variation can be neglected considering the uncertainty of the measurements. Since the form of the holes (including circularity) is expected to be largely related to the drilling process, no significant change in form related errors is expected before and after compensation.

Table 5-5 Comparison of circularity errors for the holes

Feature	**Circularity error (µm)**		
	No compensation	Regular comp.	Optimized comp.
Hole 1	11	9	4
Hole 2	8	8	7
Hole 3	7	3	4

b) Flat surface

The deviation from a plane for the face milled surface is shown in Figure 5-14. The residual vectors are smaller for the regular and optimized compensated cases compared to the uncompensated one. Calculated flatness error and the standard deviation of residuals for flat surfaces are listed in Table 5-6. Flatness error and standard deviation values are reduced by around 50% for both compensation strategies.

Table 5-6 Comparison of flatness errors for the flat surface

Parameter	No compensation	Regular comp.	Optimized comp.
Flatness error (µm)	10	4	5
Standard deviation of residuals (µm)	2	1	1

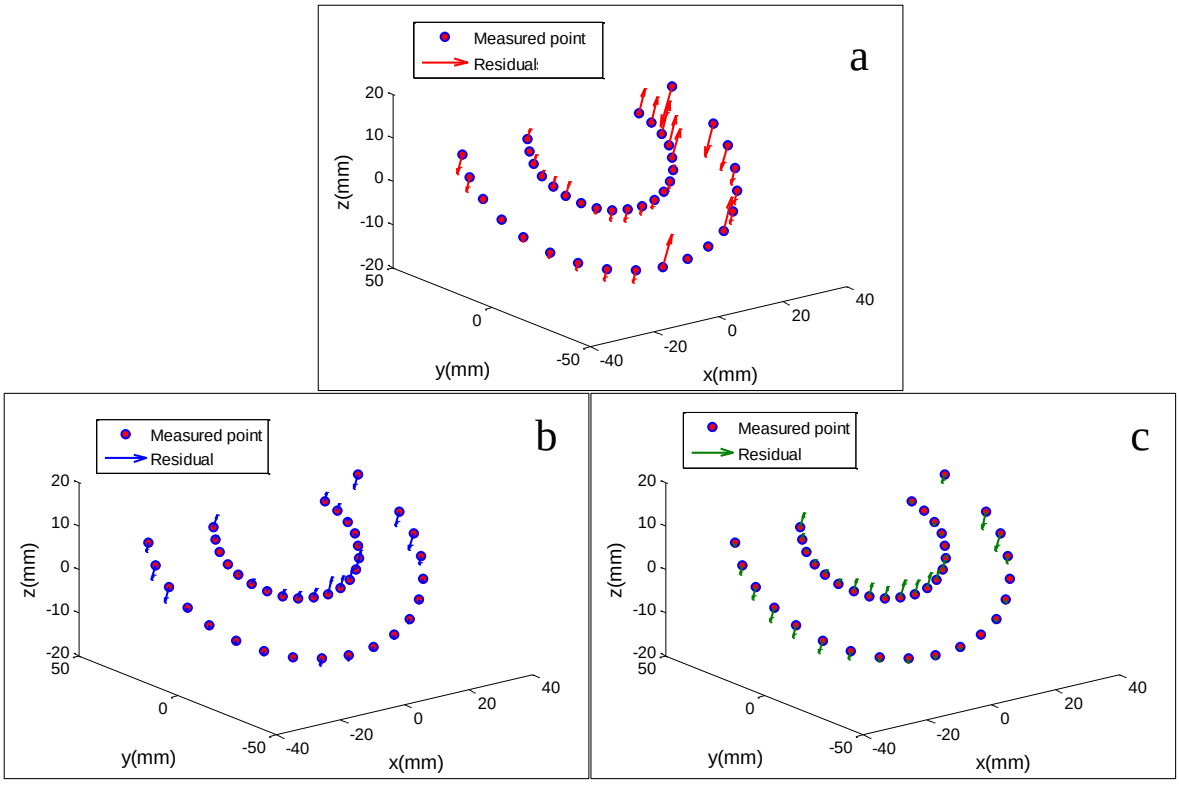

Figure 5-14 Best fit residuals for the flat surface, magnified 2000X; a) uncompensated, b) regular compensated and c) optimized compensated plane

c) Cone frustum

A conical surface is fitted to the measured points of the cones and the residual distances are shown in Figure 5-15 as residual vector at each point. The length of residual distance vectors are significantly decreased after compensation at most of the points. Statistical parameters such as range of the residual distances (maximum residual minus minimum residual) and standard deviation are also listed in Table 5-7. The results show 15% to 35% reduction for those parameters.

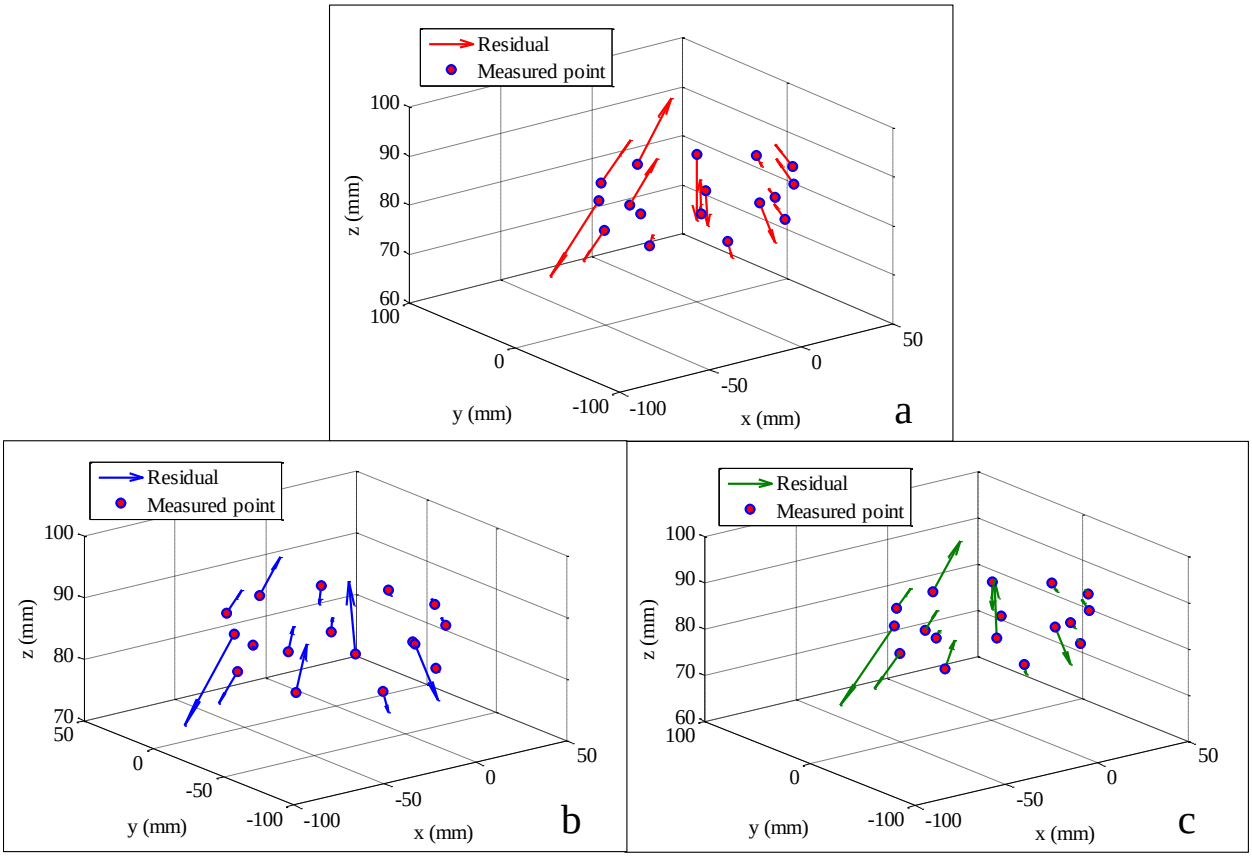

Figure 5-15 Best fit residuals for the cone surface, magnified 1000X; a) uncompensated, b) regular compensated and c) optimized compensated cone

Table 5-7 Residual analysis of the cone frustum measurement

Parameter	No compensation	Regular comp.	Optimized comp.
Range of residual distances (µm)	66	47	56
Standard deviation of residuals (µm)	17	11	13

d) Curved slot

In the case of curved slot on the spherical surface, two different surfaces are measured; the points on the slot sidewall and the points on the bottom which are nominally located on a sphere. Best fit residuals from the nominal surfaces for the sidewall and bottom surface points are illustrated

in Figure 5-16 and Figure 5-17, respectively. The range of the residual distances and standard deviation values are also listed in Table 5-8 and Table 5-9.

Table 5-8 Residual analysis of the curve sidewall measurement

Parameter	No compensation	Regular comp.	Optimized comp.
Range of residual distances (μm)	64	51	59
Standard deviation of residuals (μm)	11	8	10

Table 5-9 Residual analysis of the curve depth measurement

Parameter	No compensation	Regular comp.	Optimized comp.
Range of residual distances (μm)	72	27	30
Standard deviation of residuals (μm)	19	5	8

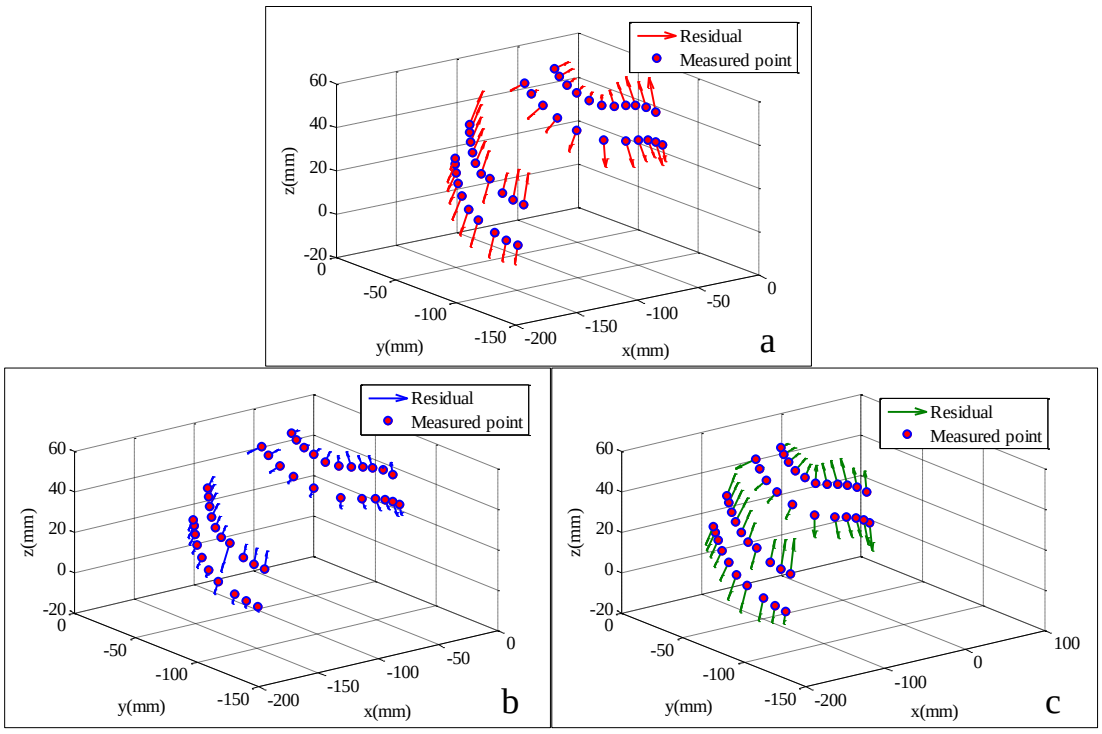

Figure 5-16 Best fit residuals for the curve sidewall, magnified 1000X; a) uncompensated, b) regular compensated and c) optimized compensated slot

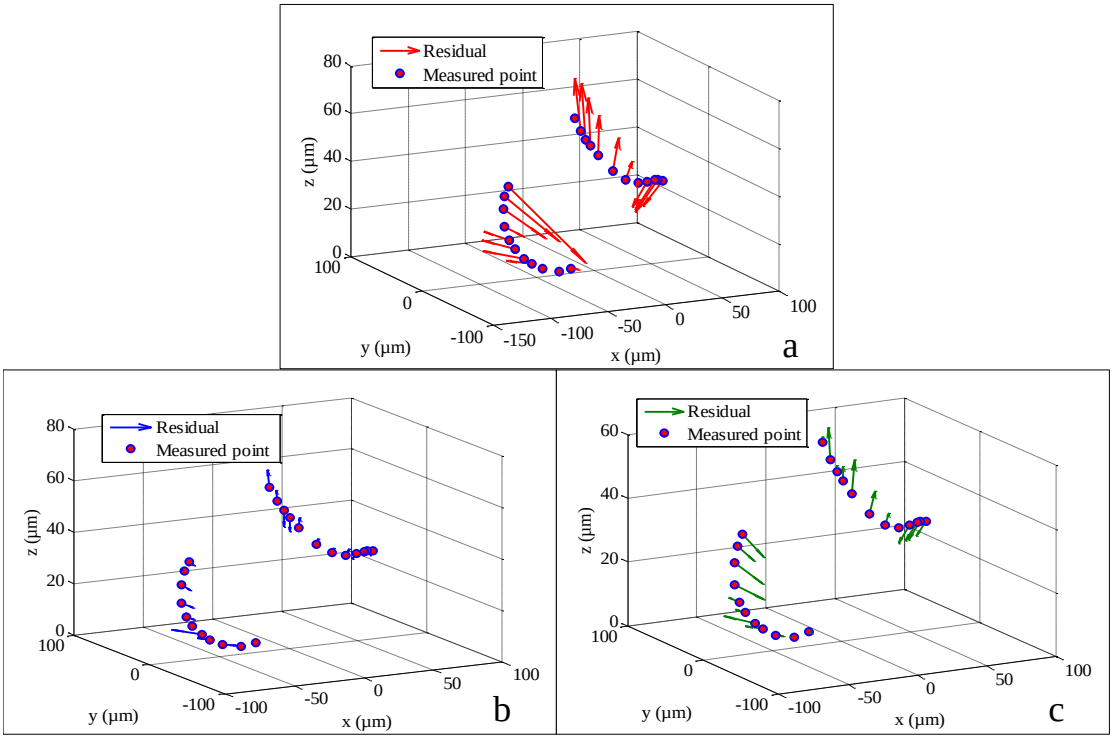

Figure 5-17 Best fit residuals for the curve depth, magnified 1500X; a) uncompensated, b) regular compensated and c) optimized compensated slot

The length of the residual distance vectors are significantly decreased after both regular and optimized compensation. Comparing the calculated statistical parameters for curved slot, a slight residual reduction for the sidewall and around 60% residual reduction for the bottom (spherical surface) are observed.

In both compensation strategies, position and orientation errors of the machine joints (inter-axis geometric error), as the main source of the machining errors are considered in the calculations. The effect of the other error sources were assumed to be negligible since the test was done for only finishing step and also aluminum parts were selected to minimize the thermal and force-induced errors. So, even after compensation, some residuals may be observed for the features' form.

In general, the residual ranges are mostly reduced after both regular and optimized compensation of the features. However, in the case of the flat surface and the curve depth, a very small (less than 3 μm) difference between the residual of regular and optimized compensation can be observed. In the cases of the cone and the curve side surface, the residuals are less after compensation but not as much as for the other features. Only form errors of the features' surfaces are measured and compared in this paper. Therefore, work is underway to conduct new tests in which the positioning errors such as holes' centre position or other positioning errors of the features could be measured and compared with respect to datum features.

5.8 Conclusion

Two new notions were introduced in five-axis machining error compensation and G-code modification. The concept of "error relevance" was described regarding the insensitivity of a machining process to some volumetric error components. In other words, only the relevant errors have to be taken into consideration in a compensation strategy and it is not necessary to make effort for the correction of those errors which are not affecting the accuracy of the machined feature. A filtration matrix was defined to mathematically obtain the relevant volumetric error vector.

The concept of "compensability" comes from the machine tool capability to correct the volumetric error components by making small and proportional variations in machine axis positions. If some of the residual volumetric error components after compensation is not negligible (i.e., volumetric error is not fully compensated due to singularity condition, for

example) or the volumetric error and calculated $\Delta axis$ are not commensurate (i.e., large changes in axes position are required to cancel the error), that part is considered as “uncompensable”.

The data of compensability ratio may not be enough to determine the capability of the machine to compensate the errors. It is recommended to check the values of volumetric errors before and after compensation, required axes motions and also machining conditions (such as depth of cut) where the compensability ratio approaches the maximum values especially in machine singularity area. The least command increments of the machine tool may also be considered for too low compensability ratios. The compensation axes positions shall be checked to see whether or not the motion directions change after compensation. Since, any change in axes motion direction may influence the positioning accuracy characteristics of the axes (such as backlash error, etc.).

Considering only relevant and compensable errors in the compensation procedure yields an optimized compensation in which there is no unnecessary or excessive change in axes commands while the accuracy is still effectively improved.

Optimized compensation was implemented to machine a test piece containing four features (hole, flat surface, curved slot and cone frustum) and compared with the results of the regular compensation. 1-norm of the linear and angular compensations were considerably reduced (up to 75%) at most of the points. Best fit residual analysis is also done for the features. For example, 60% reduction was found for the residuals range after regular and optimized compensation of the bottom surface of the curved slot.

5.9 Acknowledgements

The authors greatly appreciated the support of CNC machine technician, Guy Gironne, during the experimental validations and also CMM technician, François Menard, for the part metrology. The authors also acknowledged the collaboration of Rahman Mizanur in the best fit residual analysis section. This research was supported by the NSERC Canadian Network for Research and Innovation in Machining Technology (NSERC CANRIMT; www.nserc-canrimt.org).

5.10 References

Abbaszadeh-Mir, Y., J. R. R. Mayer, G. Cloutier and C. Fortin (2002); "Theory and simulation for the identification of the link geometric errors for a five-axis machine tool using a telescoping magnetic ball-bar." *International Journal of Production Research* 40(Compendex): 4781-4797.

Donmez, M. A., D. S. Blomquist, R. J. Hocken, C. R. Liu and M. M. Barash (1986); "A general methodology for machine tool accuracy enhancement by error compensation." *Precision Engineering* 8(4): 187-196.

Givi, M. and J. R. R. Mayer (2014); "Volumetric error formulation and mismatch test for five-axis CNC machine compensation using differential kinematics and ephemeral G-code." *The International Journal of Advanced Manufacturing Technology*: 1-9.

Hong, C., S. Ibaraki and A. Matsubara (2011); "Influence of position-dependent geometric errors of rotary axes on a machining test of cone frustum by five-axis machine tools." *Precision Engineering* 35(1): 1-11.

Ihara, Y., & Tanaka, K. (2005); "Ball bar measurement equivalent to cone frustum cutting on multi-axis machine: Comparison of ball bar measurement with cutting test on spindle-tilt type 5-axis MC." *Journal of the Japan Society for Precision Engineering* 71(12): 1553-1557.

ISO230-1, (2012); "Test code for machine tools-part 1 : geometric accuracy of machines operating under no-load or quasi-static conditions.".

ISO10791-7, (2014); "Test conditions for machining centres – Part 7: Accuracy of finished test pieces."

ISO/TR16907, (2015); "Machine tools-Numerical compensation of geometric errors.".

Jing, H. J., Yao, Y. X., Chen, S. D., & Wang, X. P. (2006); "Machining accuracy enhancement by modifying NC program." *Advances in machining and manufacturing technology eighth*: 71-75.

Lei, W. T. and Y. Y. Hsu (2003); "Accuracy enhancement of five-axis CNC machines through real-time error compensation." *International Journal of Machine Tools and Manufacture* 43(9): 871-877.

Liebrich, T., B. Bringmann and W. Knapp (2009); "Calibration of a 3D-ball plate." *Precision Engineering* 33(1): 1-6.

Mayer, J. R. R. (2012); "Five-axis machine tool calibration by probing a scale enriched reconfigurable uncalibrated master balls artefact." *CIRP Annals - Manufacturing Technology* 61(1): 515-518.

NAS979, (1969); "Uniform cutting test—NAS series. Metal cutting equipments."

Paul, R. P., B. Shimano and G. E. Mayer (1981); "Differential kinematic control equations for simple manipulators." *Systems, Man and Cybernetics, IEEE Transactions* 11(6): 456-460.

Press, W. H. (1992). Numerical recipes in Fortran 77: the art of scientific computing, Cambridge university press.

Schwenke, H., W. Knapp, H. Haitjema, A. Weckenmann, R. Schmitt and F. Delbressine (2008); "Geometric error measurement and compensation of machines—an update." *CIRP Annals - Manufacturing Technology* 57(2): 660-675.

Srivastava, A. K., S. C. Veldhuis and M. A. Elbestawit (1995); "Modelling geometric and thermal errors in a five-axis cnc machine tool." *International Journal of Machine Tools and Manufacture* 35(9): 1321-1337.

Yu, S. and J. M. Hollerbach; "Observability index selection for robot calibration". *Robotics and Automation, 2008. ICRA 2008. IEEE International Conference on*. 2008.

CHAPTER 6 GENERAL DISCUSSION

The general discussion of the thesis including the most important outcomes of the different steps of the study is provided as follows.

In the first phase of the work, a frame named “desired cutter location (DCL)” is introduced and added as the last chain of the workpiece branch. This effectively helps in definition of the volumetric error as the difference between nominal and actual tool. This definition approach is more general and beneficial in the field of five-axis machining since:

- the difference of the actual tool (position and orientation) and the actual feature (or workpiece) frame which is commonly considered in the literature as a criterion for volumetric error definition does not appear to be a good basis of comparison. Specifically, the orientation of the tool frame does not nominally coincide with the feature frame in some machining operations such as milling of a curved surface with a ball-nose end tool. Definition of the DCL frame makes it possible to generally determine the desired tool location based on the machining operation alone.
- this also helps to calculate the deviations of the desired (ideal) location of the actual tool related to the erroneous one and then, present it in the form of a volumetric error HTM, ${}^{\mathrm{DCL}}T_{\mathrm{t}'}{}^{\mathrm{actual}}$.
- the three positional components and three orientation components of the volumetric error can be extracted from the HTM matrix and taken into consideration for error relevance in the optimization phase.
- three positional components of the volumetric error twist can be graphically presented in 3D workspace as shown in the first article.
- this formulation of the volumetric error solely relies on the axes commands extracted from the G-code as well as the machine error parameters. This provides the possibility of an on-line scheme for compensation.

The local linearization hypothesis is used in different phases of the research in the form of the differential Jacobian matrix expressing the relation between differential changes in machine joint (axis) coordinates and the tool to workpiece Cartesian coordinates. The proposed compensation

formula is derived based on such local linear relation. The required $\Delta axis$ to produce the correction vector could be calculated using only the Jacobian matrix. However, since a linear system is assumed for the machine tool, an iterative approach is applied to find a numerically exact solution for $\Delta axis$ when large machine errors are present. For the proposed validation strategy also, the differential directional Jacobian is again applied for sensitivity analysis of the machining patterns to the geometric link errors. As detailed in the second article, the effect of the multiple machine geometric error parameters combines to produce a volumetric error on the machined part and at each machining point. So, some of them may cancel each other. Therefore, the proposed strategy for compensation validation can be applied to assess the "overall" accuracy improvement of the machine but not to find the effect of each error source separately.

The compensation method needs information of the estimated link geometric errors to model the erroneous machine. The results of geometric link errors estimation may change during a machine tool life due to crashes, accidents, loads from machining processes, environmental conditions etc. Two different sets of estimated link errors, gathered at a few months interval, were used for the experimental validation and compensation effectiveness was validated (88% to 91% improvements) for both sets. To get the most precise result, the latest available estimated values are used for the compensation calculations during the experimental tests in all phases of the work.

In optimized compensation, the geometry of the feature must be known in order to extract the relevant errors while the regular error compensation itself, can be implemented solely based on the G-code and machine errors parameters. Tool type and geometry also influence the error relevance. In the case of ball-end cutter face milling, for instance, small orientation errors do not leave any geometric defect on the machined surface and thus, do not require compensation. However, if a flat-end mill is used for the same operation and feature, the tool tilt angles become relevant.

Unnecessary G-code modifications are avoided in the optimized compensation and so less axes motions are required. The relevant errors are minimized in both compensation strategies while no attempt is made to compensate or control the irrelevant errors in optimized compensation. The values of irrelevant errors may become even larger after compensation. Therefore, the norm of the whole volumetric error vector (including both relevant and irrelevant components) may not be an appropriate criterion for comparison and validation purpose.

CHAPTER 7 CONCLUSION AND RECOMMENDATIONS

This chapter includes the conclusions of the thesis. Recommendations for future works are also listed.

7.1 Conclusion and contributions of the work

This thesis presented an integrated methodology for modeling the machine errors, compensation, its validation and optimization. The main contributions are summarized as below;

- a general formulation for calculation of the volumetric error twist (including translational and angular components) of a five-axis machine tool is proposed. A desired cutter location (DCL) frame is defined and used to complete the workpiece branch kinematic chain when multiplying the HTMs.
- an off-line compensation scheme is proposed based on the original axes commands (extracted from the original G-code) and the machine geometric errors information. The required adjustments in the G-code are then calculated assuming a local linearization and used to generate an ephemeral compensated G-code to be finally executed by the machine controller.
- an “all on-machine” fully automated experimental validation of the effectiveness of error compensation is proposed. A series of unidirectional machining patterns are performed on a pre-designed part where surface mismatches appear due to the machine errors. This is repeated with both uncompensated and compensated G-code on the same part. The cutter tool is replaced with a touch trigger probe for on-machine measurement (OMM) using the erroneous machine itself and without removing the part. Unidirectional probing is done in a small volume and so, provides accurate and reliable results.
- the introduced validation strategy is effective, fast and accurate and does not need CMM or other independent measurement devices. A compensation effectiveness of about 65% to 99% for the machined slots is observed using this strategy.
- amongst the volumetric error components, only “relevant” components which are affecting the total accuracy of the machined feature require compensation. Considering the machining process, the feature to be machined and also the tool geometry, a filtration

matrix is defined to mathematically filter out the irrelevant errors in the compensation process.

- Machine tool capability to correct the volumetric error components by making “small” or relatively commensurate variations in machine axes positions is quantified and verified with regard to a new notion definition, i.e. “compensability ratio” in five-axis machining. Uncompensable parts of the volumetric error can be predicted and flagged. So, no effort is made to correct them in the compensation process.
- Considering only relevant and compensable errors in the compensation procedure yields an optimized compensation in which there is no unnecessary or excessive change in axes commands (around 75% reduction in required axes motions in case of cone frustum machining, for example) while the same accuracy is reached compared to a regular compensation strategy.

7.2 Recommendations for future works

Regarding the research contributions and proposed approaches in error compensation and its validation for five-axis machine tools, the following subjects are suggested for future work;

- The compensation function needs the original axes commands as explained in the first article. Each command line of a five-axis machining G-code usually starts with G01 which is followed by the original axes commands corresponding to a specific working point. However, in some machining cases, other terms of G-code may appear (such as G02 for circular trajectories) to command the machine axes drivers. Study on how to extract the machine axes positions for working points for such trajectories could be conducted to generalize the G-code modification strategy for error compensation.
- the proposed validation strategy in the fourth chapter was implemented to compare the slots machined using uncompensated and compensated G-code. In other words, the effectiveness of G-code modification method was verified while the mismatch producing test can be used to validate any compensation strategy. It could be proven and experimentally shown if other possible compensation strategies (such as tool path correction in post processing step or real-time compensation) are implemented for machining the compensated slots.

- in the fourth chapter, the sensitivity of the machining patterns to the machine geometric link errors was analyzed. It revealed that none of the proposed machining patterns can sensitively detect the E_{BOZ} link error. A machining pattern could be imagined and performed to detect this remaining link error too.
- as mentioned in the fifth chapter, the error relevance depends on the machining operation, the feature to be machined and also the tool geometry. Some common features were already considered and tested for validation while there are still other features or tools with different geometry that could be tested. For example, optimization of the compensation can be validated in machining of a spherical surface or a flat surface using bull-end mill and ball-end mill and then compared to verify the effect of the applied tool geometry on error relevance in such cases.
- in numerical error compensation for machine tools, it may happen that some axes which are not nominally programmed are driven for the sake of error correction. For example, when a pure X-axis motion is programmed, additional small motions of Y-and Z-axis maybe executed to compensate the straightness errors of X-axis. This may results in unwanted errors or surface degradation. This could be experimentally examined so that the effect of compensation optimization on surface roughness would be approved.
- most modern industrial controllers provide entry points for compensation of some geometric errors. Such CNC controllers may contain error tables and spatial error grid tables. The limitations of their application should be studied and compared to the proposed strategies for error compensation. The development of industrial controllers using the proposed strategies also could be the subject of future works.
- the proposed integrated machine modeling, volumetric error compensation and its validation and also compensation optimization could be collected in a fully automatic process developing a software package for machine tools. This would help in the industrialization of this research work.

BIBLIOGRAPHY

Abbaszadeh-Mir, Y., J. R. R. Mayer, G. Cloutier and C. Fortin (2002); "Theory and simulation for the identification of the link geometric errors for a five-axis machine tool using a telescoping magnetic ball-bar." *International Journal of Production Research* 40(Compendex): 4781-4797.

Allen, J., S. Postlethwaite and D. Ford; "Practical application of thermal error correction--four case studies". *3rd International conference on Laser Metrology and Machine Performance- LAMDAMP*. 1997.

Andolfatto, L., S. Lavernhe and J. R. R. Mayer (2011); "Evaluation of servo, geometric and dynamic error sources on five-axis high-speed machine tool." *International Journal of Machine Tools and Manufacture* 51(10-11): 787-796.

Attia, M. H. and L. Kops (1979); "Nonlinear Thermoelastic Behavior of Structural Joints—Solution to a Missing Link for Prediction of Thermal Deformation of Machine Tools." *Journal of Manufacturing Science and Engineering* 101(3): 348-354.

Bryan, J. (1990); "International Status of Thermal Error Research (1990)." *CIRP Annals - Manufacturing Technology* 39(2): 645-656.

Bryan, J. B. (1982); "A simple method for testing measuring machines and machine tools. Part 2: Construction details." *Precision Engineering* 4(3): 125-138.

Cano, T., F. Chapelle, J. M. Lavest and P. Ray (2008); "A new approach to identifying the elastic behaviour of a manufacturing machine." *International Journal of Machine Tools and Manufacture* 48(14): 1569-1577.

Chen, J., J. Yuan, J. Ni and S. Wu (1992); "Compensation of non-rigid body kinematic effect on a machining center." *Transaction of NAMRI* 20(9): 325-329.

De Meter, E. and M. Hockenberger (1997); "The application of tool path compensation for the reduction of clampinginduced geometric errors." *International journal of production research* 35(12): 3415-3432.

Denavit, J. (1955); "A kinematic notation for lower-pair mechanisms based on matrices." *Trans. of the ASME. Journal of Applied Mechanics* 22: 215-221.

Donmez, M. A., D. S. Blomquist, R. J. Hocken, C. R. Liu and M. M. Barash (1986); "A general methodology for machine tool accuracy enhancement by error compensation." *Precision Engineering* 8(4): 187-196.

Ekinci, T. O. and J. R. R. Mayer (2007); "Relationships between straightness and angular kinematic errors in machines." *International Journal of Machine Tools and Manufacture* 47(12–13): 1997-2004.

Erkan, T., J. R. R. Mayer and Y. Dupont (2011); "Volumetric distortion assessment of a five-axis machine by probing a 3D reconfigurable uncalibrated master ball artefact." *Precision Engineering* 35(1): 116-125.

Everett, L. J. and A. H. Suryohadiprojo; "A study of kinematic models for forward calibration of manipulators". *Robotics and Automation, 1988. Proceedings., 1988 IEEE International Conference on*. 1988.

Givi, M. and J. R. R. Mayer (2014); "Volumetric error formulation and mismatch test for five-axis CNC machine compensation using differential kinematics and ephemeral G-code." *The International Journal of Advanced Manufacturing Technology*: 1-9.

Hocken, B. (1993); "Software Compensation of Precision Machines." *A Report from Precision Engineering Laboratory UNC Charlotte to National Institute of Standards and Technology*.

Hocken, R. J. (1980). Machine tool accuracy. Technology of Machine Tools. California, Lawrence Livermore Laboratory 5.

Hockenberger, M. (1994). Implementing meta-functions into a quasi-static model to analyze workpiece displacement within a machining fixture. The Pennsylvania State University Ph.D., The Pennsylvania State University.

Hong, C., S. Ibaraki and A. Matsubara (2011); "Influence of position-dependent geometric errors of rotary axes on a machining test of cone frustum by five-axis machine tools." *Precision Engineering* 35(1): 1-11.

Hsu, Y. Y. and S. S. Wang (2007); "A new compensation method for geometry errors of five-axis machine tools." *International Journal of Machine Tools and Manufacture* 47(2): 352-360.

Ibaraki, S. and W. Knapp (2012); "Indirect measurement of volumetric accuracy for three-axis and five-axis machine tools: a review." *International Journal of Automation Technology* 6(2).

Ibaraki, S., M. Sawada, A. Matsubara and T. Matsushita (2010); "Machining tests to identify kinematic errors on five-axis machine tools." *Precision Engineering* 34(3): 387-398.

Ihara, Y., & Tanaka, K. (2005); "Ball bar measurement equivalent to cone frustum cutting on multi-axis machine: Comparison of ball bar measurement with cutting test on spindle-tilt type 5-axis MC." *Journal of the Japan Society for Precision Engineering* 71(12): 1553-1557.

ISO230-1, (2012); "Test code for machine tools – Part 1: geometric accuracy of machines operating under no-load or quasi-static conditions."

ISO230-4, (2005); "Test code for machine tools – Part 4: Circular tests for numerically controlled machine tools."

ISO230-7, (2006); "Test code for machine tools – Part 7: Geometric accuracy of axes of rotation."

ISO10791-7, (1998); "Test conditions for machining centres – Part 7: Accuracy of a finished test piece."

ISO10791-7, (2014); "Test conditions for machining centres – Part 7: Accuracy of finished test pieces."

ISO/TR16907, (2015); "Machine tools-Numerical compensation of geometric errors."

J.S. Chen, J. X. Y., J. Ni and S.M. Wu, (1993); "Real-time compensation for time-variant volumetric errors on a machining centre."; *ASME Trans. Journal of Engineering for Industry* 115: pp. 472–479.

Jing, H. J., Yao, Y. X., Chen, S. D., & Wang, X. P. (2006); "Machining accuracy enhancement by modifying NC program." *Advances in machining and manufacturing technology eighth*: 71-75.

Jung, J.-H., J.-P. Choi and S.-J. Lee (2006); "Machining accuracy enhancement by compensating for volumetric errors of a machine tool and on-machine measurement." *Journal of Materials Processing Technology* 174(1–3): 56-66.

Khan, A. and W. Chen (2011); "A methodology for systematic geometric error compensation in five-axis machine tools." *The International Journal of Advanced Manufacturing Technology* 53(5): 615-628.

Koliskor, A. (1971); "Compensating for automatic-cycle machining errors." *Machines and Tooling* 5(41(1)): 1–14.

Koren, Y. (1983). Computer Control of Manufacturing Systems. New York, McGraw-Hill.

Kwon, H. D., Burdekin, M. (1996); "Development and application of a system for evaluating the feed-drive errors on computer numerically controlled machine tools." *Precision Engineering* 19(2-3): 133-140.

Lavernhe, S., C. Tournier and C. Lartigue (2008); "Kinematical performance prediction in multi-axis machining for process planning optimization." *The International Journal of Advanced Manufacturing Technology* 37(5): 534-544.

Lei, W. T. and Y. Y. Hsu (2002); "Accuracy test of five-axis CNC machine tool with 3D probe–ball. Part I: design and modeling." *International Journal of Machine Tools and Manufacture* 42(10): 1153-1162.

Lei, W. T. and Y. Y. Hsu (2003); "Accuracy enhancement of five-axis CNC machines through real-time error compensation." *International Journal of Machine Tools and Manufacture* 43(9): 871-877.

Li, X. (2001); "Real-Time Prediction of Workpiece Errors for a CNC Turning Centre, Part 4. Cutting-Force-Induced Errors." *The International Journal of Advanced Manufacturing Technology* 17(9): 665-669.

Liebrich, T., B. Bringmann and W. Knapp (2009); "Calibration of a 3D-ball plate." *Precision Engineering* 33(1): 1-6.

Lo, C.-H. H. (1994)., "Real-time error compensation on machine tools through optimal thermal error modeling.", Ph.D. 9500988, University of Michigan.

Lu, Y., Li, J.G., Gao, D., Zhou, F. (2011); "Reconstructing NC program-based geometrical error compensation for heavy-duty NC machine tool." *Advanced Materials Research* 314: 2082-2086.

Mahbubur, R. M. D., J. Heikkala, K. Lappalainen and J. A. Karjalainen (1997); "Positioning accuracy improvement in five-axis milling by post processing." *International Journal of Machine Tools and Manufacture* 37(2): 223-236.

Mayer, J. R. R. (2012); "Five-axis machine tool calibration by probing a scale enriched reconfigurable uncalibrated master balls artefact." *CIRP Annals - Manufacturing Technology* 61(1): 515-518.

Mou, J. (1997); "A Method of Using Neural Networks and Inverse Kinematics for Machine Tools Error Estimation and Correction." *Journal of Manufacturing Science and Engineering* 119(2): 247-254.

Mou, J., M. A. Donmez and S. Cetinkunt (1995); "An Adaptive Error Correction Method Using Feature-Based Analysis Techniques for Machine Performance Improvement, Part 1: Theory Derivation." *Journal of Manufacturing Science and Engineering* 117(4): 584-590.

Murray, R. M., Z. Li, S. S. Sastry and S. S. Sastry (1994). A mathematical introduction to robotic manipulation. Boca Raton,, CRC press.

NAS979, (1969); "Uniform cutting test—NAS series. Metal cutting equipments."

Ni, J. (1997); "CNC Machine Accuracy Enhancement Through Real-Time Error Compensation." *Journal of Manufacturing Science and Engineering* 119(4B): 717-725.

Paul, R. P., B. Shimano and G. E. Mayer (1981); "Differential kinematic control equations for simple manipulators." *Systems, Man and Cybernetics, IEEE Transactions* 11(6): 456-460.

Press, W. H. (1992). Numerical recipes in Fortran 77: the art of scientific computing, Cambridge university press.

Ramesh, R., M. A. Mannan and A. N. Poo (2000); "Error compensation in machine tools -- a review: Part I: geometric, cutting-force induced and fixture-dependent errors." *International Journal of Machine Tools and Manufacture* 40(9): 1235-1256.

Ramesh, R., M. A. Mannan and A. N. Poo (2000); "Error compensation in machine tools -- a review: Part II: thermal errors." *International Journal of Machine Tools and Manufacture* 40(9): 1257-1284.

Roberts, L. G. (1966). Homogeneous matrix representation and manipulation of N-dimensional constructs, Massachusetts Institute of Technology Lincoln Laboratory.

S.P. Moylan, D. B., M.L. McGlauflin, R.R. Fesperman, and M.A. Donmez; "Evaluation of Proposed Test Artifacts for Five-Axis Machine Tools". *the 26th ASPE Annual Meeting*. 2011.

Sartori, S. and G. X. Zhang (1995); "Geometric Error Measurement and Compensation of Machines." *CIRP Annals - Manufacturing Technology* 44(2): 599-609.

Schmitz, T. and J. Ziegert (1999); "Examination of surface location error due to phasing of cutter vibrations." *Precision Engineering* 23(1): 51-62.

Schmitz, T. L., J. C. Ziegert, J. S. Canning and R. Zapata (2008); "Case study: A comparison of error sources in high-speed milling." *Precision Engineering* 32(2): 126-133.

Schultschik, R. (1977); "The components of the volumetric accuracy." *Annals of CIRP* 25, No.1: 223-227.

Schwenke, H., W. Knapp, H. Haitjema, A. Weckenmann, R. Schmitt and F. Delbressine (2008); "Geometric error measurement and compensation of machines—an update." *CIRP Annals - Manufacturing Technology* 57(2): 660-675.

Sencer, B., Y. Altintas and E. Croft (2009); "Modeling and Control of Contouring Errors for Five-Axis Machine Tools---Part I: Modeling." *Journal of Manufacturing Science and Engineering* 131(3): 031006-031008.

Spaan, H. A. M. (1995). Software error compensation of machine tools. PhD, Technische Universiteit Eindhoven.

Srivastava, A. K., S. C. Veldhuis and M. A. Elbestawit (1995); "Modelling geometric and thermal errors in a five-axis cnc machine tool." *International Journal of Machine Tools and Manufacture* 35(9): 1321-1337.

Takeshima, H., & Ihara, Y. ; "Finished Test Piece Example for Fiveaxis Machining Centers". *The 5th Int. Conf. on Leading Edge Manufacturing in 21st century (LEM21)*, Osaka, Japan. 2009.

Uddin, M. S., S. Ibaraki, A. Matsubara and T. Matsushita (2009); "Prediction and compensation of machining geometric errors of five-axis machining centers with kinematic errors." *Precision Engineering* 33(2): 194-201.

Wang, S.-M. and J.-J. Lin (2013); "On-machine volumetric-error measurement and compensation methods for micro machine tools." *International Journal of Precision Engineering and Manufacturing* 14(6): 989-994.

Wang, S.-M., Y.-L. Liu and Y. Kang (2002); "An efficient error compensation system for CNC multi-axis machines." *International Journal of Machine Tools and Manufacture* 42(11): 1235-1245.

Weikert, S. (2004); "R-Test, a New Device for Accuracy Measurements on Five Axis Machine Tools." *CIRP Annals - Manufacturing Technology* 53(1): 429-432.

Yee, K. W. and R. J. Gavin (1990). Implementing fast part probing and error compensation on machine tools. NIST Report 4447, National Institute of Standards and Technology, Gaithersburg, MD 20899.

Yu, S. and J. M. Hollerbach; "Observability index selection for robot calibration". *Robotics and Automation, 2008. ICRA 2008. IEEE International Conference on*. 2008.

Zargarbashi, S. H. H. and J. R. R. Mayer (2009); "Single setup estimation of a five-axis machine tool eight link errors by programmed end point constraint and on the fly measurement with Capball sensor." *International Journal of Machine Tools and Manufacture* 49(10): 759-766.

Zhu, S., G. Ding, S. Qin, J. Lei, L. Zhuang and K. Yan (2012); "Integrated geometric error modeling, identification and compensation of CNC machine tools." *International Journal of Machine Tools and Manufacture* 52(1): 24-29.